

STABILITY OF AN EMBANKMENT ON
A PARTIALLY CONSOLIDATED FOUNDATION - INTERSTATE 95

by

FRANCISCO SILVA - TULLA
BS, University of Illinois
(1971)

Submitted in partial fulfillment
of the requirements for the degree of
Master of Science in Civil Engineering

at the

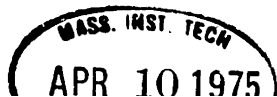
Massachusetts Institute of Technology
February, 1975

Signature of Author.....
Department of Civil Engineering, 22 January 1975

Certified by.....
Thesis Supervisor

and.....
Thesis Co-Supervisor

Accepted by.....
Chairman, Departmental Committee on Graduate Students of the
Department of Civil Engineering



ABSTRACT

-2-

STABILITY OF AN EMBANKMENT
ON A PARTIALLY CONSOLIDATED
FOUNDATION - INTERSTATE 95

by

FRANCISCO SILVA-TULLA

Submitted to the Department of Civil Engineering on 22 January 1975 in partial fulfillment of the requirements for the degree of Master of Science in Civil Engineering.

A test fill was built on a section of the I-95 embankment north of Boston in an effort to resolve the uncertainties involved in selecting strength parameters of Boston Blue Clay for stability analyses. Predictions of the fill elevation to cause failure, made before the field test began, are based on Unconfined Compression, Unconsolidated Undrained triaxial, field vane and SHANSEP (Stress History and Normalized Soil Engineering Properties) undrained strength. The Simplified Bishop and the Morgenstern-Price procedures of stability analyses are utilized for the predictions which are compared with the actual field test results.

The test fill failed at an elevation of +56.5 feet, after placing 18.7 feet of additional fill on an embankment which had been in place for five years. The field instrumentation was not as successful in warning against impending failure as was expected. The only consistent but very conservative sign of instability was provided by the settlement plates. The uncorrected field vane and SHANSEP yielded the most accurate predictions. The field vane prediction was 52.5 feet (7.1% underestimate) and the SHANSEP prediction was 60.7 feet (7.4% overestimate). The UC and UU strength were much too low, underestimating the failure elevation by 33%.

Thesis Supervisor:

T. William Lambe

Title:

Edmund K. Turner Professor of Civil Engineering

ACKNOWLEDGEMENT

The Author wishes to thank the following persons and organizations:

- Professor T. William Lambe and Dr. W. Allen Marr, my thesis supervisors, for their interest and guidance in my professional development.
- Professor Charles C. Ladd for his assistance during the preparation of the predictions.
- The Massachusetts Department of Public Works and the Department of Transportation, sponsors of the I-95 research project that supported my studies.
- All the members of the I-95 test fill project team who worked in the field and in the laboratory collecting the data that made this thesis possible.

I am specially grateful to my wife, Arlyn, for her patience and invaluable support during my graduate work.

TABLE OF CONTENTS

-4-

	<u>Page</u>
Title Page	1
Abstract	2
Acknowledgement	3
Table of Contents	4
List of Tables	7
List of Figures	8
List of Symbols	10
1. Introduction	12
1.1 The Failure at the I-95 Test Embankment	12
1.2 Background Information on the I-95 Research Project	14
1.3 Outline of Present Investigation	15
2. Stability Analyses of the I-95 Test Section	20
2.1 Subsurface Conditions and Soil Properties	20
2.1.1 Geologic History of the Area	20
2.1.2 Soil Properties	21
2.2 Methods of Stability Analyses Utilized	23
2.2.1 Simplified Bishop Method	23
2.2.2 Morgenstern and Price's Method	26
2.2.3 Procedure for Predicting Maximum Embankment Height with Limiting Equilibrium Analysis	27
2.3 Analysis with Unconfined Compression Strengths	28
2.4 Analysis with Unconsolidated Undrained Strengths	29
2.5 Field Vane Analysis	30

		-5-	
	2.5.1	Uncorrected Field Vane Analysis	30
	2.5.2	Corrected Field Vane Analysis	31
		2.5.2.1 Bjerrum Correction	31
		2.5.2.2 1.1 x Field Vane S_u	31
	2.6	SHANSEP Analysis	32
		2.6.1 Simplified Bishop Analysis	35
		2.6.2 Morgenstern Price Analysis	35
3.		Performance of the Station 263 Test Section	65
	3.1	Field Instrumentation and Exploration at the Test Section	65
	3.2	Field Test Construction Sequence	66
	3.3	Field Measurements	67
		3.3.1. Pore Pressures	67
		3.3.2 Settlement and Heave	67
	3.4	Failure	67
4.		Comparison of Predictions and Observed Performance	85
	4.1	Factors Contributing to Inaccuracies in All Predictions	85
		4.1.1 Properties of Sand Fill	85
		4.1.2 Mode of Failure	86
		4.1.3 Time Effects	87
	4.2	U.C. and U.U. Case	87
	4.3	Field Vane Analyses	88
	4.4	SHANSEP Analysis	88
5.		Post Failure Analyses	93
	5.1	Field Vane Analyses	93
	5.2	SHANSEP Analyses	95

5.3	Effective Stress Analyses	96
5.4	Effectiveness of Field Measurements as Indication of Impending Failure	97
5.4.1	Pore Pressures	98
5.4.2	Settlements and Heave	99
5.4.3	Summary	100
6.	Conclusions	109

LIST OF TABLES

-7-

<u>Table</u>	<u>Page</u>
2-1 Soil Properties for Unconfined Compression Analysis	37
2-2 Unconsolidated-Undrained Tests on Boston Blue Clay	38
2-3 Soil Properties for Unconsolidated-Undrained Stability Analysis	39
2-4 Soil Properties for Uncorrected Field Vane Stability Analysis	40
2-5 Soil Properties for Bjerrum Corrected Field Vane Stability Analysis	41
2-6 Soil Properties for 1.1 Field Vane Stability Analysis	42
2-7 SHANSEP Undrained Strength for Boston Blue Clay	43
3-1 Field Instrumentation at the Station 263 Test Section	70
4-1 Comparison of Predictions with Observed Behavior	90
4-2 SHANSEP STABILITY ANALYSES - Effects of Varying Fill Properties	91
4-3 Field Density Tests	92
5-1 Post Failure Field Vane Analyses	101
5-2 Post Failure SHANSEP Analyses	102
5-3 Piezometer Water Elevation Before and After Failure	103
5-4 Post Failure Effective Stress Analyses	104

LIST OF FIGURES

-8-

<u>Figure No.</u>	<u>Page</u>
1-1 Aerial View of Test Embankment After Failure	13
1-2 Location Map	18
1-3 Station 263 Test Section	19
2-1 Atterberg Limits vs. Elevation - Station 263	45
2-2 Unit Weight vs. Elevation - Station 263	46
2-3 Stress History - Station 263	47
2-4 Forces and Locations involved in the Equilibrium of an Individual Slice	48
2-5 Unconfined Compression Shear Strengths	49
2-6 Unconfined Compression Stability Analysis	50
2-7 Unconsolidated-Undrained Shear Strengths	51
2-8 Unconsolidated-Undrained Stability Analysis	52
2-9 Vane Shear Strength at Station 263	53
2-10 Vane Shear Strength at Station 263	54
2-11 Uncorrected Field Vane Stability Analyses	55
2-12 Field Vane Correction Factor vs. Plasticity Index	56
2-13 Bjerrum Corrected Field Vane Stability Analysis	57
2-14 $1.1 \times$ Field Vane S_u Stability Analysis	58
2-15 Embankment Elevation vs. Factor of Safety for Field Vane Analyses	59
2-16 SHANSEP Cross Section	60
2-17 Existing Stresses - Station 263	61
2-18 Undrained Strength Ratio vs. OCR for Boston Blue Clay	62
2-19 LEASE - SHANSEP Stability Analysis	63

<u>Figure No.</u>	<u>Page</u>
2-20 Results of M-P SHANSEP Analysis	64
3-1 Location of Field Instrumentation	71
3-2 Location of Field Instrumentation (Plan View)	72
3-3 Embankment Elevation vs. Time	73
3-4 Excess Pore Pressure vs. Embankment Elevation (P-14-A, P-14-B, P-14-C)	74
3-5 Excess Pore Pressure vs. Embankment Elevation (P-1, P-2)	75
3-6 Excess Pore Pressure vs. Embankment Elevation (P-3, P-4, P-5)	76
3-7 Excess Pore Pressure vs. Embankment Elevation (P-12, P-13, P-14)	77
3-8 Excess Pore Pressure vs. Embankment Elevation (P-6, P-8, P-9, P-10, P-11)	78
3-9 Excess Pore Pressure vs. Embankment Elevation (P-7, P-15)	79
3-10 Settlement vs. Embankment Elevation (SP-44, SP-2, SP-3, SP-4)	80
3-11 Vertical Movement vs. Embankment Elevation (East Side)	81
3-12 Station 263 Test Section Before and After Failure	82
3-13 Horizontal Displacement of Surface Stakes	83
3-14 View of the East Side of the Embankment After Failure	84
3-15 Large Crack East of Station 263 After Failure	84
5-1 Bjerrum Field Vane Correction Plot with I-95 Test Embankment Results	105
5-2 Post Failure SHANSEP Analyses (M-P)	106
5-3 Pore Pressures Used for Effective Stress Analysis	107
5-4 Graphical Representation of ESA	108

LIST OF SYMBOLS

a	= Henkle's pore pressure parameter
\bar{c}	= cohesion, in terms of effective stresses
CIU	= Isotropically Consolidated Undrained triaxial test
DSS	= Direct Simple Shear
ESA	= Effective Stress Stability Analysis
E_j	= total interslice normal force
FS	= factor of safety
$f(x)$	= distributional relationship assumed for the side force inclination
Δg	= distance between the location of the normal force and the center of the base of a slice
h_t	= vertical distance between the line of thrust and the shear surface
K_o	= coefficient of earth pressure at rest; ratio of lateral to axial stress for conditions of uniaxial strain
k_α	= dimensionless number depending on the values of α , ϕ and FS
N	= normal force acting on the base of a slice
OCR	= Over Consolidation Ratio
P - 1	= piezometer #1
PI	= Plasticity Index
PSA	= Plane Strain Active
PSP	= Plane Strain Passive
r	= radius of a circle
S	= shear force on the base of the slice
S_u	= undrained shear strength
SHANSEP	= Stress History and Normalized Soil Properties

SI - 1 = Sope Indicator #1; inclinometer

TSA = Total Stress Stability Analysis

UC = Unconfined Compression test

UU = Unconsolidated Undrained triaxial test

Δu = excess pore pressure

W = weight of an individual slice

w = water content

w_L = liquid limit

w_N = natural water content

w_P = plastic limit

X_j = shear force between slices

Δx = width of a slice

y_t = y coordinate of the line of thrust

α = angle of inclination of the base of a slice measured in a clockwise direction from the horizontal

λ = scaling factor for side force inclinations

$\bar{\sigma}_{vo}$ = initial vertical effective stress

$\bar{\sigma}_{vm}$ = maximum vertical effective stress

σ_1 = major principal stress

σ_3 = minor principal stress

γ_t = total unit weight

ϕ = angle of internal friction for a soil in terms of total stresses

$\bar{\phi}$ = angle of internal friction for a soil in terms of effective stresses

1. INTRODUCTION

1.1 THE FAILURE OF THE I-95 TEST EMBANKMENT

Early in the morning of 20 September 1974 a failure of extraordinary proportions occurred on a test fill located on the Interstate 95 embankment north of Boston. Within minutes, a simultaneous failure to both sides of the embankment caused the crest to drop about 30 feet and the sides to heave as much as 14 feet. An aerial view of the slide areas as shown in Figure 1-1. Unfortunately, no one was present to witness the failure take place since no advance warning was noticed. The fill never cracked at the surface nor was any clear indication of impending failure obtained from the field instrumentation at the site. The test section failed at an elevation of 56.5 feet, after placing 18.7 feet of additional fill on an embankment which had been in place for five years.

The test fill was planned on an effort to resolve the uncertainties involved in selecting strength parameters for use in stability analyses of embankments on Boston Blue Clay. The I-95 test fill problem was further complicated by having a partially consolidated foundation under the embankment.

The construction of full scale test embankments for the solution of engineering problems is by no means uncommon. In his state-of-the-art report, "Embankments on Soft Ground", Bjerrum (1972) discusses 11 embankment failures of which 8 were test fills. La Rochelle, et. al (1974) report the results of a more recent test fill located in Canada. The test fills



Figure 1-1 Aerial view of the I-95 test embankment after failure

are selected because they are the only test which models ⁻¹⁴⁻ precisely the site conditions (soil properties and state of stress). Results from these full size field tests are very useful in the interpretation of the routinely performed laboratory and field strength tests.

This thesis is a study of the stability of the I-95 test embankment. The objective is to evaluate prediction techniques by comparing the predictions with the measured field performance. Predictions of the embankment elevation at failure were made based on Unconfined Compression tests (UC), Unconsolidated Undrained triaxial tests (UU), Field Vane shear tests (with and without corrections), and Stress History And Normalized Soil Properties (SHANSEP) undrained strengths. The Simplified Bishop and the Morgenstern-Price procedures of stability analyses were utilized. The predictions varied from 39.7 ft (zero ft of additional fill) for the UC and 61.1 ft for the field vane with a correction factor of 1.1. The uncorrected field vane, on the low side, and the SHANSEP approach, on the high side, yielded the most accurate predictions. The stability methods utilized were unsuccessful in predicting the location of the failure surface.

Based on the results presented in this thesis, a stability analysis with field vane shear strengths and the Simplified Bishop procedure should yield a prediction within 10% of the actual value for embankments on Boston Blue Clay. To investigate the stability of an embankment on a partially consolidated foundation (e.g. an embankment built in various stages) analyses

based on SHANSEP strengths should be used. With SHANSEP the⁻¹⁵⁻ increase in strength with consolidation is easily evaluated without performing additional tests and the results obtained should also be within 10% of the actual value.

1.2 BACKGROUND INFORMATION ON THE I-95 RESEARCH PROJECT

The Interstate 95 research project was begun in September 1965 with preconstruction activities for a 2.4 mile section of the highway north of Boston. Much of the section required construction of a high embankment across a low tidal marsh in the Revere-Saugus area (Fig. 1-2). The marsh was covered with peat and underlain with a thick deposit of a medium to soft clay called Boston Blue Clay.

Construction operations began in August 1967 with removal of the top layer of silt and peat and placement of a ten foot thick sand and gravel working mat. By July 1969, when filling was completed, the embankment crest elevation ranged from +25 to + 40 feet. Fill above elevation +18 feet represented a surcharge placed to accelerate consolidation deformations.

An extensively instrumented section was established by M.I.T. and the Massachusetts Department of Public Works (MDPW) at Station 246 of the highway embankment. The study of the M.I.T. MDPW test section was focused at predicting, measuring and evaluating the deformations and pore pressure performance during construction, after construction and upon removal of the surcharge in 1973. However, final surcharge removal and paving was cancelled.

To complete the objectives of the research program at Station 246, M.I.T. and the MDPW planned to remove the surcharge

from a 300 foot long section of the embankment at the M.I.T.-MDPW test section. During planning for surcharge removal, the research participants realized that substantial field performance information regarding stability of the clay foundation could be obtained at little extra cost by placing the removed surcharge fill as an additional fill on another section of the embankment until a stability failure occurred. Accordingly, a construction and instrumentation program was developed to load a 300 foot section of embankment to failure.

1.3 OUTLINE OF PRESENT INVESTIGATION

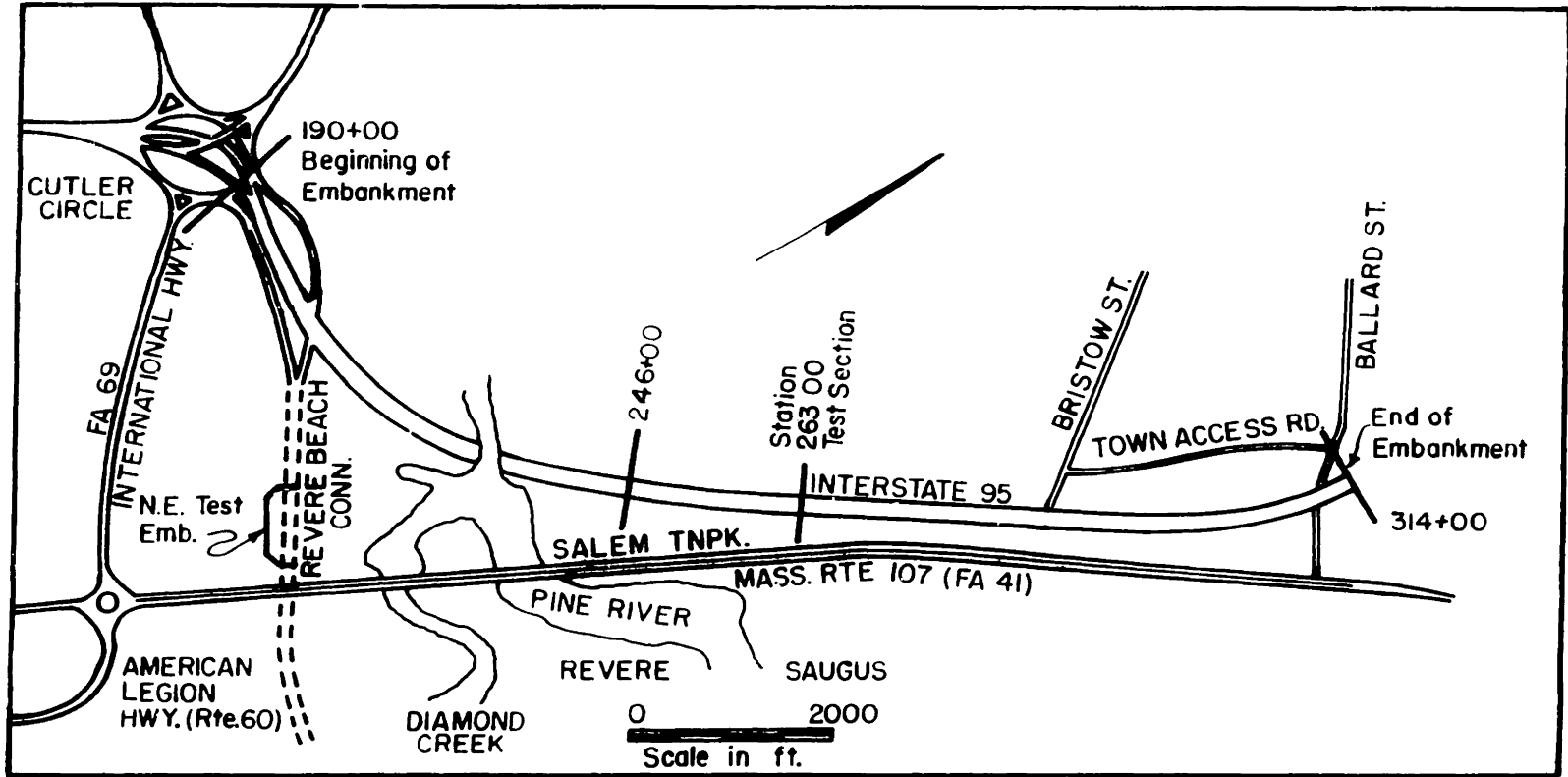
Station 263 was selected as the new test section for the loading operation which was scheduled for the summer of 1974. At this location, lateral movements in the foundation of up to 10 inches on the west side and 8 inches on the east side were measured during initial construction. These movements were larger than those measured at any other station and lead the project engineer to recommend the installation of a stabilizing berm on the west side as shown in Figure 1-3.

The geometry for the placement of additional fill, also shown in Fig. 1-3, was designed to force the failure to occur to the east side to minimize disturbance of the marsh area on the west side. A wider embankment crest needed to accommodate construction equipment during the later stages of loading required steepening of the east slope. Fill was to be dumped from the crest of the original embankment until the east slope was equal to the angle of repose of the sand. Then fill was to be

placed in even lifts for the entire 300 feet length of the test section. No compaction, other than that provided by the construction equipment, was planned.

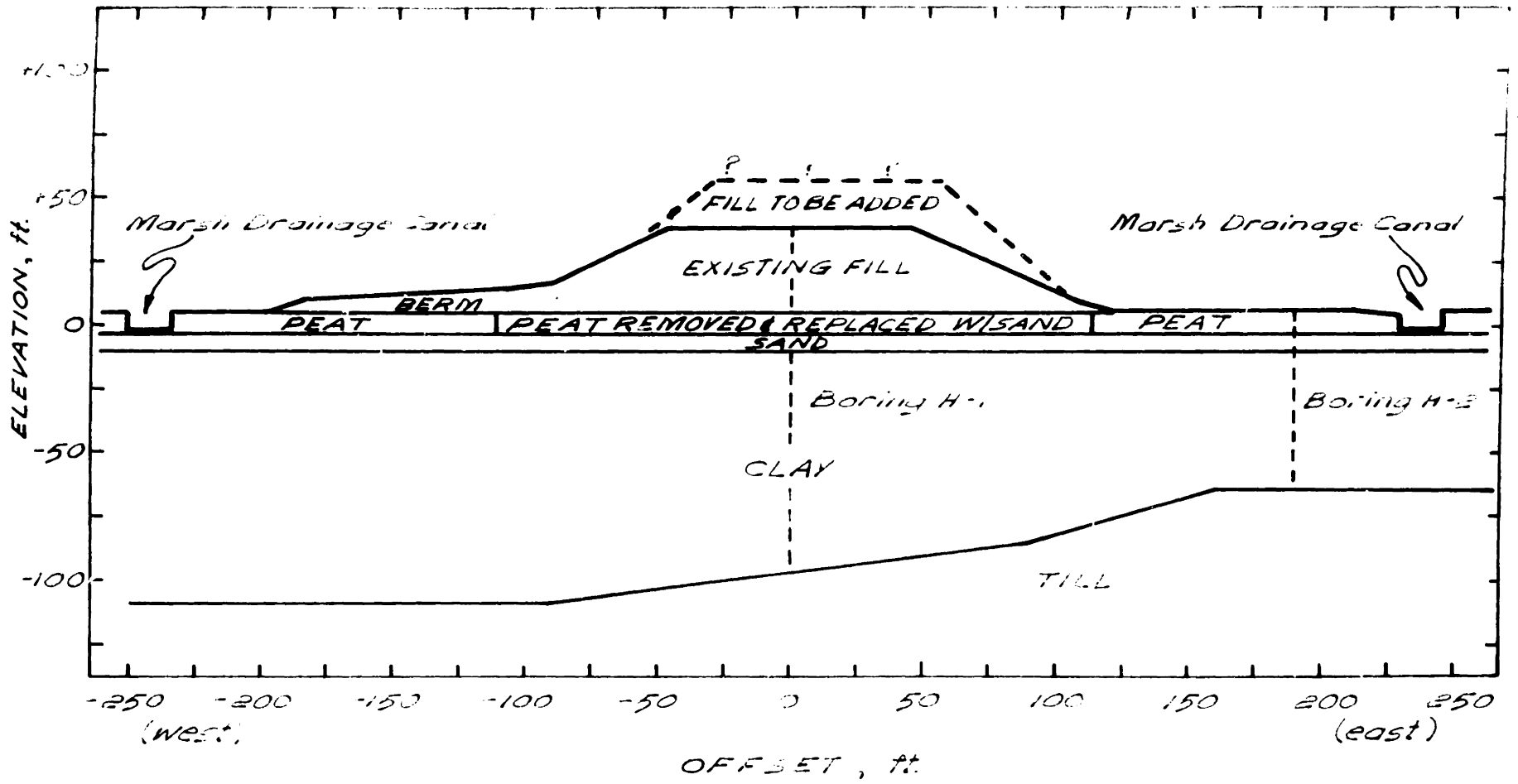
In his Rankine lecture, Lambe (1973) classified predictions into three types. A "Type A" is made before the event to be predicted takes place. A "Type B" prediction is made as the event is taking place and a "Type C" prediction after the event has occurred. Type A predictions are the most useful in civil engineering projects since they are the only means to prove that a prediction technique is correct. Furthermore, design decisions are always based on Type A predictions.

The predictions of height of fill required to cause failure, presented in Chapter 2, were all made before the event, thus falling into Lambe's category of "Type A". The performance of the test section is given in Chapter 3, and Chapter 4 compares predicted and observed behavior. After failure occurred, analyses considering the best estimate of the failure surface were done in order to gain further insight into the various methods and soil parameters used. Results from these post-failure stability analyses and a short evaluation of the field measurements are the subject of Chapter 5. Conclusions from the study are presented in Chapter 6.



LOCATION MAP , I- 95

FIGURE 1-2



STATION 263 TEST SECTION - I-95

FIGURE 1-3

2. STABILITY ANALYSES OF THE I-95 TEST SECTION

2.1 SUBSURFACE CONDITIONS AND SOIL PROPERTIES

2.1.1 Geologic History of the Area⁽¹⁾

Geologists believe that the 5 to 45 feet thick layer of glacial till underlying the Greater Boston area was deposited during the Wisconsin glaciation on a gray shale bedrock (Cambridge Aegillite) which is found at depths of 70 to 204 feet. Radiocarbon dates indicate that the Boston area became free of glacial ice at least 14,000 years ago and deposition of a marine illitic clay, called Boston Blue Clay, was in progress at that time. The clay, which consists of sediments of glacial origin, was deposited in a brackish water environment.

During the Valdres glacial substage (12,250 to 11,740 years ago) sea level fell with respect to land. The clay sediments emerged from below sea level and were eroded by streams and weathered subaerially. The weathering and subsequent desiccation formed a stiff "crust" which exhibits the properties of over consolidation. The Valdres glacial substage was followed by warmer climates during which sea level rose rapidly and sand were deposited in depressions in the clay surface. As the sea continued to rise at a slower rate to its present level, the entire area was further covered with organic silt, shells and peat. The geologic processes at the I-95 site have

⁽¹⁾ From Kenney (1964) and Storch Engineers (1971)

produced a deposit with a very complex stress history. The stiff crust is underlain by a clay layer of varying but generally decreasing overconsolidation with depth. As shown in Fig. 2-3, the clay becomes normally consolidated at around elevation -70 ft. A generalized soil profile at Station 263 is shown in Figure 1-3 together with a cross section of the original 40 feet high embankment.

2.1.2 Soil Properties

Boston Blue Clay - Figures 2-1 and 2-2 present plots of Atterberg Limits, water content (w) and total unit weight (γ_t) with depth. Tests were performed on samples obtained from borings at the centerline of the embankment (boring H-1) and at 190 ft right of the centerline (boring H-2) as shown in Figure 1-3. The samples were taken during April 1974, about 5 months prior to the start of loading. Average total unit weight values of 121.5 lb/ft^3 for clay above elevation -30 ft and 114.0 lb/ft^3 for that below -30 ft were used in all the stability analyses performed. The maximum past pressure of the clay deposit, determined from the April 1974 samples, is presented in Figure 2-3. The M.I.T. constant rate of strain consolidometer (Wissa et al, 1971) was used for the consolidation tests and maximum past pressures were obtained by the Casagrande method. Detailed information on the strength characteristics of the clay are given in subsequent sections where the different types of stability analyses are discussed.

Natural sand - The natural sand overlying the clay is a well graded silty sand with some gravel. Standard penetration tests at Station 246 before construction indicated blow counts of 8 to 25 with an average of 17 for this material. A unit weight, $\gamma = 113 \text{ lb/ft}^3$, and a friction angle, $\bar{\phi} = 35^\circ$, were used in the stability analyses.

Till - The glacial till is quite dense with blow counts generally in excess of 50 but varying from 24 to 171. This material is of no significance for the stability analyses since it is highly unlikely that the failure surface will go below the clay strata.

Peat - No tests have been performed on samples from the fibrous peat found over the sand. Values of $\gamma = 75 \text{ lb/ft}^3$ and undrained shear strength, $S_u = 300 \text{ lb/ft}^2$ were considered reasonable and used in all the analyses.

Embankment sand - The fill for the embankment consists of well graded fine to coarse sand with some fine to medium gravel. The particles are angular with the predominant minerals being quartz and some mica. Density tests performed during initial construction at Station 246 ranged from 101.8 lb/ft^3 to 134.6 lb/ft^3 with an average of 119 lb/ft^3 . During initial fill placement, material was end dumped up to elevation +5 and compacted with rubber tired rollers thereafter. Maximum and minimum dry densities of 110.5 lb/ft^3 and 95.2 lb/ft^3 , respectively, were obtained during laboratory tests. Unit weights of 110 lb/ft^3 for the end dumped material

and 119 lb.ft³ for the compacted material were utilized for all the analyses. Drained triaxial compression tests on the embankment sand yielded an average $\bar{\phi} = 43.8$ for $\gamma_t = 135\text{lb/ft}^3$. The friction angle used in the stability analyses was 35° for the end dumped sand and 40° for the compacted sand. The reduction in $\bar{\phi}$ reflects the difference in unit weight between the laboratory test specimens and the field material.

2.2 Methods of Stability Analyses Utilized

Stability of the embankment for different fill heights was predicted by two different methods - the Simplified Bishop Procedure and the Morgenstern and Price Procedure. Different types of analyses were run depending on the basis for evaluating the strength of the soils. These types include strengths computed by unconfined compression (UC) tests, unconsolidated undrained (UU) triaxial tests, field vane shear tests and the stress history and normalized soil engineering properties (SHANSEP). The slice equilibrium equations were solved with computer programs available at M.I.T.

2.2.1 Simplified Bishop Method

Bishop (1955) presented a method of slices for slope stability analysis in which the normal and weight forces were assumed to act through a point on the center of the base of each slice. With this assumption the moment equilibrium equation for a circular arc failure surface can be expressed as:

$$\sum_{\text{all slices}} W r \sin\alpha - \sum_{\text{all slices}} S r = 0 \quad (2.1)$$

where:

W = weight of the slice

r = radius of circle

α = angle of inclination of the base of the slice

and act as shown in Figure 2-4. From this figure it is also clear that the expression for vertical force equilibrium is:

$$- W + (X_j - X_{j-1}) + S \sin\alpha + N \cos\alpha = 0 \quad (2.2a)$$

And for horizontal force equilibrium:

$$(E_j - E_{j-1}) + S \cos\alpha - N \sin\alpha = 0 \quad (2.2b)$$

where:

S = shear force at bottom of slice

N = normal force at bottom of slice

X_j = interslice shear force

E_j = interslice normal force

In addition, Bishop assumed that S and N are related by the Mohr-Coulomb strength criterion and a constant factor of safety (FS) such that:

$$S = \frac{1}{FS} [\bar{c} \Delta x + (N - u \Delta x) \tan \bar{\phi}] \quad (2.3)$$

By substituting Eqn 2.3 into 2.2a, we find that:

$$S = \frac{1}{FS} \bar{c} \Delta x [W - (X_j - X_{j-1}) - u \Delta x] \tan \phi k_\alpha \quad (2.4)$$

in which

$$k = \frac{\sec\alpha}{1 + \frac{\tan\alpha \tan\phi}{FS}}$$

Substituting equation 2.4 into the moment equilibrium equation (2.1) the factor of safety can be expressed as:

$$FS = \frac{\sum c' \Delta x + [W - (X_j - X_{j-1}) - u \Delta x] \tan\phi}{\sum W \sin\alpha} k_\alpha \quad (2.5)$$

The simplest solution for Eqn. 2.5 is obtained by assuming that there are no interslice shear forces ($X_j = X_{j-1} = 0$). This method of solution is commonly referred to as the Simplified Bishop Method.

Three important assumptions were made in arriving at the solution:

- 1) The soil behaves as a Mohr-Coulomb material.
- 2) The factors of safety of the cohesive component of strength and the frictional component of strength are equal.
- 3) The factor of safety is the same for each slice.

This solution, in common with all other simplified solutions, does not satisfy static equilibrium.

Wright (1969) presents a comprehensive treatment of stability analysis by limiting equilibrium. He concludes that the Simplified Bishop Method is, for all practical purposes, a suitably accurate procedure of analysis for cases where the critical shear surface is likely to be approximated by a circular arc.

The solution to Eqn. 2.5 was obtained with program LEASE I (Limiting Equilibrium Analysis in Soil Engineering). The program is described in detail by Bailey and Christian (1969). With LEASE, a large number of trial circles can be analyzed at a reasonable cost which simplifies the problem of identifying the most critical failure surface. The description of the problem geometry and soil boundaries with a numbered set of straight line segments as suggested by Little and Price (1958) makes the program easy to use. The soil properties can be given either as undrained parameters for total stress analysis or drained parameters and pore pressure for effective stress analysis.

2.2.2 Morgenstern and Price's Method

In the Morgenstern and Price (1965, 1967) analysis of slope stability, moment equilibrium of individual slices is considered instead of overall moment equilibrium. The Morgenstern-Price analysis is also an application of the method of slices and thus contains the same three assumptions made above in arriving at the Simplified Bishop Method. In addition, the relationship between the shear and normal forces at slice interfaces is assumed to be of the form:

$$X_j = \lambda f(x) E_j \quad (2.6)$$

where $f(x)$ is a function representing the relationship between forces X and E (see Fig. 2-4). λ is an unknown scaling factor defining the relationship between X and E in terms $f(x)$. If $f(x)$ is specified the location of the normal force.

on the base of each slice is fixed and the problem becomes statically determinate. λ and the factor of safety with respect to shear strength, FS, are then found from a solution of the differential equations that satisfy the appropriate boundary conditions.

From Fig. 2-4, the moment equilibrium equation about point M is:

$$\begin{aligned} X_{j-1} \Delta X + (X_j - X_{j-1}) \frac{\Delta X}{2} + E_{j-1} \Delta y_t \\ + (E_j - E_{j-1}) \left(h_t + \Delta y_t + \frac{\Delta y}{2} \right) \\ + (N \Delta g) = 0 \end{aligned} \quad (2.7)$$

Eqn. 2.7 can be expressed as:

$$-X = E \frac{dy_t}{dX} + h_t \frac{dE}{dX} \quad (2.8)$$

The solution to this differential equation for moment equilibrium and to the force equilibrium equations (Eqn. 2.2) yields the required answer.

The advantage of the Morgenstern and Price Method is that the analysis of non circular failure surfaces is made much simpler by considering the moment equilibrium of each individual slice. Several examples of analysis of non-circular surfaces will be presented in section 2.6.2. These were analyzed with the aid of computer program MGSTRN (Madera 1969).

2.2.3 Procedure for Predicting Maximum Embankment Height with Limiting Equilibrium Analysis

The approach to predicting the maximum embankment height is the same with either LEASE or MGSTRN. Both programs

have identical input except for the shape of the assumed failure surface. Figure 2-6 is a graphical representation of the problem description required by the computer. The geometry and boundaries between soils of different characteristics are delineated by numbered line segments. For clarity, the numbers have been omitted from the figure. Each soil type is identified by a number to which particular soil properties have been assigned.

After the problem is correctly defined, a series of trial failure surfaces are analyzed. The trial surface with the lowest factor of safety and reasonable location is taken as the critical one. Then, the height of the embankment is increased and a new critical surface and factor of safety is calculated. Factors of safety for critical surfaces of different embankment elevations are plotted as shown in Figure 2-15. From this plot, the height of fill producing a $FS = 1$ is determined.

2.3 Analysis with Unconfined Compression Strengths

A total stress stability analysis (TSA) was performed based on strengths determined from Unconfined Compression (UC) tests. The strength tests were conducted according to the procedure given by Lambe (1951).

Figure 2-5 shows the results from UC tests on samples taken at Station 263 from borings H-1 and H-2. The solid line represents the variation of undrained shear strength with

depth on which the LEASE analysis was based. Figure 2-6 is a graphical representation of the problem and its solution. As in all subsequent analyses, the geometry of the soil layers has been modified to account for the settlement that took place from the beginning of initial construction in 1967 to July 1974. The computed factor of safety (Simplified Bishop Method) along the critical failure surface shown in Fig. 2-6 was 0.983. A stability analysis using unconfined compression strengths would indicate that the embankment could not have originally been constructed to elevation +40. The predicted elevation of fill for $FS = 1$ was essentially +37.8, the average elevation of the embankment prior to placing additional fill for the loading of the test section.

2.4 Analysis with Unconsolidated Undrained Strengths

The results from Unconsolidated Undrained (UU) tests shown in Table 2-2 and Figure 2-7 were the basis for the UU analysis. The UU tests were performed according to the procedure given by Lambe (1951) with non porous end caps and thin latex membranes (prophylactics).

The results of the analysis for the embankment prior to loading are depicted in Fig. 2-8. The Simplified Bishop Method factor of safety for the critical circle is 1.003 and thus, as in the UC case, the predicted embankment elevation for $FS = 1$ was +37.8 ft.

Two types of field vane analyses were performed. The first type was based on the uncorrected vane results and the second on the corrected field vane strengths as suggested by Bjerrum (1972).

The most recent field vane tests run at the site of the station 263 test section were performed in June 1973 (Fig.2-9). These vane tests were performed by M.I.T. using vane shear equipment manufactured by Geonor. A 5.5 cm by 11.0 cm vane was used for all tests and the tests were performed according to ASTM D2573-63T. In order to use the 1973 tests for the 1974 analyses it was necessary to correct the shear strength to account for the additional consolidation or to show that the increase in strength would have been very small. Figure 2-10 shows field vane tests run at station 244 at five year intervals. The increase in strength measured in the five years of consolidation at station 244 was very small. The strength increase at the test section corresponding to 13 additional months of consolidation would have been negligible and thus it was considered reasonable to use the 1973 tests for the 1974 analyses at station 263

2.5.1. UNCORRECTED FIELD VANE ANALYSIS

The strength profile represented by the solid lines in Fig.2-9 was the basis for the computer model shown in Fig.2-11. The sliding mass was divided in slices 5 ft wide. LEASE ignores the two end slices but for the station 263 test section the additional resistance through the peat layer and the nearly vertical failure plane in the sand would be very small.

Figure 2-15 shows the results of the simplified Bishop analyses for various embankment elevations. The predicted elevation for

FS=1 is 52.5 ft with the failure surface shown in Figure 2-11.

2.5.2 CORRECTED FIELD VANE ANALYSIS

2.5.2.1 Bjerrum Correction

Simplified Bishop analyses were performed with the model described in the previous section modified by using the corrections to field vane strengths proposed by Bjerrum(1972). Figure 2-12 shows Bjerrum's correction factor for field vane shear strength as a function of the Plasticity Index (PI)of the clay. The variation of PI with depth for the clay foundation at Station 263 was shown in Figure 2-1. The corrected strengths for the cross section of Figure 2-13 using Bjerrum's recommended curve are given in Table 2-5. The correction factor for each soil layer was determined using the average value of PI within the layer. The net effect of the correction is an overall reduction of the clay strength ($u_{ave}=0.94$). Results of analyses at various embankment heights are shown in Figure 2-15 from which a fill elevation for FS=1 of +50.5 fr is predicted. The approximate critical failure surface is shown in Figure 2-13

2.5.2.2 1.1 x Field Vane S_u

Since Bjerrum published his field vane correction factor in 1972, several case studies have been added to the literature. These are shown plotted in Figure 2-12. If the new points are considered, it is apparent that Bjerrum's recommended correction for $PI \approx 20$ is too low. A correction factor of 1.1 was considered more appropriate and was used for an additional Field Vane

The results of the FV \times 1.1 analysis are plotted in Figure 2-15. The failure elevation predicted is +61.1 ft. Figure 2-14 presents the analysis and critical failure surface for an embankment elevation of 60 feet. In addition to the analysis of the east slope, the west side of the embankment at elevation +60 was examined with the 1.1 \times F.V properties. The computed factor of safety was 0.977. Since this is somewhat lower than the safety factor for the east side at the same embankment elevation, it was an indication of the possible need for preventive measures during construction to force the failure to the east side, where the majority of the instrumentation had been installed.

2.6 SHANSEP ANALYSIS

SHANSEP (Stress History And Normalized Soil Engineering Properties) is a procedure for determining soil properties from the results of laboratory tests assuming that the soil follows a normalized behavior. A series of strength tests are performed to obtain plots such as S_u/σ_{vc} and E_u/S_u v.s. OCR. With these plots one needs only to determine the OCR with depth and the appropriate soil parameters can be obtained. The main advantages of SHANSEP are: 1) minimizes effects of sample disturbances by reconsolidating (under K_o conditions) normally consolidated clays to 2 to 4 times $\bar{\sigma}_{vm}$ and over consolidated clays to about 1.5 times $\bar{\sigma}_{vm}$, where normalized behavior is observed. 2) Once the plots have been obtained they can be used for

similar deposits in the area. 3) Provides a rational way of estimating increase in strength with consolidation.

The disadvantages of the SHANSEP approach are: 1) An accurate determination of the maximum past pressure is essential since everything is based on OCR (the in situ effective vertical stress ($\bar{\sigma}_{vo}$) can generally be determined accurately). 2) For clays with a lot of structure (e.g., quick clays) the consolidation beyond $\bar{\sigma}_{vm}$ will destroy the structure and the test results will not be reliable. 3) In order to simulate actual field conditions the strength tests require equipment not generally found in commercial laboratories. SHANSEP should be complemented with a good strength index test, such as field vane, to provide an idea of the variability of properties through the soil deposit and to help in determining the stress history. SHANSEP is described in detail by Ladd (1971).

The soil parameters for the SHANSEP analyses were derived by Ladd (1975) from normalized properties plots for Plane Strain Active (PSA), Direct Simple Shear (DSS) and Plane Strain Passive (PSP) conditions for resedimented Boston Blue Clay. The embankment cross-section shown in Figure 2-16 was divided into four sections (55' West to 40' East, 40'E to 90' E, 90'E to 140' E and East of 140' E) based on the magnitude and orientation of the existing effective stresses. The total stresses induced by the construction of the original embankment (+40 ft elevation) were computed with program FEECON, a finite element program for analysis of embankment construction, described by Simon et al (1972). The details of the FEECON analysis of the I-95 test

embankment are presented by Hawkes (1975). To find the existing effective stresses, pore pressures measured in the field were subtracted from the total stresses computed by FEECON, as shown in Figure 2-17. With the maximum past pressure shown in figure 2-3 and the magnitude of the existing stresses the present Over Consolidation Ratio (OCR) was computed. The undrained strength was then determined from the plots shown in Figure 2-17.

Table 2-6 presents the input shear strengths for each of the four sections of Figure 2-16. Values of Su for each of the possible stress systems along the failure surface are given for each section. The following criteria were used in selecting the value of Su along the failure surface in order to represent the actual field conditions as closely as possible:

Stress System	Angle of Failure Surface with Horizontal	Su
PSA	45°	qf
PSA	45° + φ / 2 ≈ 60°	τh
DSS	0° ± 20°	τh
PSP	45°	qf
PSP	45 - φ / 2 ≈ 30°	τff

Where $q_f = \frac{\sigma_1 - \sigma_2}{2}$ and $\tau_{ff} = q_f \cos \phi$

The properties of the granular soils and peat are the same as in the previous analyses.

2.6.1 Simplified Bishop Analysis

The result of the LEASE-SHANSEP analysis for the embankment at elevation +65 feet is shown in Figure 2-19. The factor of safety computed was 0.917. As shown in Figure 2-20, the fill elevation for FS=1 was estimated to be 59 feet using only the analysis at +65 feet. A formal prediction was not made using the LEASE-SHANSEP approach for two reasons: 1) the analyses would involve a time consuming trial and error procedure to obtain the correct value of S_u on the different segments of the critical surface. 2) Since the problem geometry suggests a non circular failure surface, the more sophisticated Morgenstern-Price analysis was considered to be suitable to use with the more sophisticated SHANSEP approach.

2.6.2 Morgenstern-Price Analysis

The results of the MGSTRN analyses are presented in Appendix A. Unlike LEASE, each MGSTRN run represents the analysis of only one assumed failure surface. The user has the option of specifying any arbitrary function $f(x)$ (see equation 2.6). The value of λ compatible with the $f(x)$ assumed is computed by the program. Run M-17, shows that the difference between the three basic $f(x)$ assumptions (constant, sine and bell) described by Whitman and Bailey, (1967), is very small. Consequently, only the sine assumption was used for the majority of the analyses.

The results of selected runs are plotted in Figure 2-20. Initially runs M-6, M-12 and M-14-C were plotted. These runs

were selected because of their similar geometry. However, it was necessary to adjust run M-14-C to reflect the decrease in F.S. caused by lowering the failure surface from -60ft to -70ft. The analyses indicated that the deeper failure surface was more critical. The adjustment was made by multiplying FS(m-14-c) by the ratio $\frac{FS_{m-12}}{FS_{m-1-A}} = 0.95$. (see appendix A for runs M-12 and M-1-A). Secondly, the FVx 1.1 results from section 2.5.2 were plotted and finally the most critical runs at elevation +62.5 and +65 (runs M-18 and M-20) were plotted. In Figure 2-19, the lines joining the three sets of M-P analyses are approximately parallel.

The fill elevation for FS=1 predicted from Figure 2-20 is +60.7 feet.

**UNCONFINED COMPRESSION
STABILITY ANALYSIS
SOIL PROPERTIES FOR FIGURE 2-6**

SOIL NO.	$\bar{\sigma}_t, lb/ft^2$	C or S_u lb/ft ²	ϕ°	SOIL TYPE
1	119	0	40	Embankment Sand
2	110	0	40	End Dumped Sand
3	110	0	30	End Dumped Sand
4	75	300	0	PEAT
5	113	0	35	Foundation Sand
7	121	1000	0	Boston Blue Clay
8	114	950	0	"
9	114	800	0	"
10	114	430	0	"
11	114	250	0	"
12	114	480	0	"
13	114	800	0	"
14	114	1030	0	"
15	121	1250	0	"
16	121	850	0	"
17	117	675	0	"
18	114	530	0	"
19	114	500	0	"
20	114	540	0	"
21	114	600	0	"
22	120	0	40	TILL

TABLE 2-1

**UNCONSOLIDATED UNDRAINED TESTS ON
BOSTON BLUE CLAY, I-95 STATION 263**

TEST NO.	BORING	ELEV., (ft.)	$\sigma_1 = \sigma_3 \text{ max}$ lb/ft ²	$\frac{\sigma_1 - \sigma_3}{2}$ lb/ft ²	REMARKS
UU-19-74	H-1	-37.0	1044.6	522.	
UU-20-74	H-1	-62.5	645.2	322.	
UU-21-74	H-1	-81.6	583.7	292.	
UU-22-74	H-2	-24.3	1556.6	778.	$\sigma_c \neq \sigma_v$
UU-23-74	H-2	-45.2	1044.6	522.	
UU-24-74	H-2	-64.2	1671.3	836.	
UU-25-74	H-3	-70.5	1429.6	715.	
UU-26-74	H-3	-70.5	870.5	435.	$\beta = 45^\circ$
UU-27-74	H-3	-70.5	1126.5	563.	$\beta = 90^\circ$
UU-28-74	H-2	-45.2	921.7	460.	$\beta = 45^\circ$
UU-29-74	H-2	-44.2	194.6	097.	$\beta = 90^\circ$
UU-30-74	H-1	-27.0	1683.6	841.	
UU-31-74	H-1	-91.8	1700	850.	
UU-32-74	H-1	-14.7	2201.8	1100.	
UU-33-74	H-1	-62.5	684.7	312.	$\sigma_c = 0.5\sigma_v$
UU-34-74	H-1	-62.5	327.7	164.	$\sigma_c = 2.0\sigma_v$

TABLE 2-2

**UNCONSOLIDATED UNDRAINED
STABILITY ANALYSIS
SOIL PROPERTIES FOR FIGURE 2-8**

SOIL NO.	$\gamma_t, \text{lb/ft}^3$	$C \text{ or } S_u$ lb/ft^2	ϕ°	SOIL TYPE
1	119	0	40	Embankment Sand
2	110	0	40	End Dumped Sand
3	110	0	30	End Dumped Sand
4	75	300	0	PEAT
5	113	0	35	Foundation Sand
7	121	820	0	Boston Blue Clay
8	114	610	0	"
9	114	450	0	"
10	114	370	0	"
11	114	355	0	"
12	114	475	0	"
13	114	650	0	"
14	114	820	0	"
15	121	1085	0	"
16	121	900	0	"
17	117	675	0	"
18	114	540	0	"
19	114	530	0	"
20	114	660	0	"
21	114	850	0	"
22	120	0	40	TILL

TABLE 2-3

**UNCORRECTED FIELD VANE STABILITY ANALYSIS
SOIL PROPERTIES FOR FIGURE 2 - 11**

SOIL NO.	$\gamma_s, lb/ft^3$	C or S_u lb/ft ²	ϕ°	SOIL TYPE
1	119	0	40	Embankment Sand
2	110	0	40	Fill Dumped Sand
3	100	0	30	"
4	75	300	0	PEAT
5	113	0	35	Foundation Sand
6	110	0	37	Test Fill Sand
7	121	1270	0	Boston Blue Clay
8	114	118	0	"
9	114	1075.3	0	"
10	114	973	0	"
11	114	870.5	0	"
12	114	717	0	"
13	114	594.0	0	"
14	114	717	0	"
15	114	1024.1	0	"
16	121	1936	0	"
17	121	1638.5	0	"
18	121	1331.3	0	"
19	114	1126.5	0	"
20	114	921.7	0	"
21	114	758	0	"
22	120	0	40	TILL
24	114	860.2	0	Boston Blue Clay

TABLE 2-4

**BJERRUM CORRECTED FIELD VANE
STABILITY ANALYSIS
SOIL PROPERTIES FOR FIGURE 2-13**

SOIL NO.	γ_t , lb/ft ³	C or Su lb/ft ²	ϕ°	SOIL TYPE
1	119	0	40	Embankment Sand
2	110	0	40	End Dumped Sand
3	100	0	30	"
4	75	300	0	PEAT
5	113	0	35	Foundation Sand
6	113	0	37	Test Fill Sand
7	121	1224	0	Boston Blue Clay
8	114	1165	0	"
9	114	1064	0	"
10	114	973	0	"
11	114	879	0	"
12	114	731	0	"
13	114	612	0	"
14	114	745	0	"
15	114	1086	0	"
16	121	1548	0	"
17	121	1344	0	"
18	121	1092	0	"
19	114	1104	0	"
20	114	912	0	"
21	114	750	0	"
22	120	0	40	TILL
24	114	860	0	Boston Blue Clay

TABLE 2-5

SOIL NO.	$\delta_t, lb/ft^2$	C or S_u lb/ft^2	ϕ°	SOIL TYPE
1	119	0	40	Embankment Sand
2	110	0	40	End Dumped Sand
3	100	0	30	"
4	75	300	0	Peat
5	113	0	35	Foundation Sand
6	110	0	37	Test Fill Sand
7	121	1398	0	Boston Blue Clay
8	114	1305	0	"
9	114	1172	0	"
11	114	878	0	"
13	114	653	0	"
14	114	848	0	"
15	114	1128	0	"
16	121	1915	0	"
18	121	1397	0	"
19	114	1160	0	"
21	114	839	0	"
22	120	0	40	Till
24	114	990	0	Boston Blue Clay
25	114	946	0	"
26	114	1137	0	"

1.1 x FIELD VANE STABILITY ANALYSIS
SOIL PROPERTIES FOR FIGURE 2-

TABLE 2-6

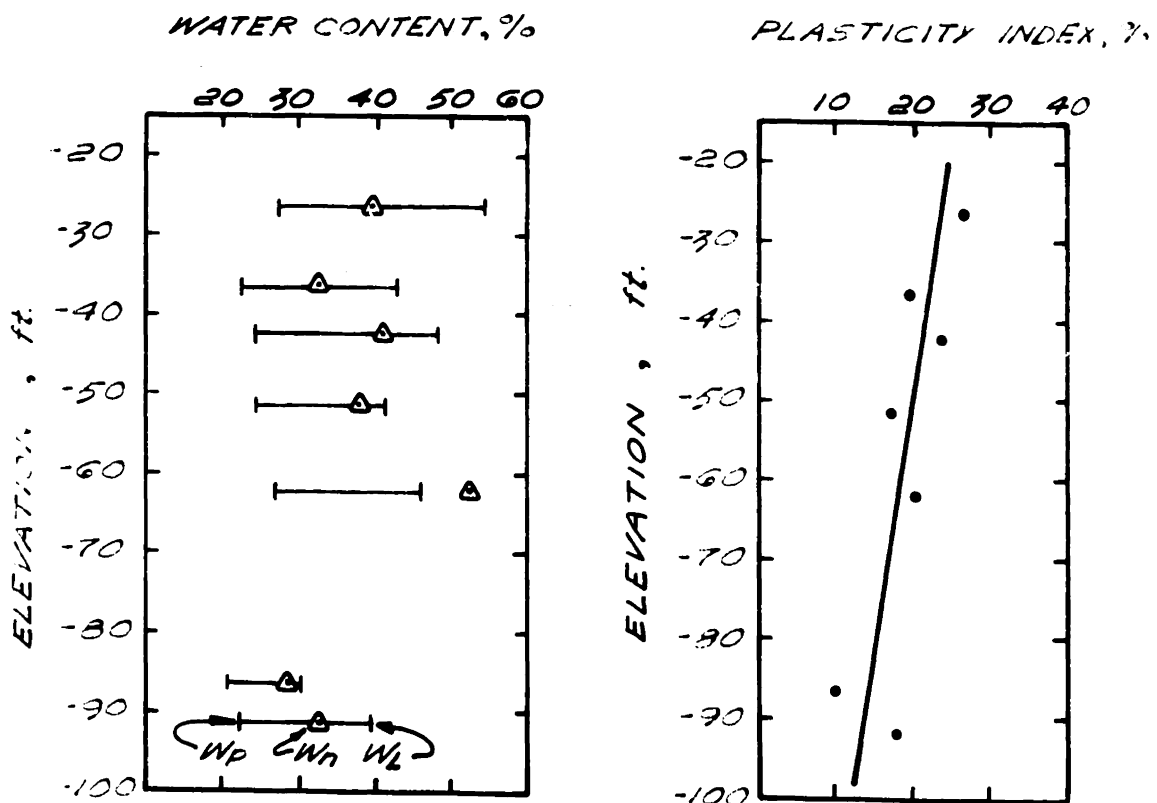
TABLE 2-7
SHANSEP UNDRAINED STRENGTH FOR BOSTON BLUE CLAY
I-95 STA. 263

ALL UNITS: ft., lbs.				PSA			OSS	
OFFSET	ELEV.	$\bar{\sigma}_{vc}$	OCR	$q_f/\bar{\sigma}_{vc}$	q_f	T_{ff}	$T_h/\bar{\sigma}_{vc}$	T_h
					$\theta = 45^\circ$	$\theta = 60^\circ$		$\theta = 0 \pm 20^\circ$
55'W ↓ 44'E	-12.5	5000	1.75	0.51	2544	2150		
	-20	5100	1.57	0.47	2400	2000		
	-30	4550	1.54	0.46	2090	1750		
	-40	4140	1.35	0.42	1735	1520		
	-50	3800	1.13	0.37	1405	1270		
	-60	3700	1.0	0.34	1260	1100		
	-70	4150	1.0	0.34	1410	1230		
	-80	4700	1.0	0.34	1600	1400		
	-90	6000	1.0	0.34	2040	1785		
40'E ↓ 30'E	-12.5	3900	2.24	0.625	2440	2040	1.6	1200
	-20	3950	2.02	0.57	2250	1885	1.1	1330
	-30	3720	1.88	0.54	2010	1685	0.6	1060
	-40	3600	1.55	0.46	1655	1390	0.3	1080
	-50	3500	1.23	0.39	1365	1190	0.24	840
	-60	3440	1.09	0.36	1240	1085	0.22	755
	-70	3880	1.0	0.34	1320	1150	0.20	775
	-80	4700	1.0	0.34	1600	1400	0.20	940
	-87	6300	1.0	0.34	2140	1870	0.20	1260

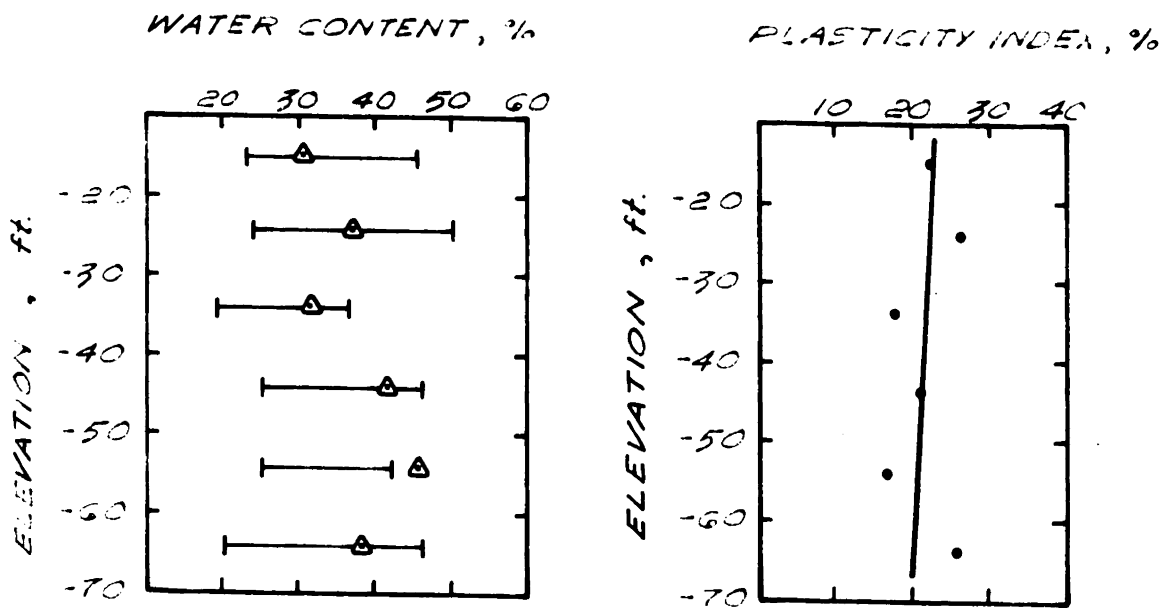
TABLE 2-7 (CONT.)

ALL UNITS: ft., lbs.				DSS		PSP		
OFFSET	ELEV.	$\bar{\sigma}_{vc}$	OCR	$T_h/\bar{\sigma}_{vc}$	T_h	$q_f/\bar{\sigma}_{vc}$	q_f	T_{ff}
					$\theta = 0 \pm 20^\circ$		$\theta = 45^\circ$	$\theta = 60^\circ$
90'E ↓ 140'E	-12.5	750	18.7	1.6	1200	2.02	1515	1200
	-20	1200	10.0	1.11	1330	1.34	1610	1280
	-30	1770	3.98	0.60	1060	0.665	1175	935
	-40	2300	2.18	0.39	900	0.40	920	730
	-50	2820	1.42	0.275	775	0.265	745	590
	-60	3330	1.20	0.24	800	0.22	735	585
	10' above fill	4100	1.0	0.20	820	0.19	780	620
	5' above fill	4500	1.0	0.20	900	0.19	855	680
>140'E	12.5	750	18.7	1.6	1200	2.02	1515	1200
	-20	1200	10.0	1.11	1330	1.34	1610	1280
	-30	1770	3.98	0.60	1060	0.665	1175	935
	-40	2300	2.18	0.39	900	0.40	920	730
	-50	2820	1.42	0.275	775	0.265	745	590
	-60	3330	1.20	0.24	860	0.22	735	585
	-70	3850	1.035	0.205	790	0.195	750	595

CENTERLINE

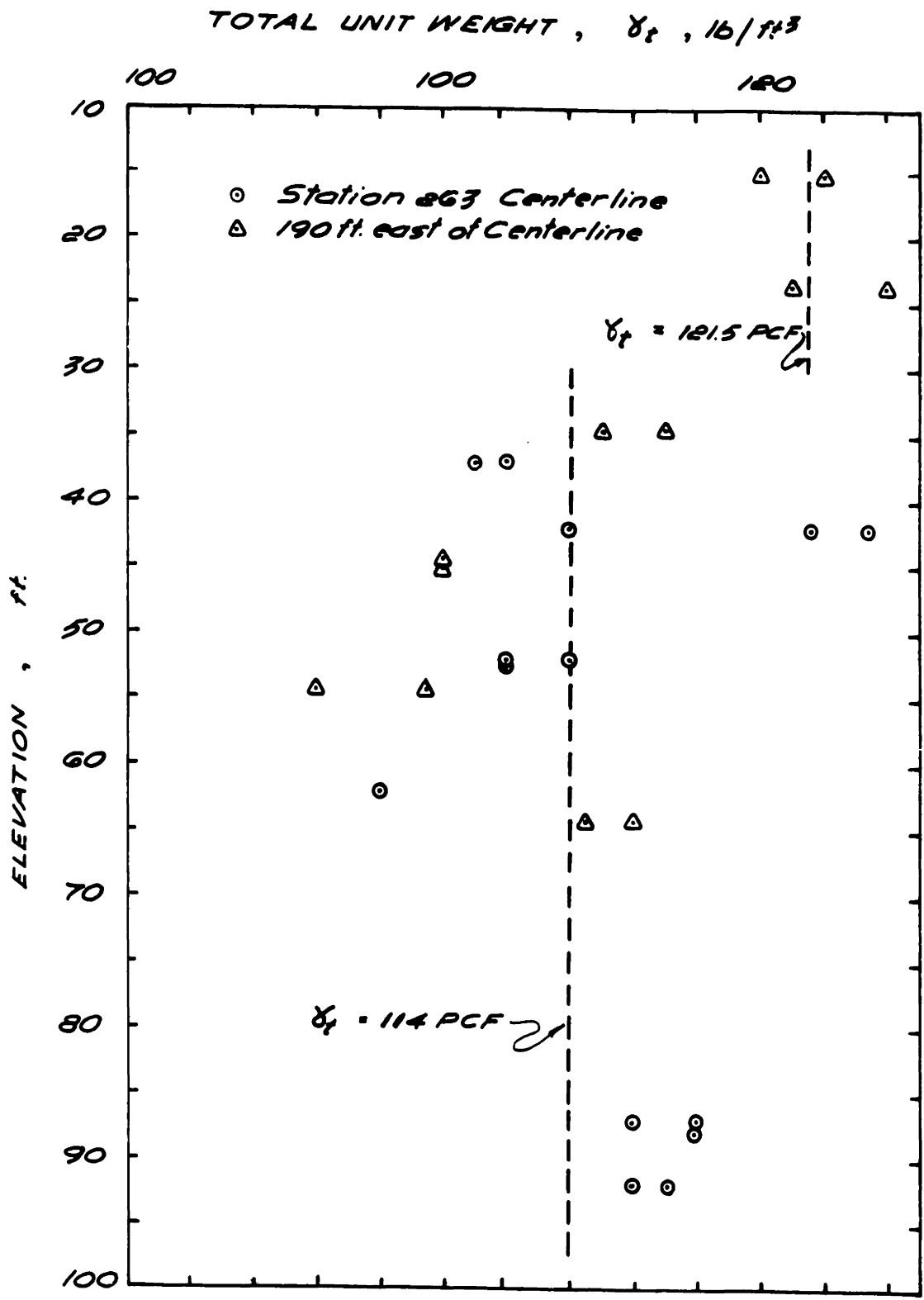


190' EAST OF CENTERLINE



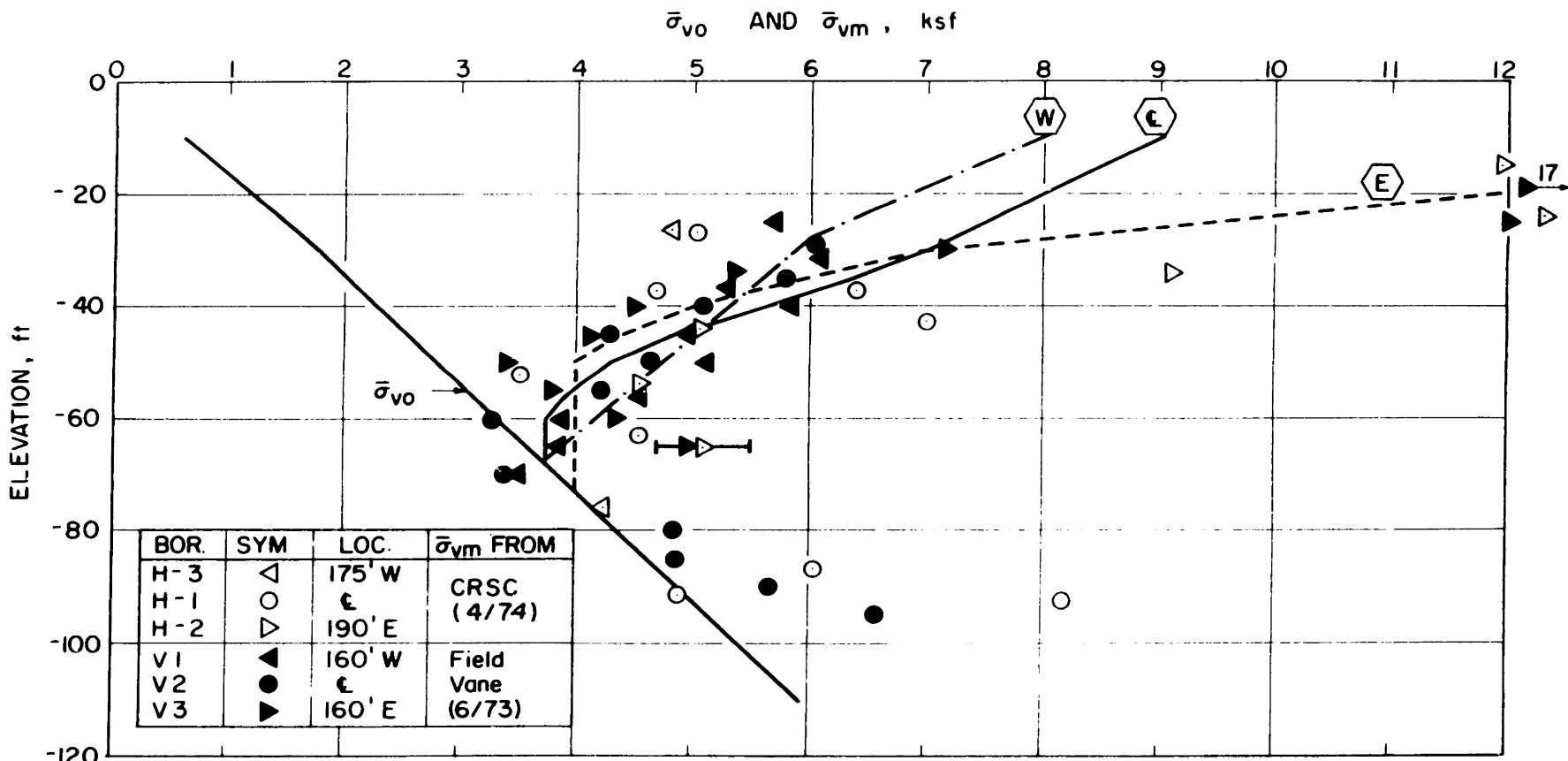
STATION 263 - ATTERBERG LIMITS VS ELEVATION

FIGURE 2-1



STATION 263 - UNIT WEIGHT VS ELEVATION

FIGURE 2-2

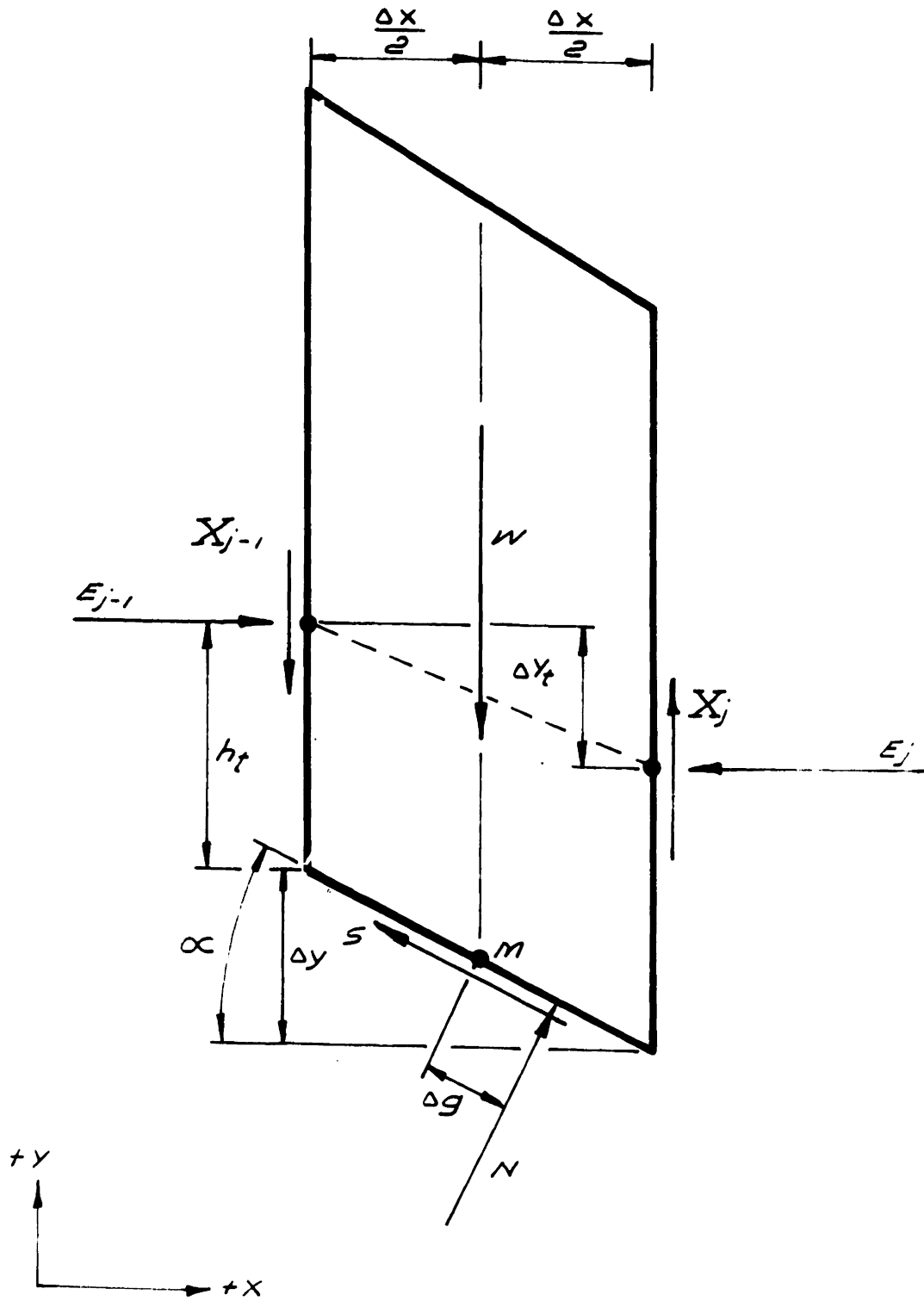


STRESS HISTORY, I - 95
 STATION 263 (FROM LADD, 1975)

Selected values of preconstruction $\bar{\sigma}_{vm}$

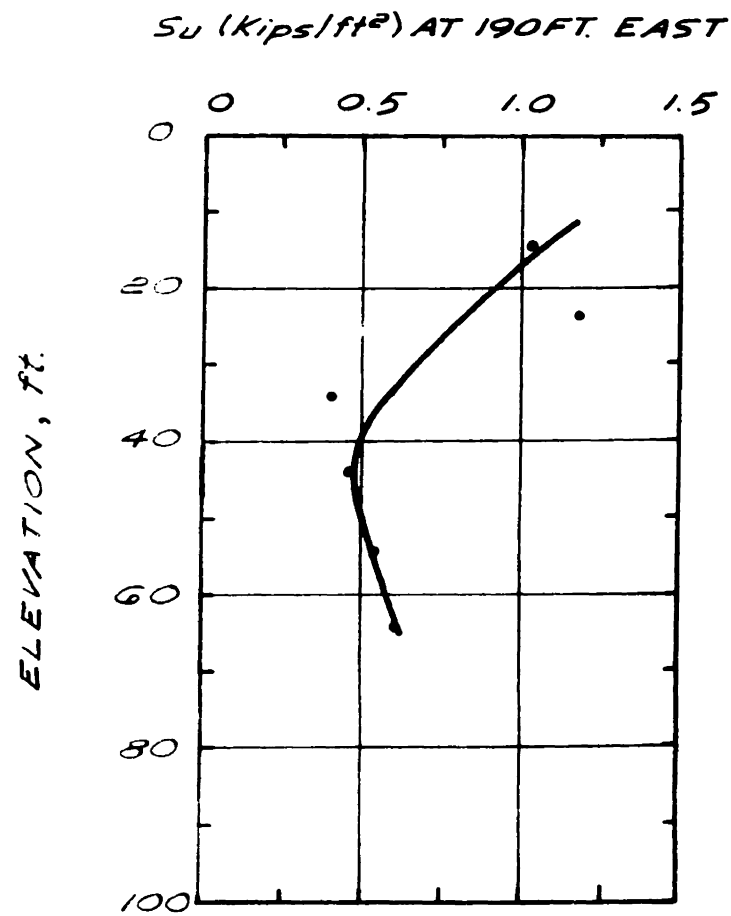
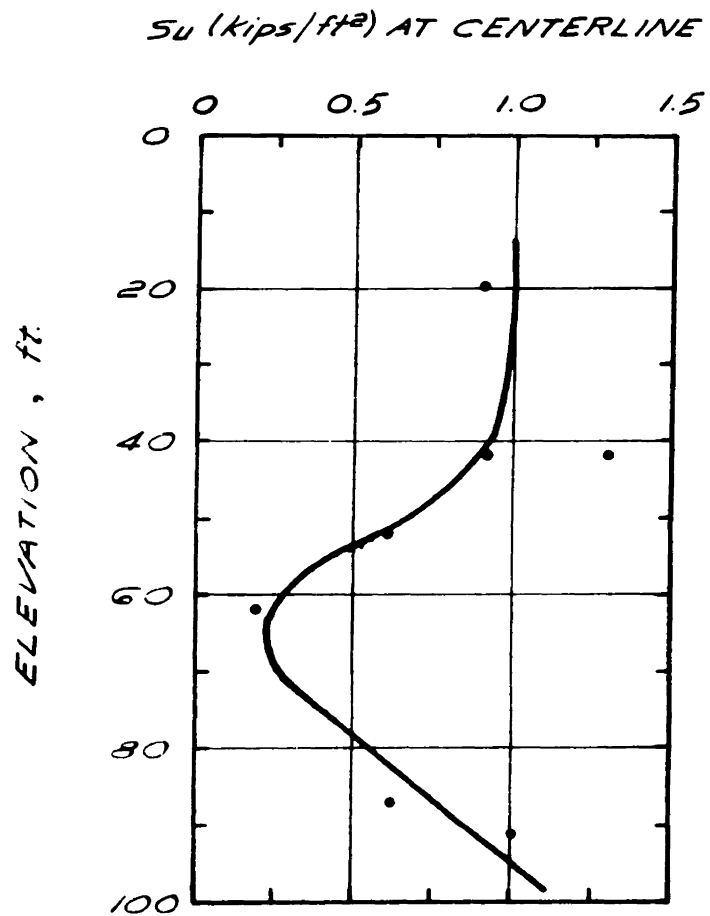
- (W) --- Beyond 50' West
- (ε) --- Centerline ± 50'
- (E) --- Beyond 50' East

FIGURE 2-3



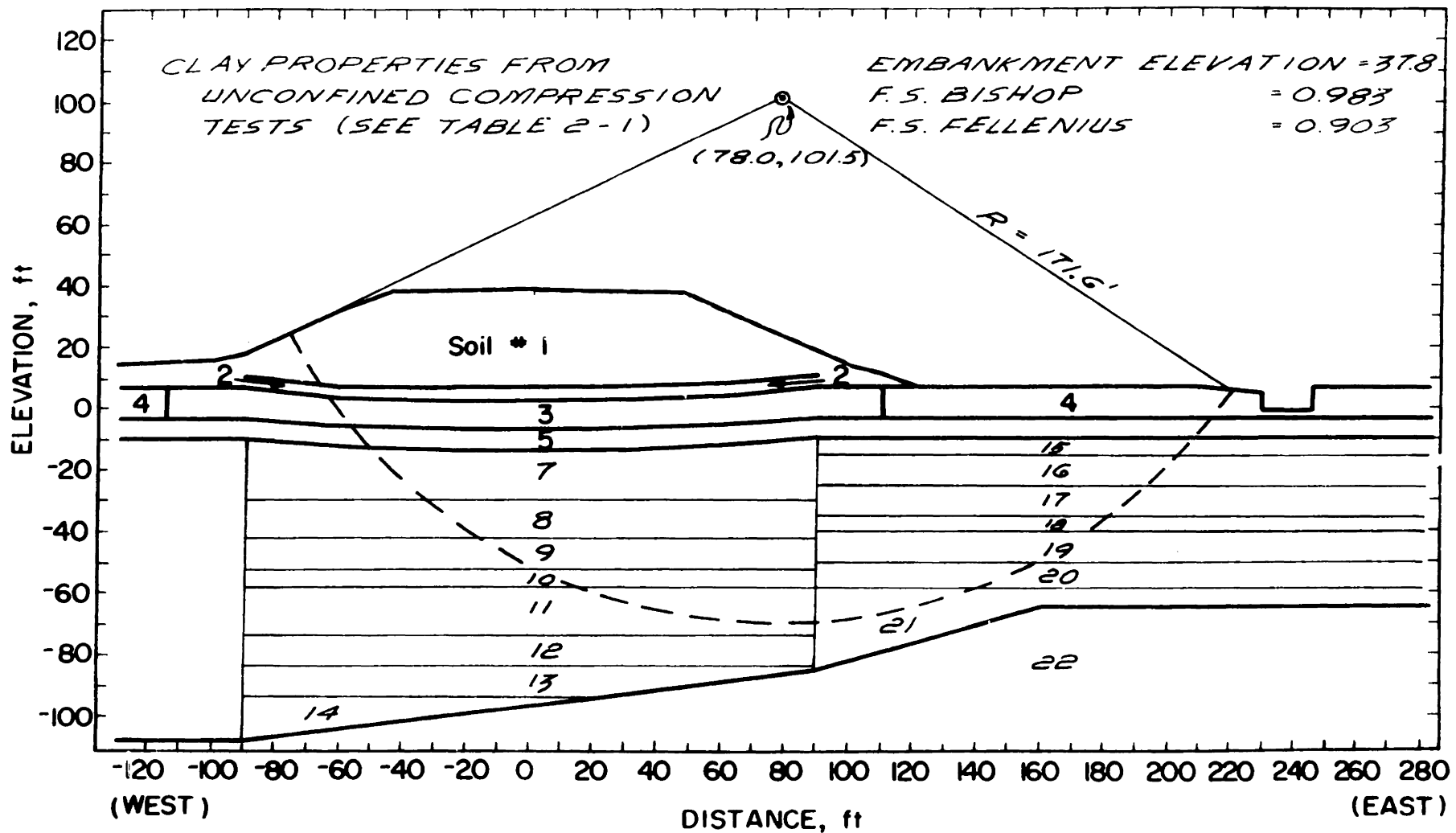
FORCES AND LOCATIONS INCLUDED IN THE EQUILIBRIUM OF AN INDIVIDUAL SLICE

FIGURE 2-4

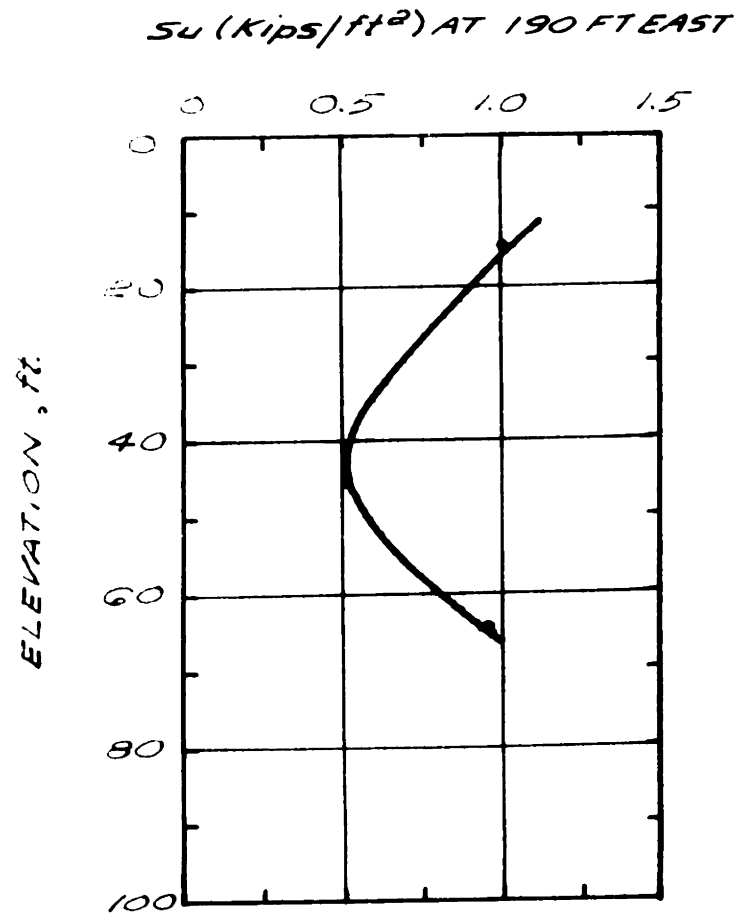
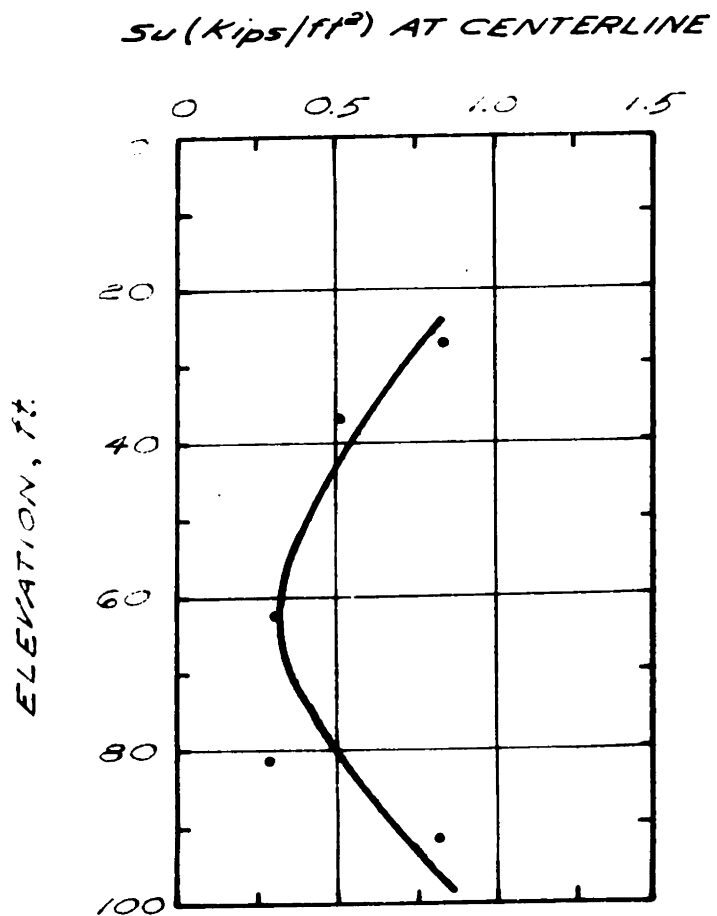


**UNCONFINED COMPRESSION SHEAR STRENGTHS
AT CENTERLINE AND 190 FT EAST FOR STABILITY
ANALYSES, I-95 STATION 263**

FIGURE 2-5

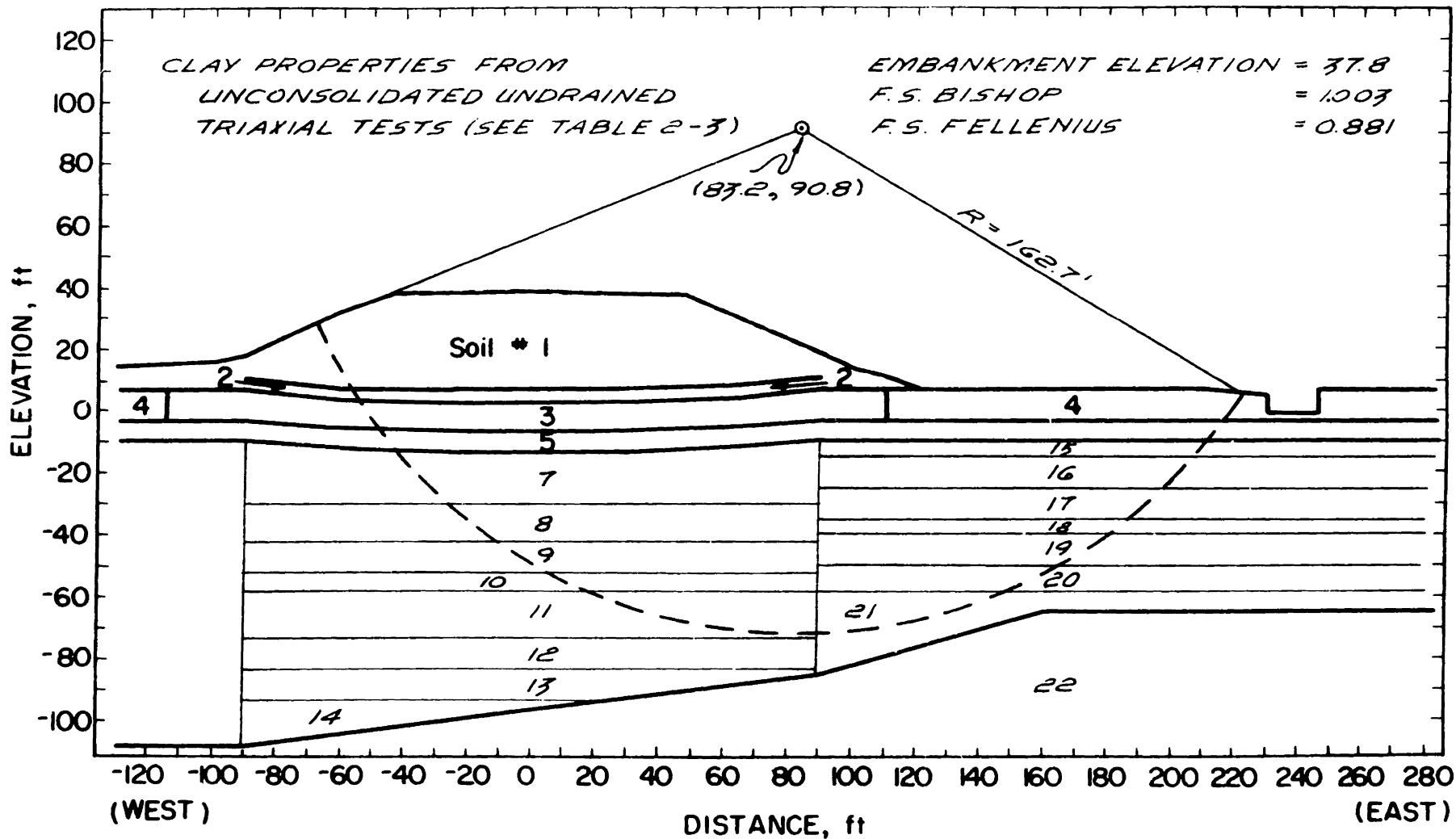


STABILITY ANALYSES I - 95 STATION 263
 FIGURE 2-6



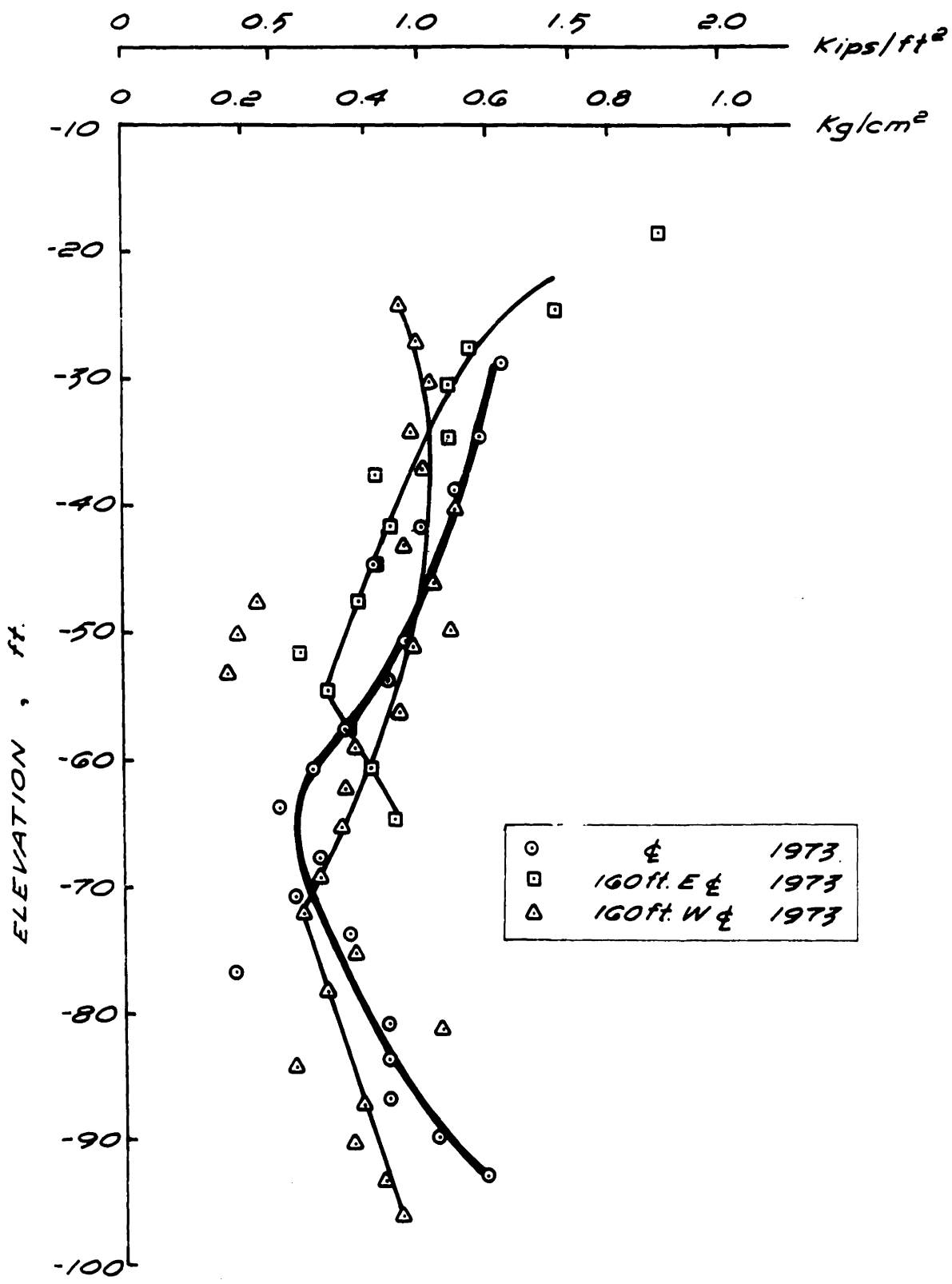
**UNCONSOLIDATED - UNDRAINED SHEAR STRENGTHS
AT CENTERLINE AND 190 FT EAST FOR STABILITY
ANALYSES, I-95 STATION 263**

FIGURE 2-7



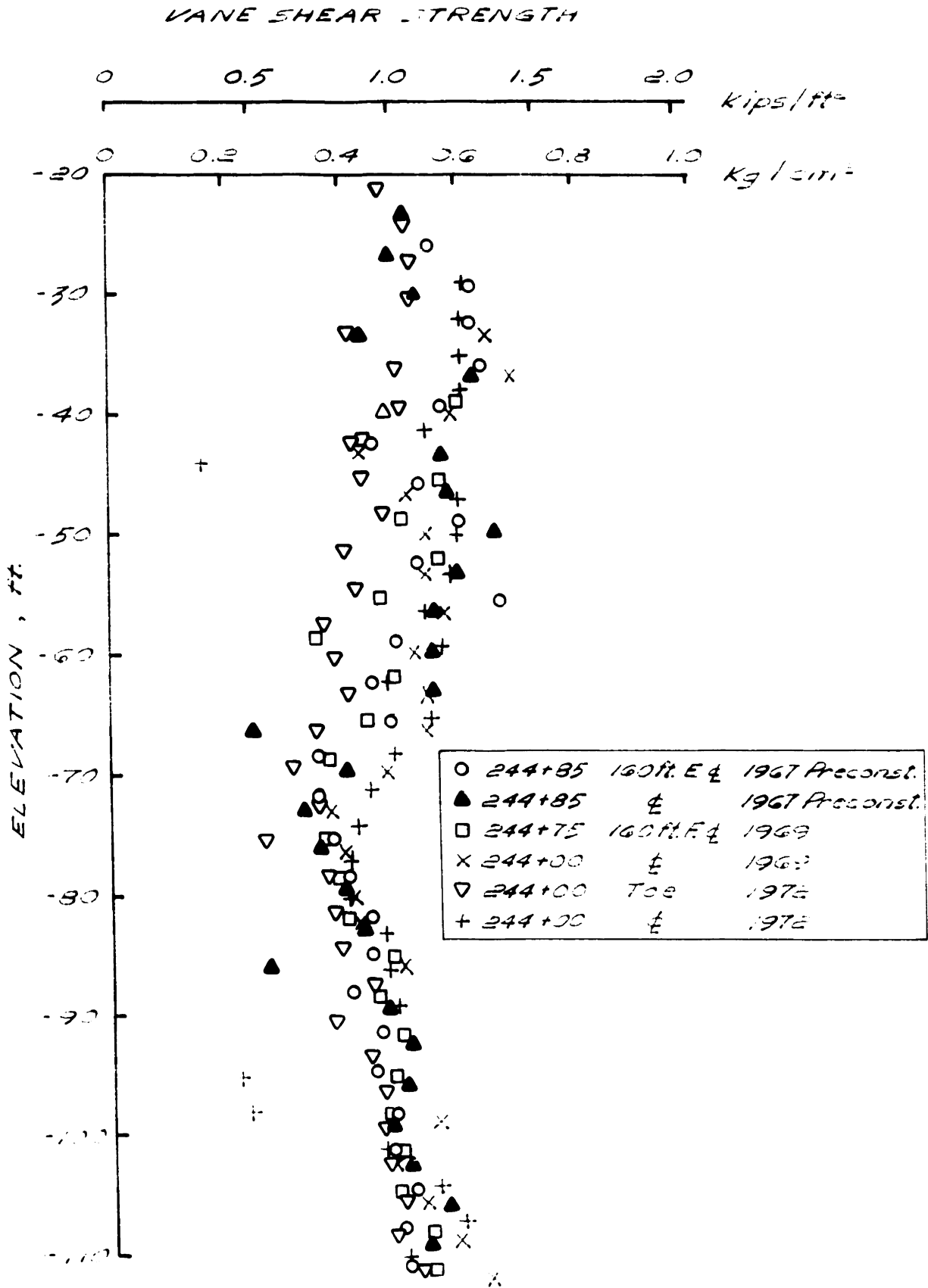
STABILITY ANALYSES I-95 STATION 263
FIGURE 2-8

VANE SHEAR STRENGTH

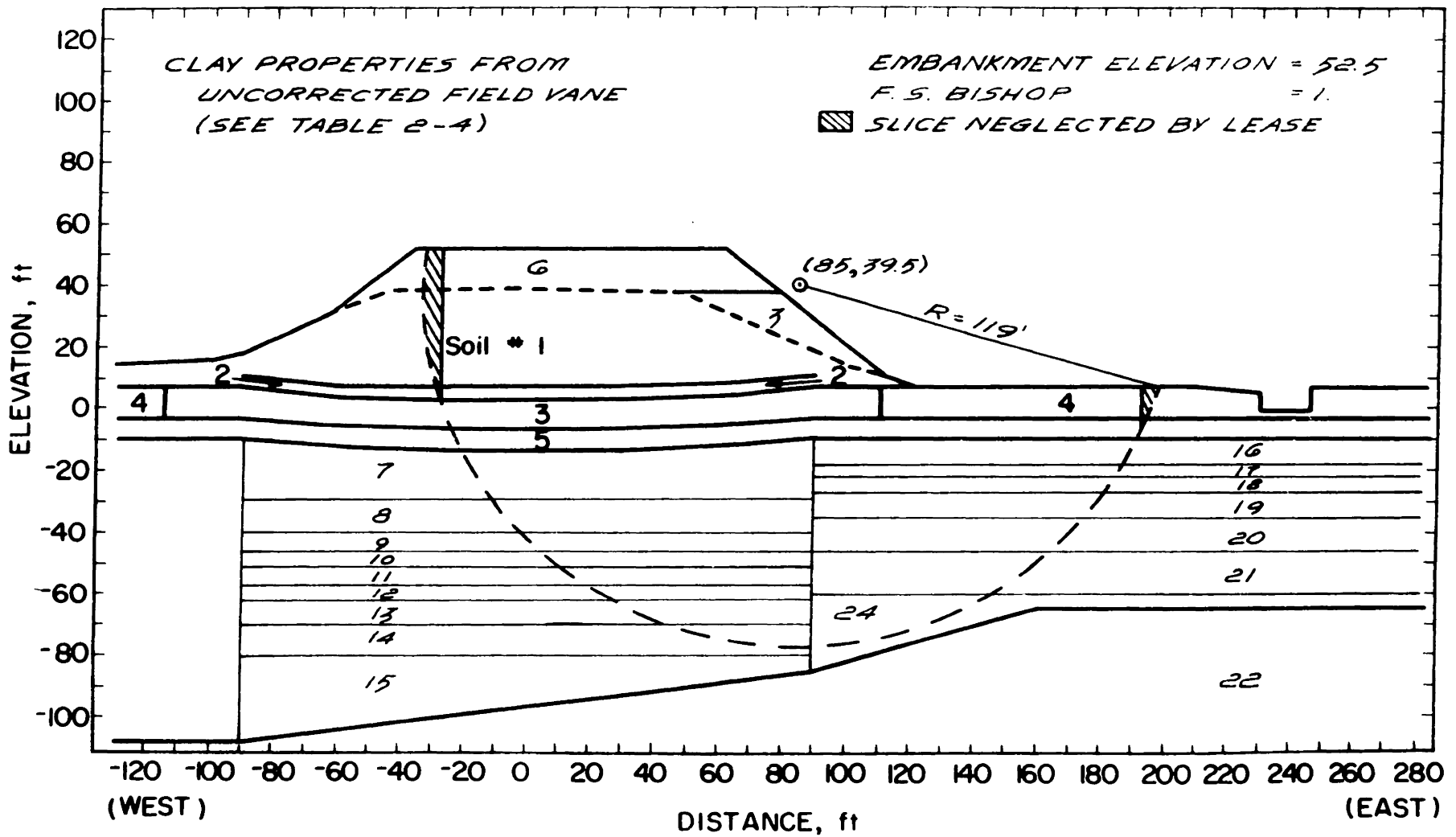


FIELD VANE TESTS AT TEST SECTION 263

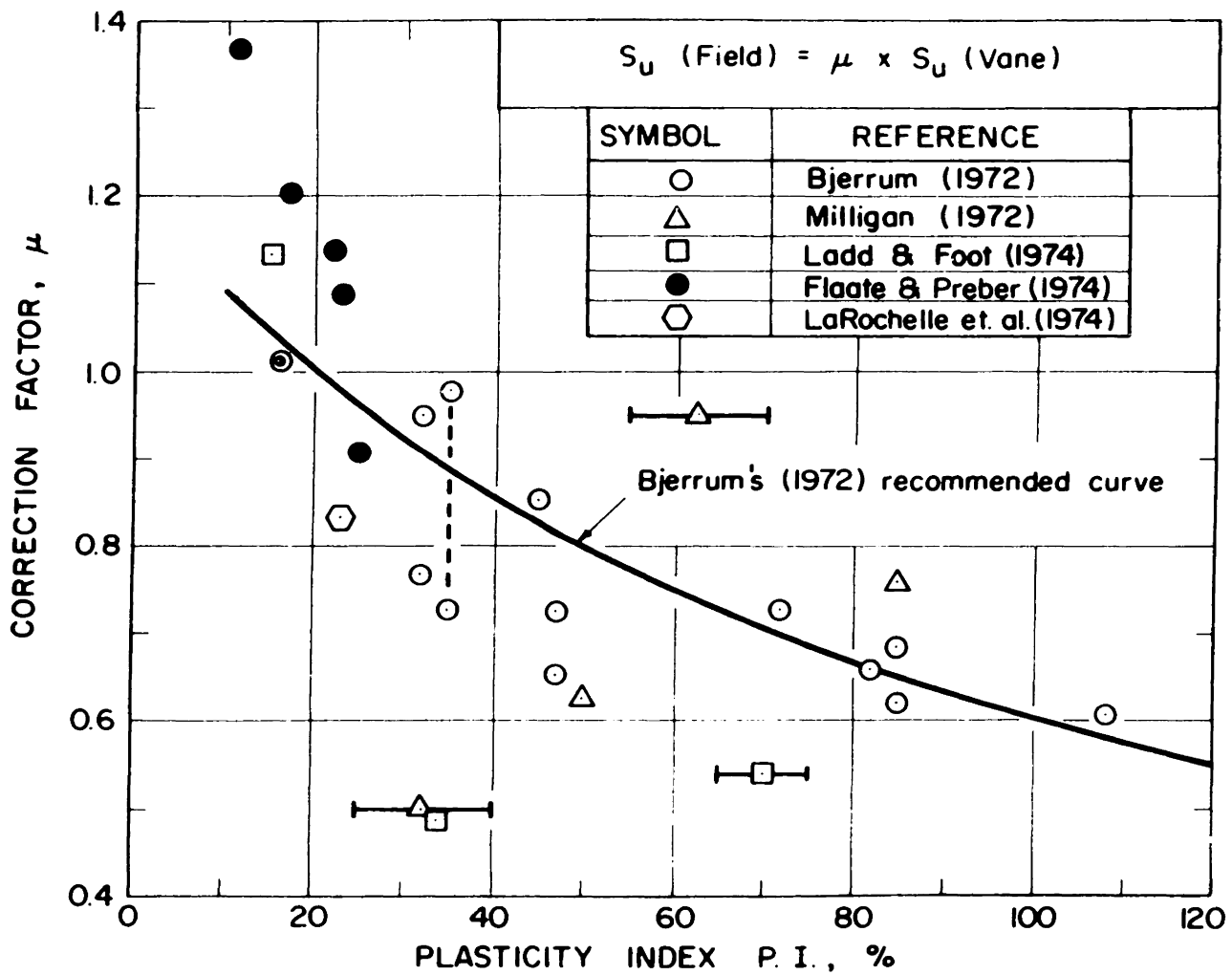
FIGURE 2-9



FIELD VANE TESTS AT THE MIT-MDPW TEST SECTION
FIGURE 2-10

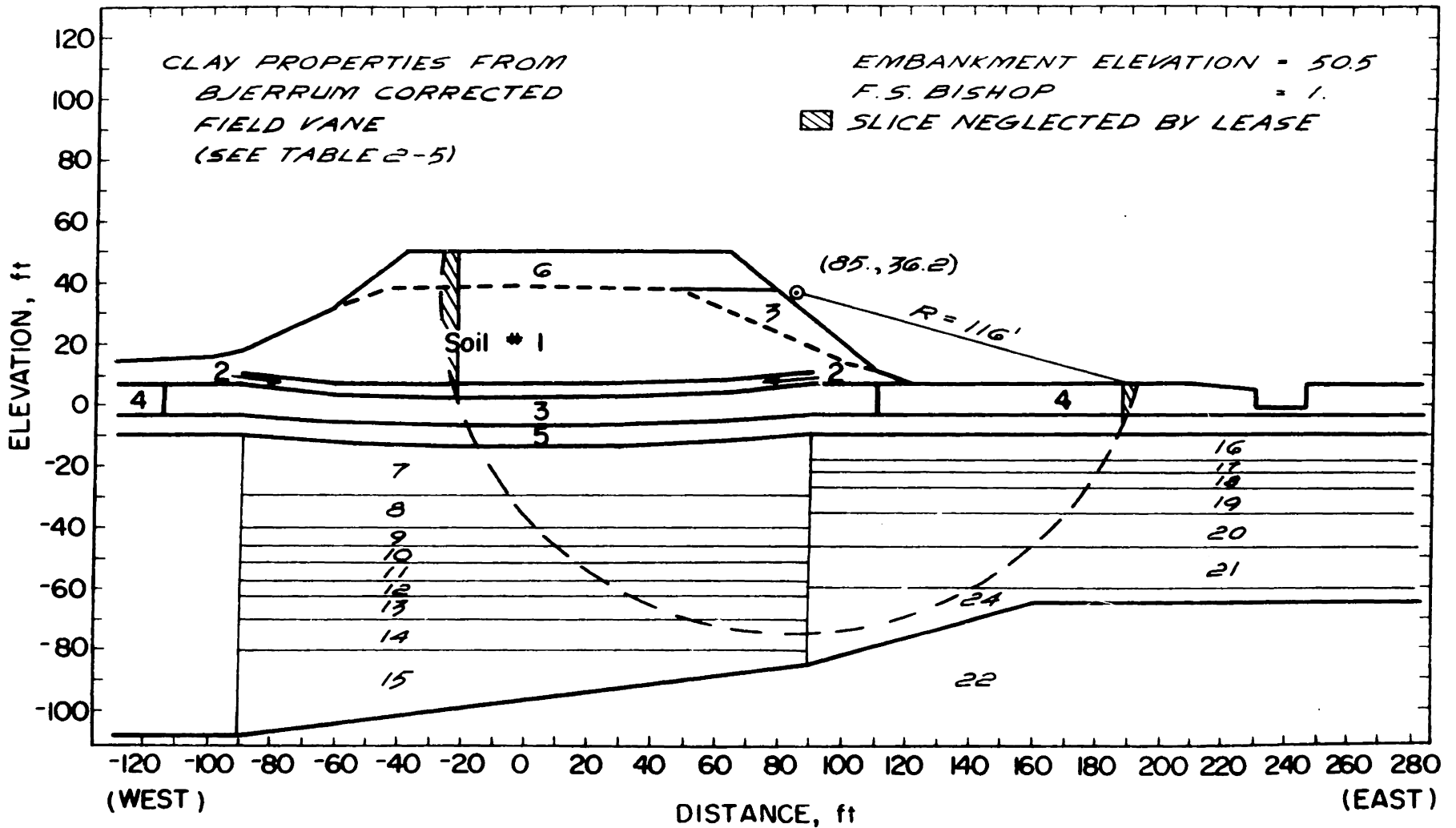


STABILITY ANALYSES I-95 STATION 263
FIGURE 2-11

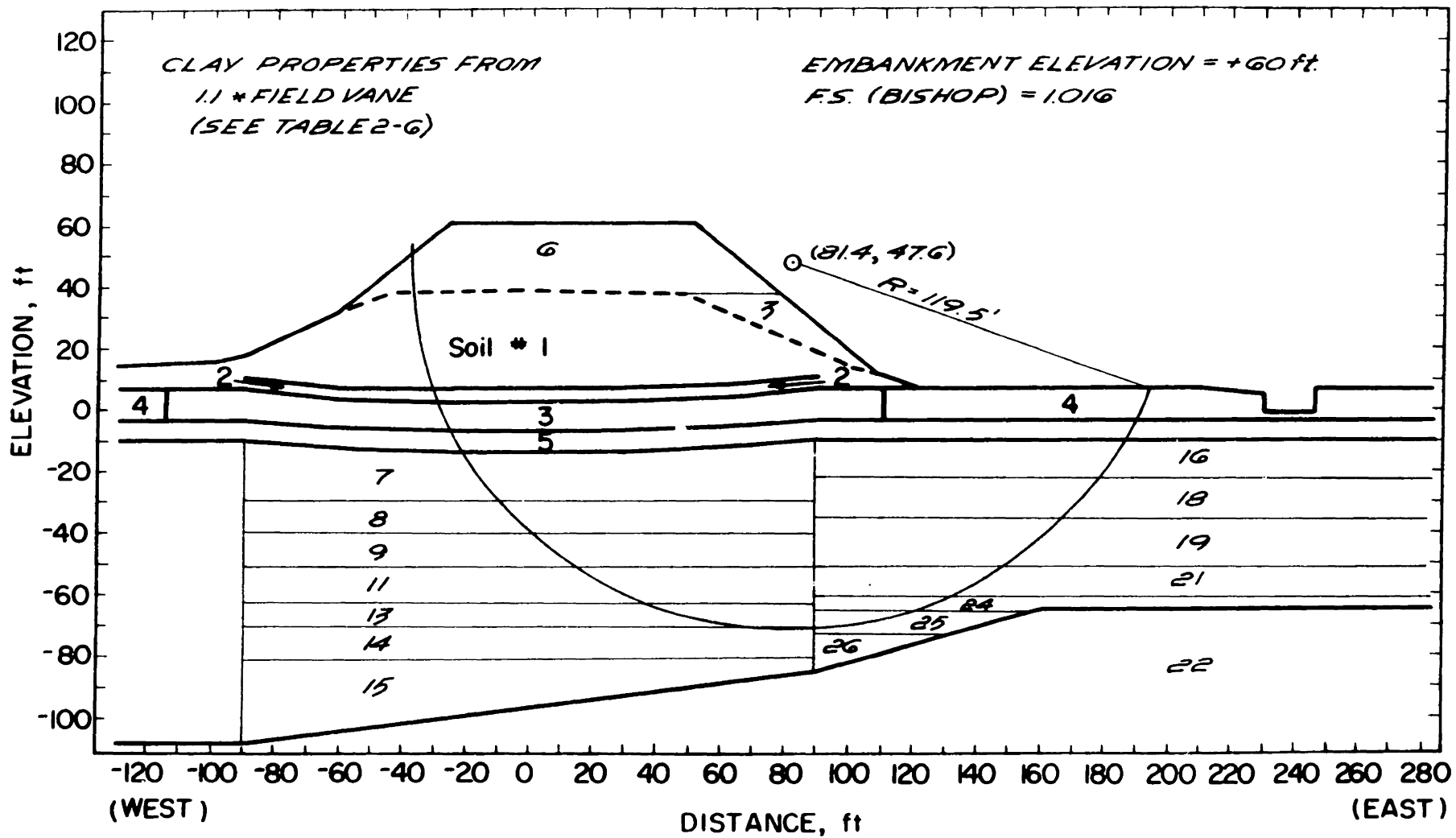


FIELD VANE CORRECTION FACTOR VS. PLASTICITY INDEX DERIVED FROM
EMBANKMENT FAILURES (FROM LADD, 1975)

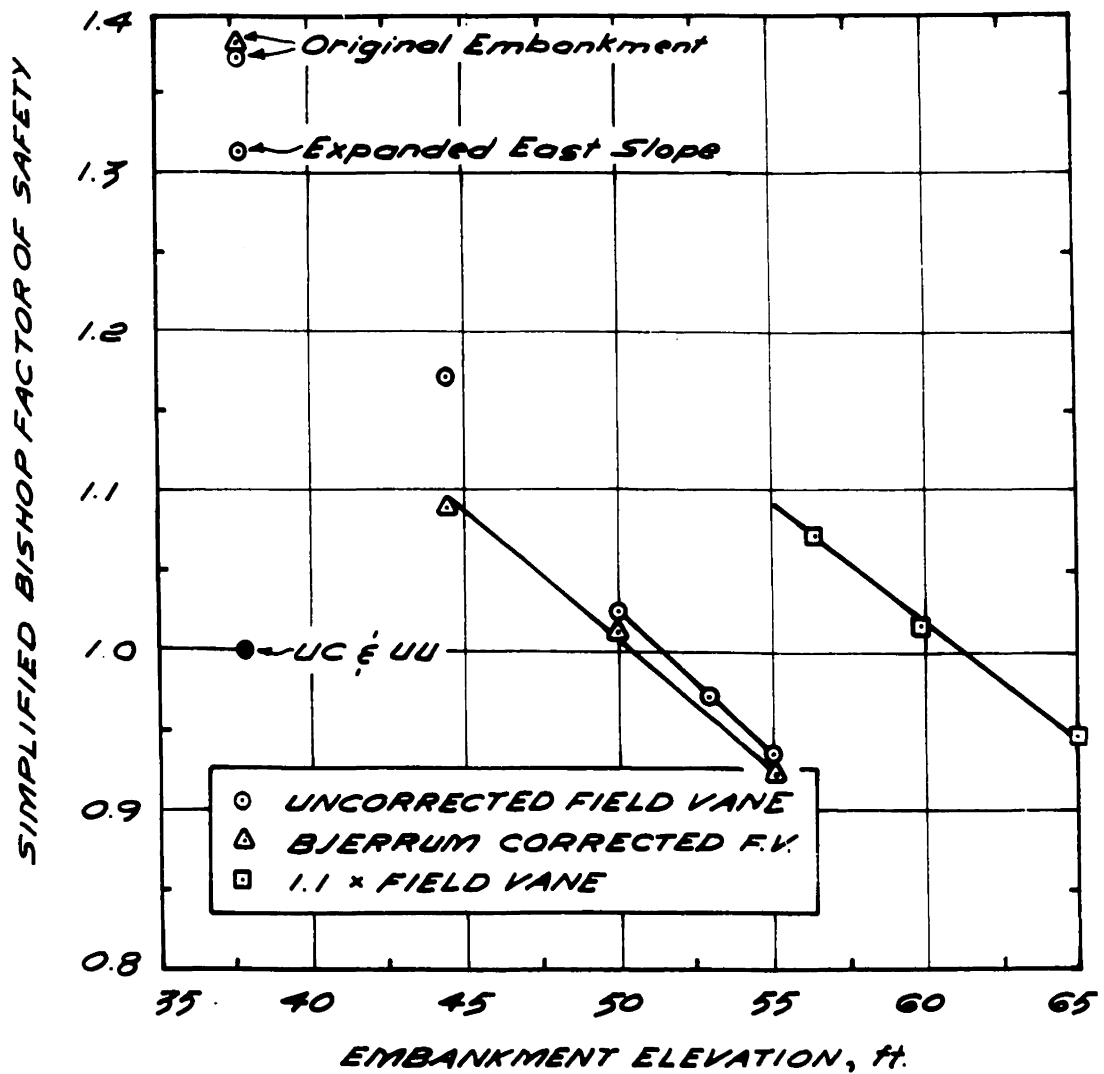
FIGURE 2-12



STABILITY ANALYSES I-95 STATION 263
FIGURE 2-13

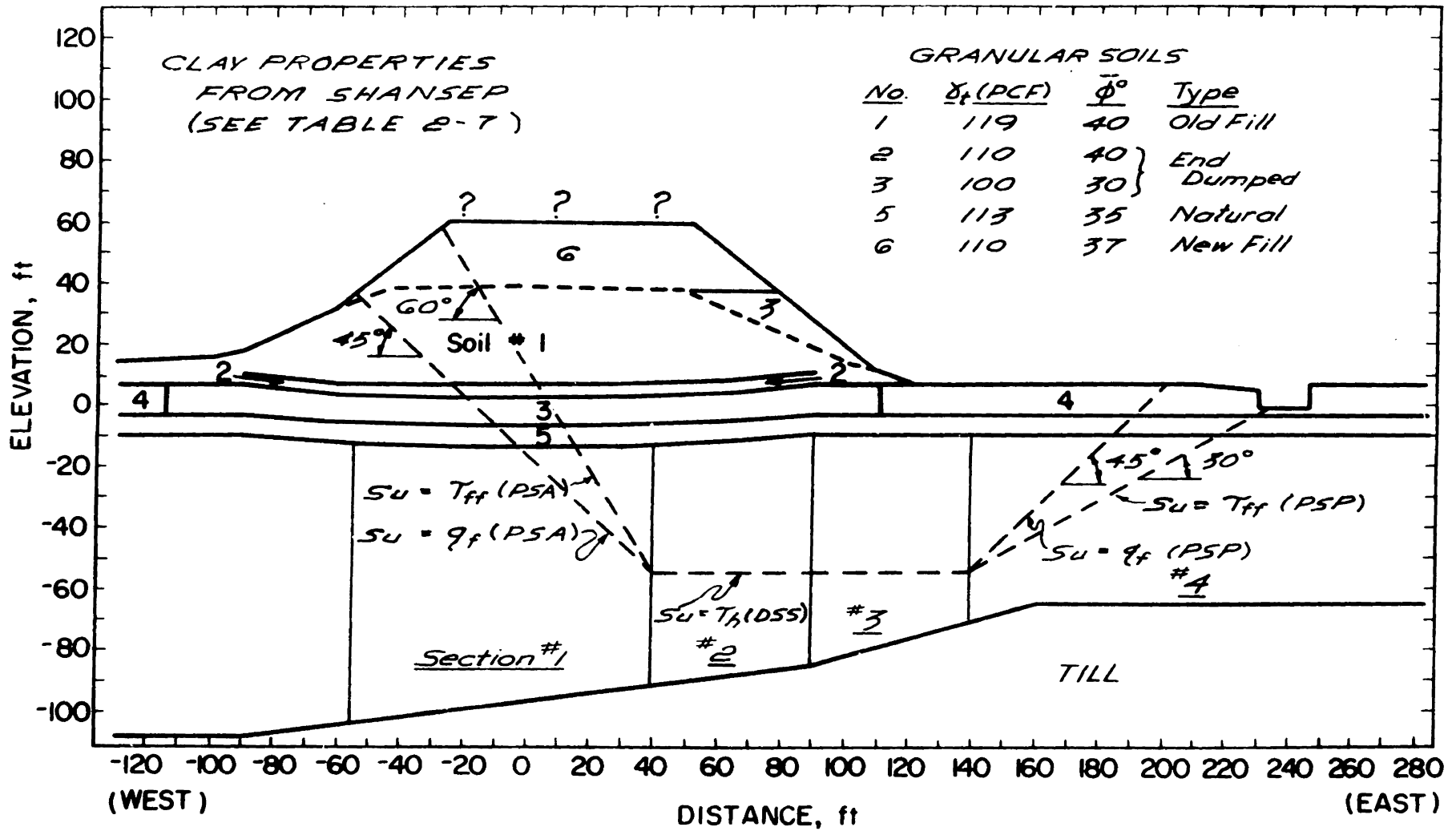


STABILITY ANALYSES I - 95 STATION 263
FIGURE 2-14

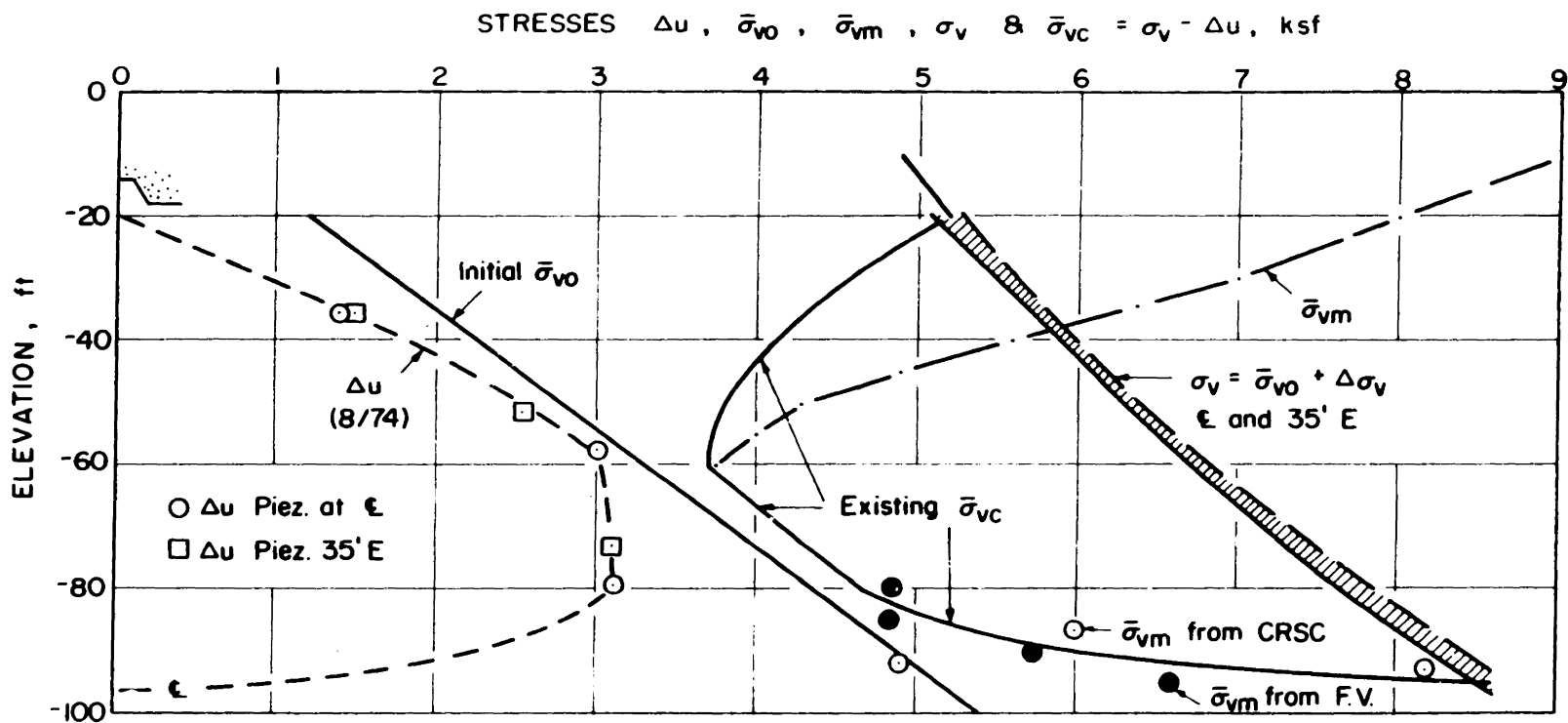


**EMBANKMENT ELEVATION VS FACTOR OF SAFETY
FIELD VANE STABILITY ANALYSIS
I-95 STATION 263**

FIGURE 2-15



STABILITY ANALYSES I-95 STATION 263
 FIGURE 2-16



EVALUATION OF EXISTING STRESSES AUGUST 1974, I-95 STATION 263
CENTERLINE TO 35 FEET EAST (FROM LADD, 1975)

FIGURE 2-17

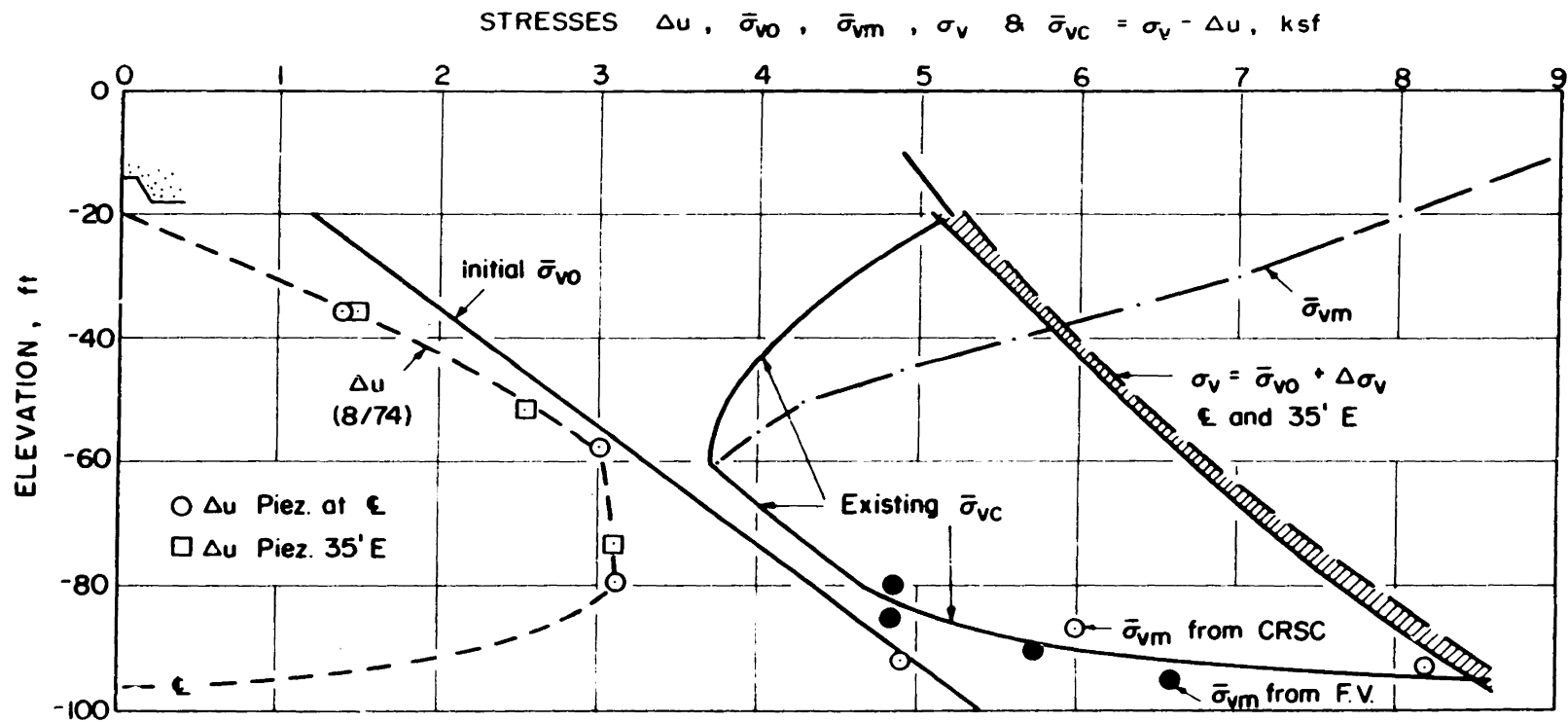
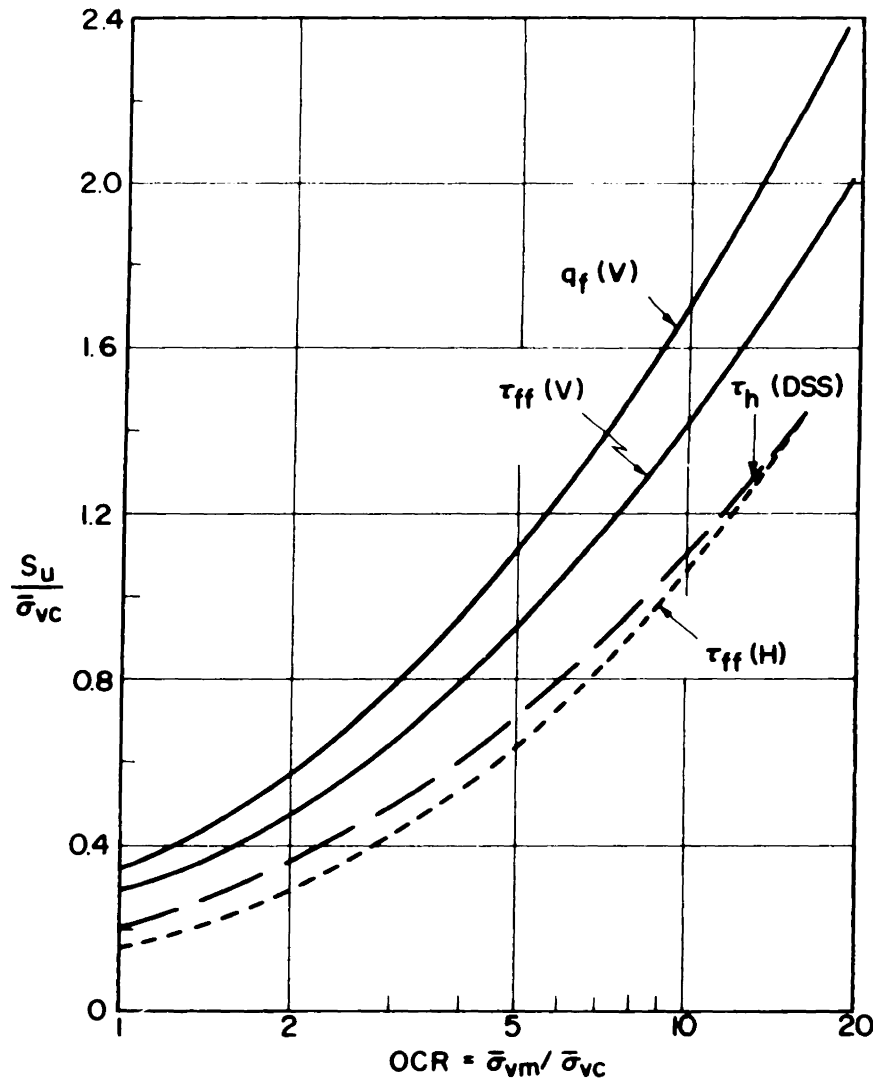


FIGURE 2-17



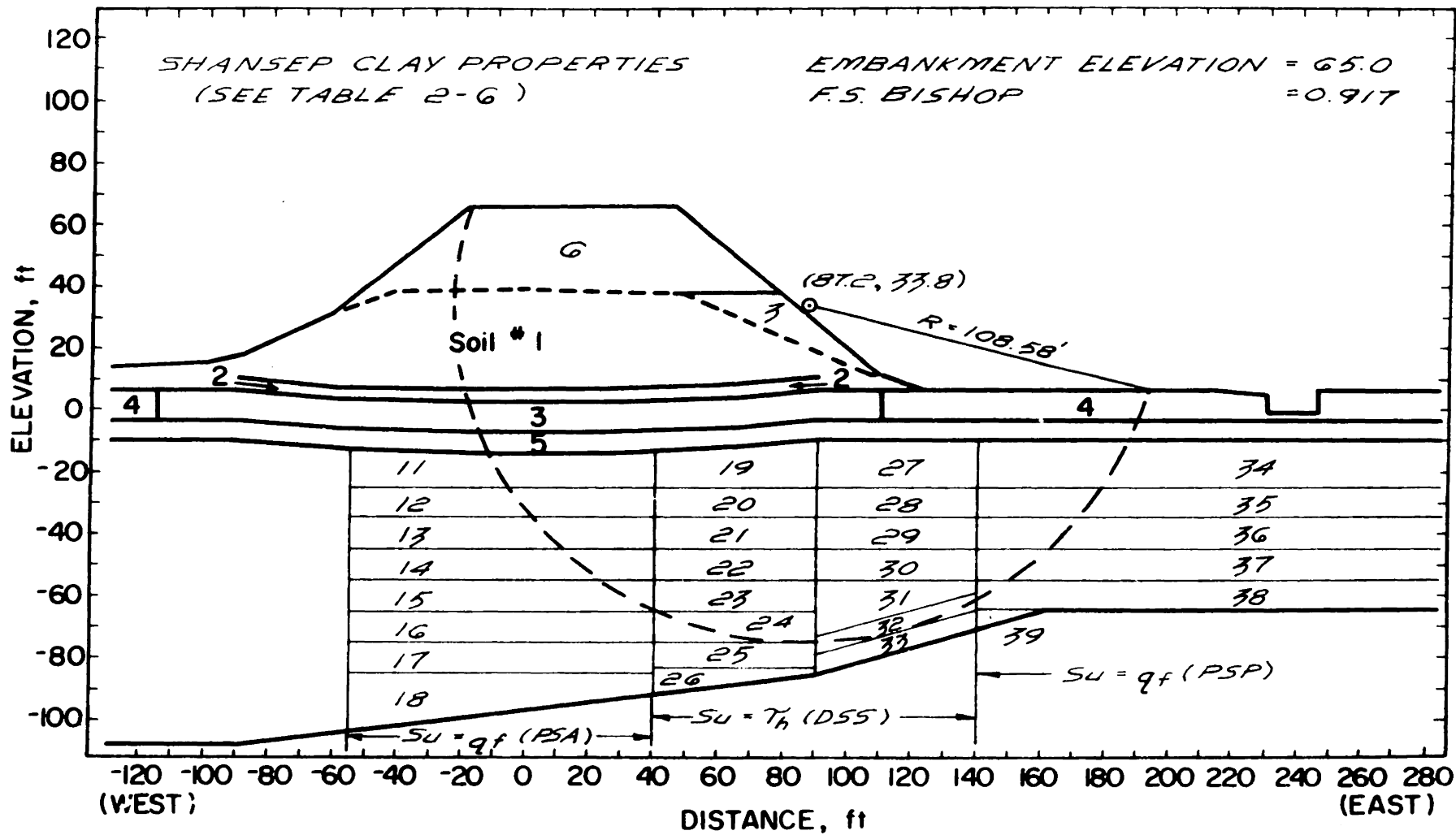
TYPE OF SHEAR	DEFINITION OF S_u	$\bar{\phi}^\circ$	SYMBOL
Plane strain (V) active	q_f ($\theta = 45^\circ$)	—	—
	τ_{ff} ($\theta = 60^\circ$)	29-33	—
Direct - simple shear	τ_h (max) ($\theta = 0 \pm^\circ$)	—	—
Plane strain (H) passive	τ_{ff} ($\theta = 30^\circ$)	37.5	---

- Notes : (1) $q_f = 0.5 (\sigma_1 - \sigma_3)_f$
 (2) $\tau_{ff} = q_f \cos \bar{\phi}$
 (3) θ = angle between failure plane and horizontal

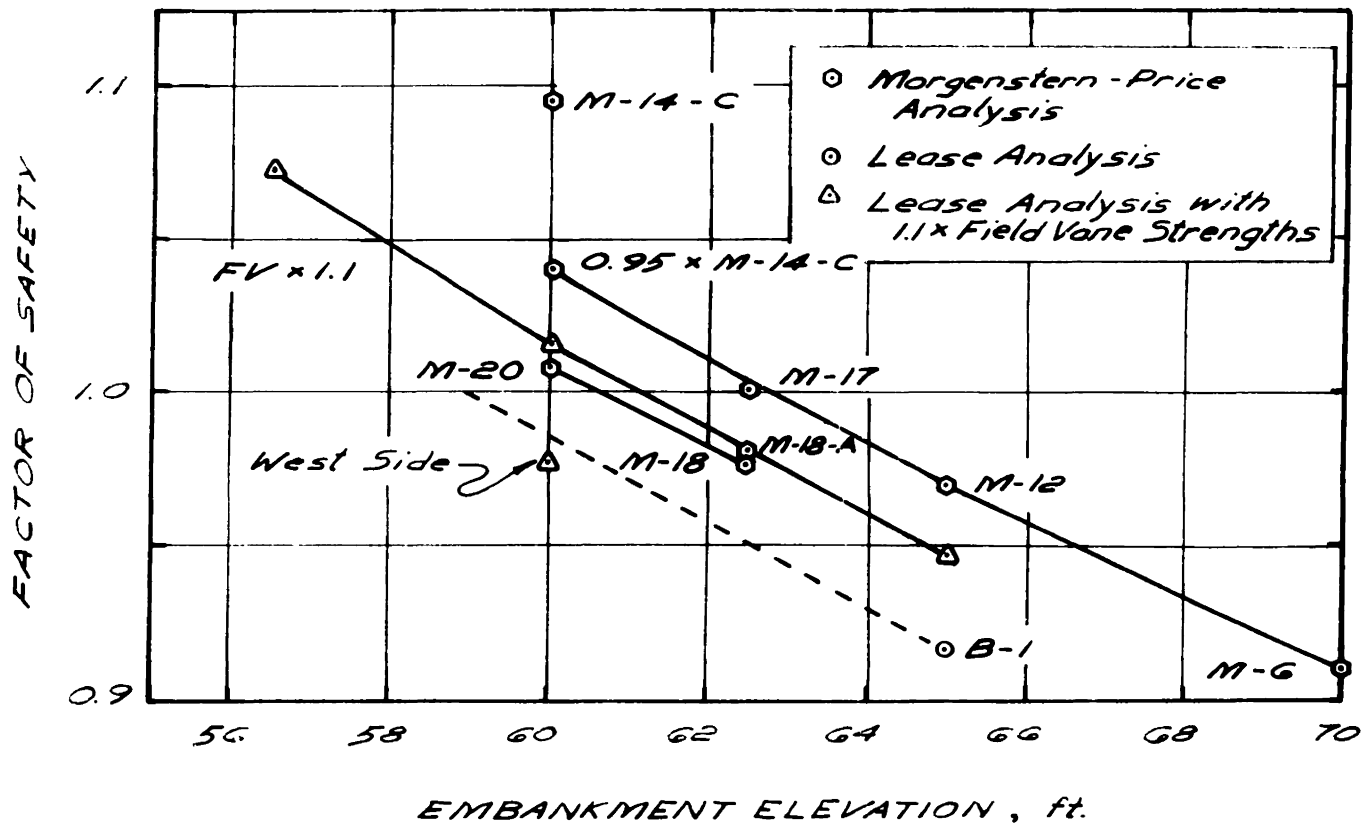
Data from Ladd et. al. (1971) and Ladd and Edgers (1972)

FIGURE 2-18

UNDRAINED STRENGTH RATIO VS. OCR FOR TOTAL STRESS M-P STABILITY ANALYSES WITH BOSTON BLUE CLAY (FROM LADD, 1975)



STABILITY ANALYSES I-95 STATION 263
FIGURE 2-19



RESULTS OF STABILITY ANALYSES BASED ON SHANSEP

FIGURE 2-20

3.1 Field Instrumentation and Exploration at the Test Section

The original construction control instrumentation at station 263 consisted of 3 hydraulic piezometers, one settlement plate and four inclinometers. None of the piezometers were working by June 1970 and one of the inclinometers was filled with sand by vandals. Part of the preparation for the field test was to replace inoperative instruments, install new ones at selected locations and conduct a field exploration program to obtain samples of the foundation material for testing.

The inoperative piezometers, P-14-A, P-14-B, P-14-C, were replaced in July 1973 by P-3, P-4 and P-5 respectively. At that time four additional piezometers were installed (P-1, P-2, P-6 and P-7). During the Spring of 1974 the sand in inclinometer SI-1 was washed out, the rest of the piezometers, inclinometers and settlement plates were installed and a grid of stakes to measure surface displacements was established. Table 3-1 summarizes the field instrumentation installed at the test section prior to the start of loading and the instrument locations are shown in Figures 3-1, 3-2 and 3-14. The 3.89 feet of settlement of SP-1 measured since the start of the original construction have been considered in determining its sensor elevation.

The piezometers were single lead Geonor A/S M-206 instruments and most were fitted with bourdon gauges to obtain quick response and to measure the high pore pressures expected. Whenever the piezometric water elevation was below ground level,

readings were obtained with capillary or electric probes. The piezometers were read twice daily through the field test. The inclinometers were aluminum Wilson Slope Indicators. They were read with a Wilson Manual torpedo and with the Beaver System, an automatic recording accelerometer developed at M.I.T. and described by Bromwell et al (1971). The stakes for the surface grid were set in concrete about 2 feet into the peat layer. As with the settlement plates, readings were obtained by optical surveys performed by the Massachusetts Department of Public Works.

In April, 1974, 5 inch fixed piston samples were obtained from borings H-1 and H-2 shown in Figure 1-3. Atterberg Limits, UC and CRSC tests reported in this thesis were run on the samples from H-1 and H-2. Additionally, boring H-2 provided one more determination of the till surface. The known elevations for the top of the till are as follows:

Location	Elevation (ft).
SI-1	-109
SI-2	-108
SI-3	-87
SI-4	-65
SI-5	-87
SI-6	-79.5
Boring H-2	-68

3.2 Field Test Construction Sequence

The loading operation began on 26th of August, 1974 with the steepening of the embankment east slope to an angle of 40°. The embankment was then raised in lifts of about one feet. Fill was carried by trucks from station 246 and spread by bulldozer

on rubber tired loader at the test section. The only compaction was that provided by the construction equipment. Figure 3-3 shows the progress of the fill movement which proceeded at an average rate of 1.5 feet per day, excluding weekends.

3.3 FIELD MEASUREMENTS

3.3.1 Pore Pressures

Pore Pressure data for the initial embankment construction (crest elevation = +40 feet) are shown in figure 3-4. Figures 3-5 through 3-9 present the data obtained during the field test. The computation of excess pore pressure is based on a water table elevation of +2.5 feet and an artesian pressure in the till of 5 feet of water as reported by Whittle (1974).

3.3.2 Settlements and Heave

Figure 3-10 is a plot of settlement v.s. embankment elevation for the four settlement plates located at station 263. Since the surveys were conducted around the middle of the working day, the embankment elevation selected for the settlement and heave plots was the average elevation during the day of the measurement.

Figure 3-11 shows the vertical movement of two heave points at Station 263. The offset for H-1 was 130 feet east and for H-2 183 feet east.

3.4 Failure

Failure occurred on Friday, 20 September, 1974 at about 6:30 A.M. Unfortunately, no one was present to observe the failure take place. Figure 1-1 shows the massive lateral and

longitudinal extension of the embankment failure. A surface examination immediately after the failure indicated cracks and movements on the embankment crest and sides from station 257 to station 267 and 30. Thus failure occurred for a length of 1030 feet! The length of the failure, compared to the 300 feet long loaded section was surprising. To the south of the test section, the embankment crest was at its original 40 ft. elevation minus a settlement of the order of two-to three feet. To the north, however, the 40 ft. high embankment continued only to station 266 after which the embankment elevation decreased to +25 ft.

Failure occurred to both sides as shown in Figure 3-12. A single frame of an unsuccessful time-lapse film made during the failure indicates failure occurring to both sides simultaneously. Also shown in Figure 3-12 are the depths at which the inclinometer ruptured as indicated by probing after the failure and the zones of maximum horizontal strain up to the day before failure. The horizontal strain data was obtained from inclinometer data presented by Hawkes (1975).

The rupture points shown in Fig. 3-12 represent at best an upper boundary for the failure surface. Particularly at SI-4, the inclinometer casing may have separated due to the large heave and the actual failure surface may be deeper than the location shown. The slip circles in the figure represent the best circular arc fit through the locations of inclinometer rupture. The center for the circles were determined by rotating the pre-failure geometry about different points, until a reasonable agreement with the

surface of the failed embankment was obtained.

-69-

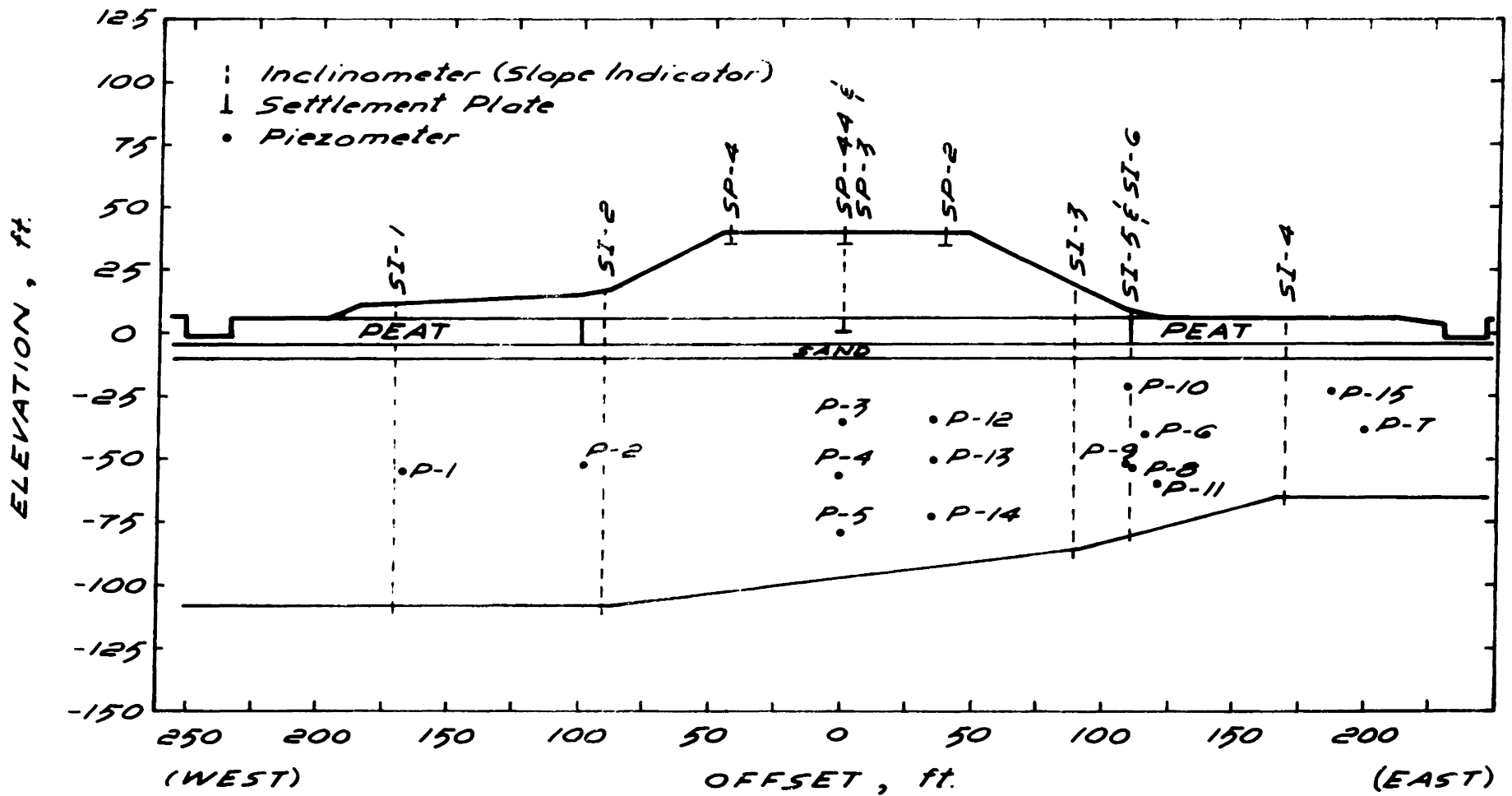
At station 263, the top of the embankment dropped a maximum of about 30 feet. A heave of 14 feet was measured on the east side and 10 feet on the west side. The movements to the east side of the embankment were very uniform as shown in Figure 3-14. A very large crack (14 ft. wide at the top and 8 ft. deep) formed on the east side as shown in the photographs of Figures 3-15 and 3-16 and schematically in Figure 3-14.

More detailed information of the failure including the surveys before and after failure will appear in an M.I.T. Department of Civil Engineering Report to be published in 1975.

**FIELD INSTRUMENTATION AT THE
STATION 263 TEST SECTION**

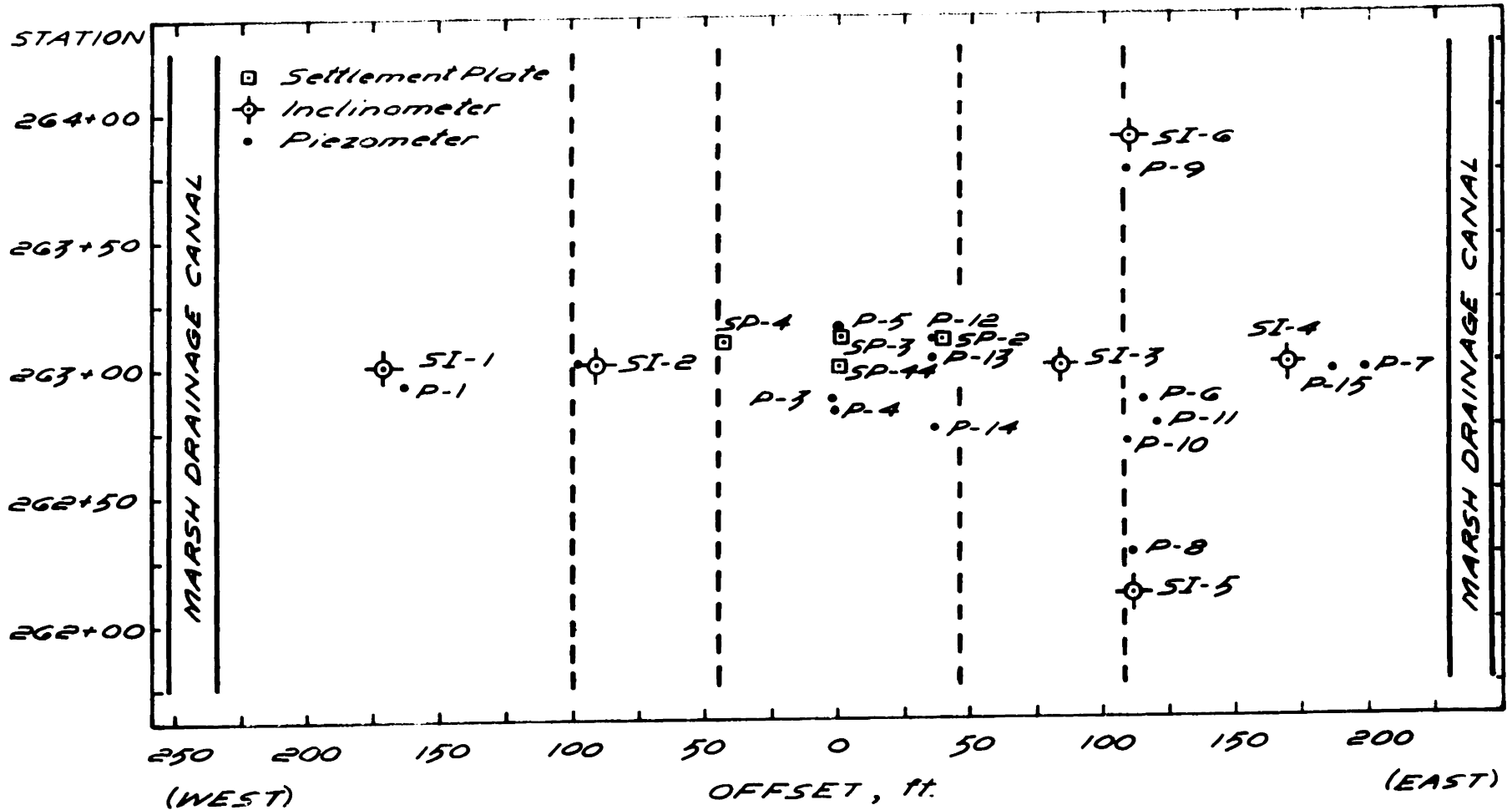
INSTRUMENT NO.	TYPE OF INSTRUMENT	LOCATION		SENSOR ELEV. (ft.)
		STATION	OFFSET (ft.)	
SP-44	Settlement Plate	263+00.75	0.3E	-4.272
SP-2	"	263+11.15	39.60E	+37.0
SP-3	"	263+11.0	0.60E	+37.0
SP-4	"	263+10.28	43.80W	+37.0
SI-1	Inclinometer	263+00.94	171.22W	-
SI-2	"	263+01.32	91.2W	-
SI-3	"	263+00.	28.85E	-
SI-4	"	263+00.35	169.54E	-
SI-5	"	262+11.64	110.73E	-
SI-6	"	263+89.25	109.38E	-
P-1	Hydraulic Piezometer	262+94.18	167.31W	-56.5
P-2	"	263+02.15	97.99W	-53.5
P-3	"	262+82.5	0.4W	-35.5
P-4	"	262+78.15	0.15W	-57.5
P-5	"	263+15.33	0.15W	-78.5
P-6	"	262+86.06	115.26E	-40.5
P-7	"	262+98.35	198.13E	-38.5
P-8	"	262+26.21	111.16E	-58.8
P-9	"	263+77.85	108.91E	-54.7
P-10	"	262+70.58	109.96E	-22.7
P-11	"	262+76.11	120.22E	-59.8
P-12	"	263+08.15	35.181E	-35.8
P-13	"	263+21.5	35.94E	-51.7
P-14	"	262+74.75	35.63E	-73.1
P-15	"	262+97.52	186.82E	-23.6

TABLE 3-1



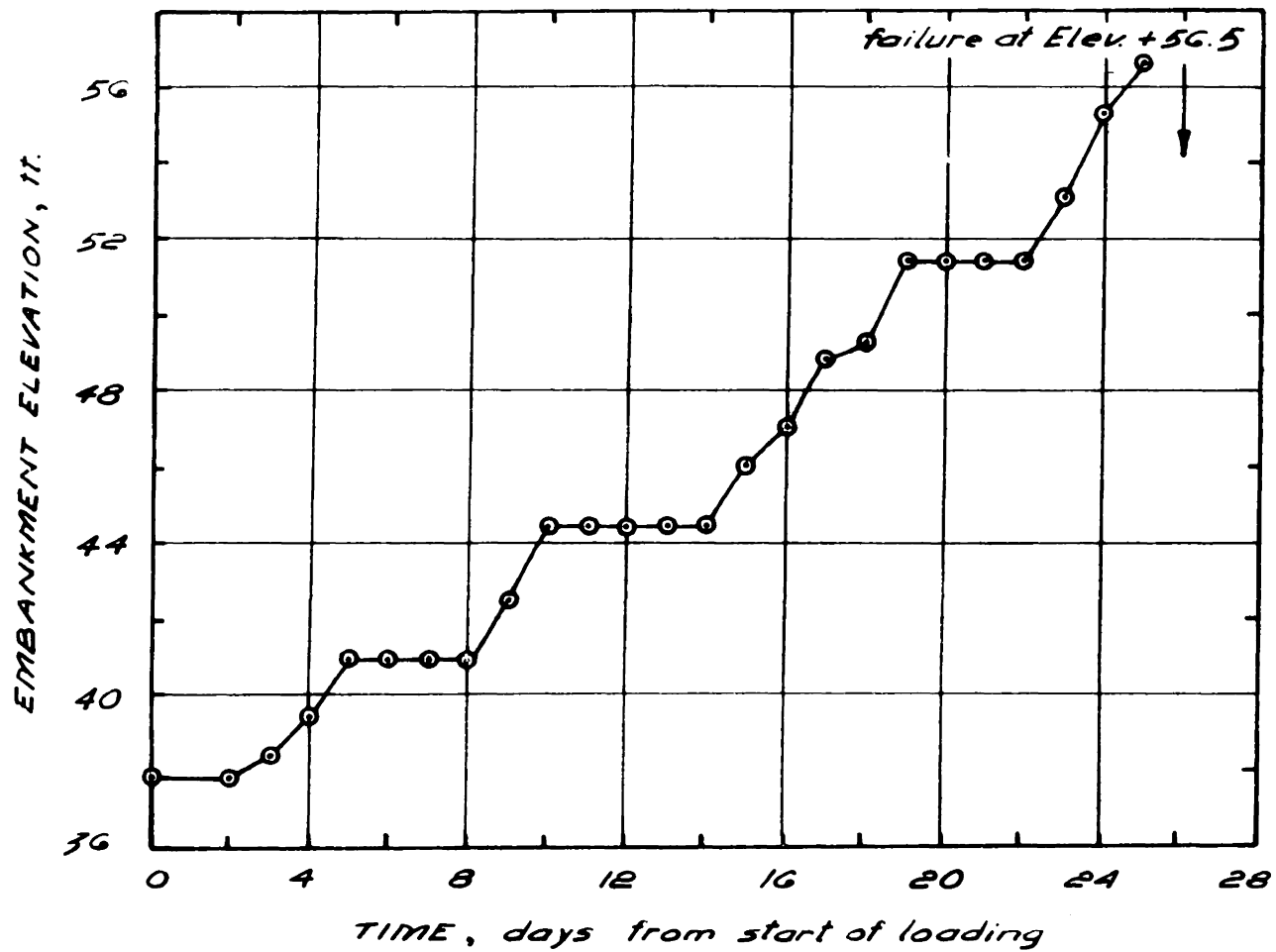
LOCATION OF FIELD INSTRUMENTATION
I-95 STATION 263 TEST SECTION

FIGURE 3-1

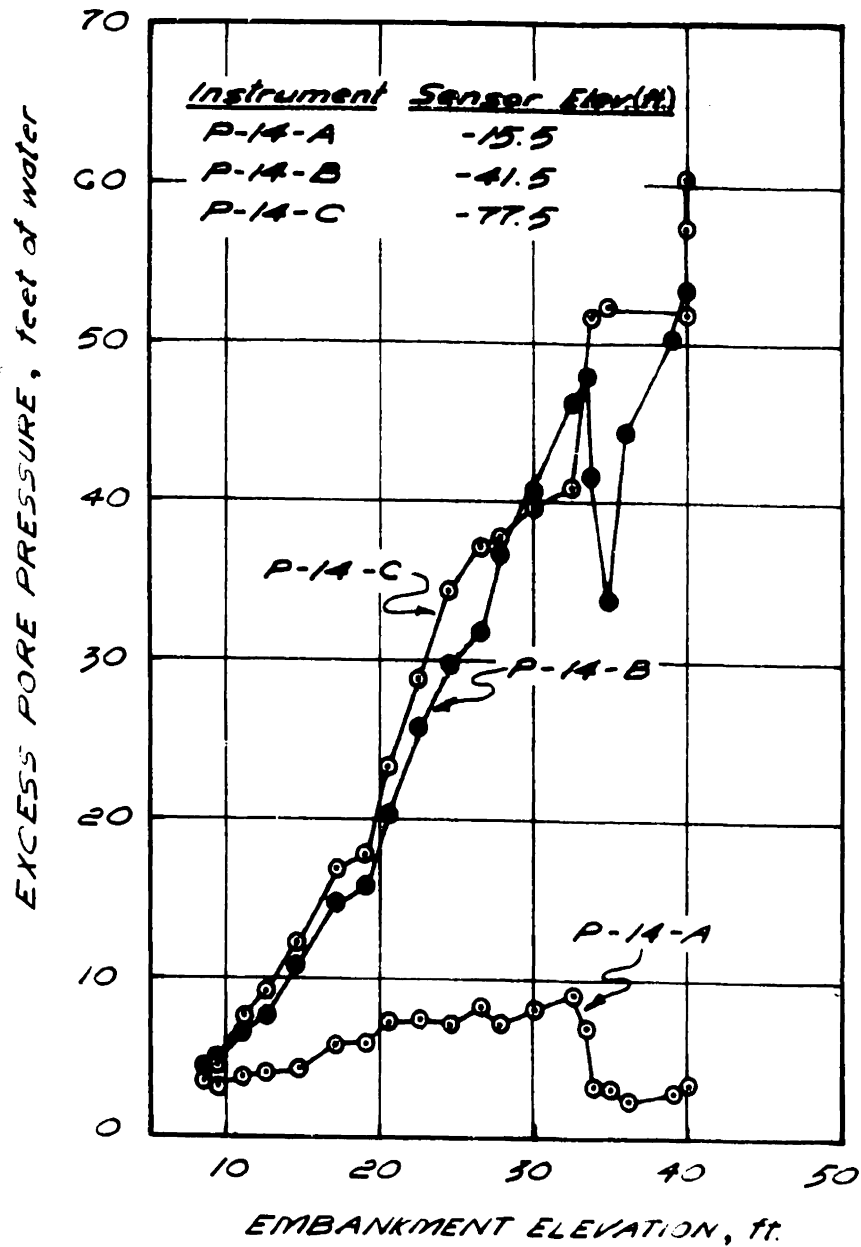


LOCATION OF FIELD INSTRUMENTATION (PLAN VIEW)
 I-95 STATION 263 TEST SECTION

FIGURE 3-2

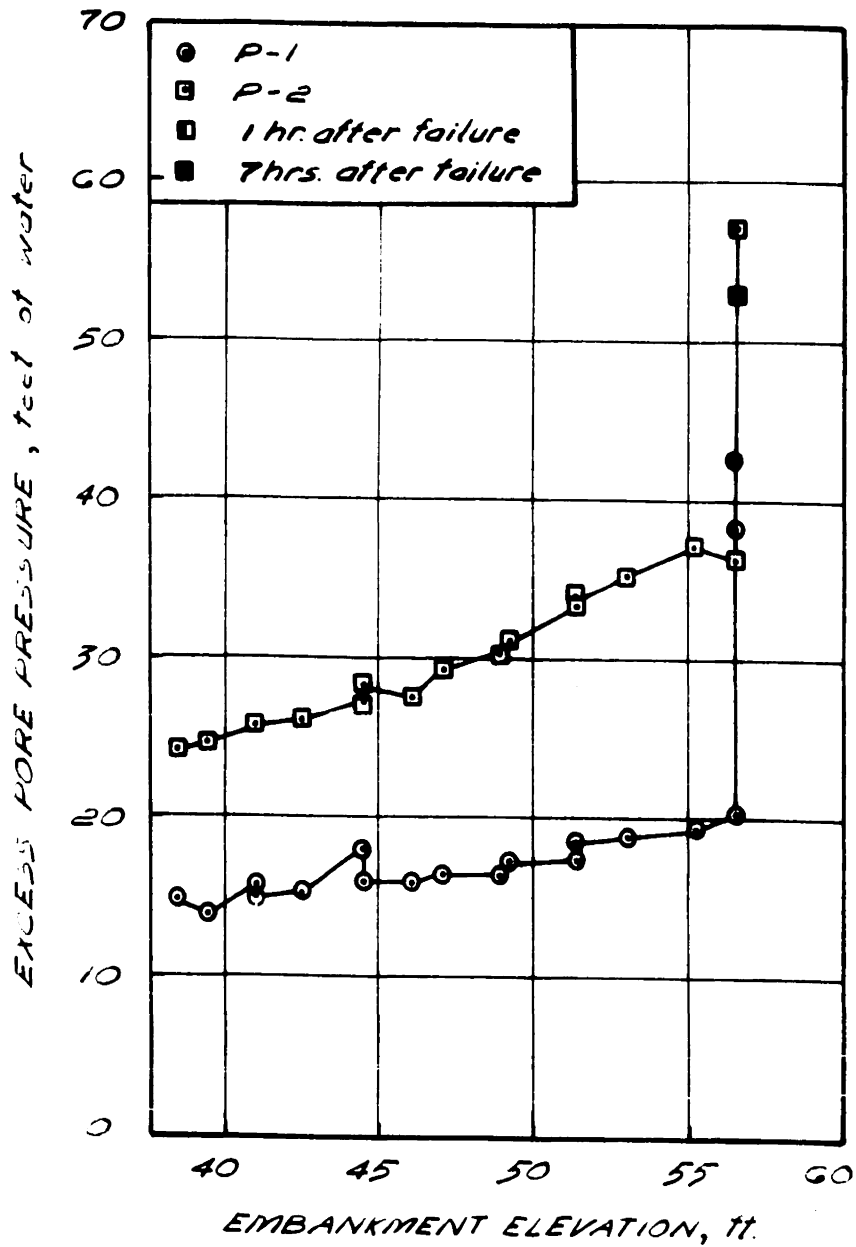


EMBANKMENT ELEVATION VS TIME
 STATION 263 TEST SECTION
 FIGURE 3-3



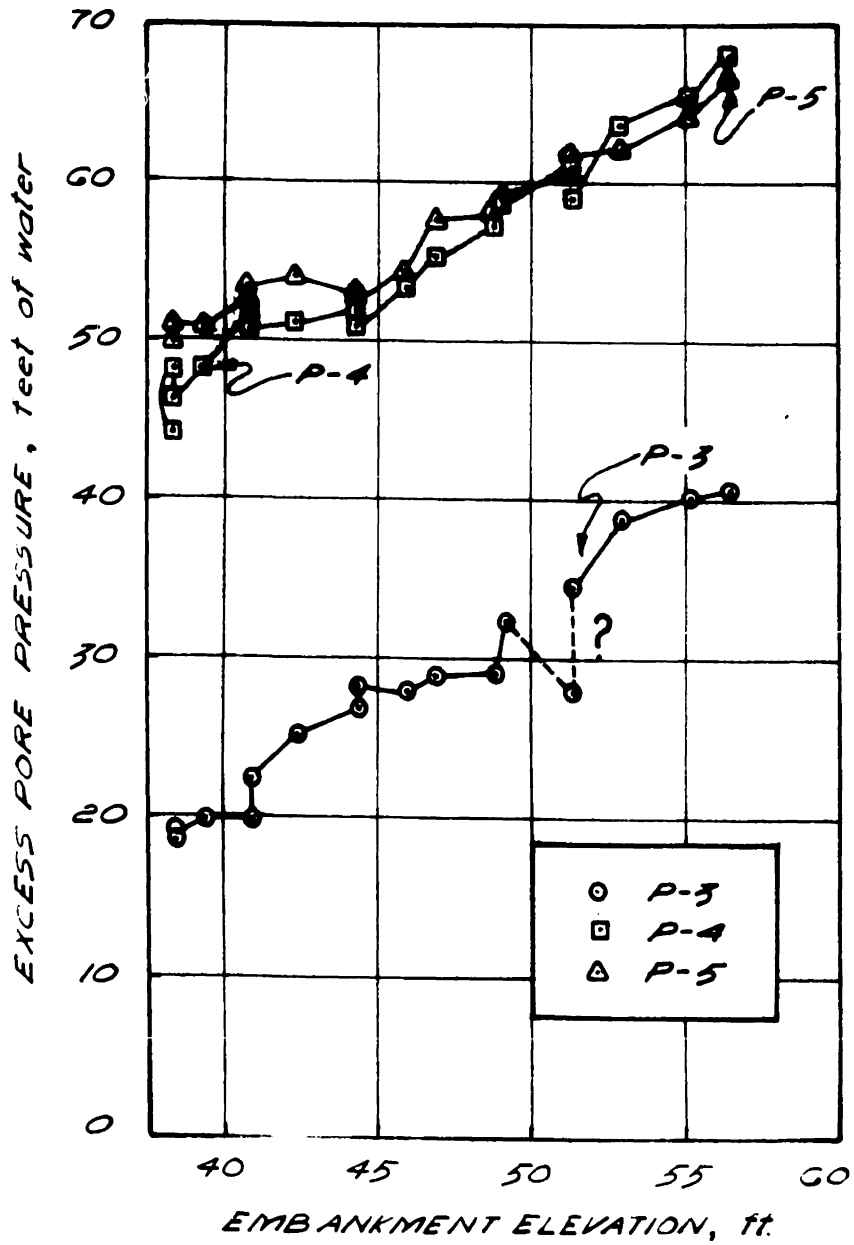
EXCESS PORE PRESSURE VS EMBANKMENT ELEVATION
STATION 263, INITIAL CONSTRUCTION

FIGURE 3-4



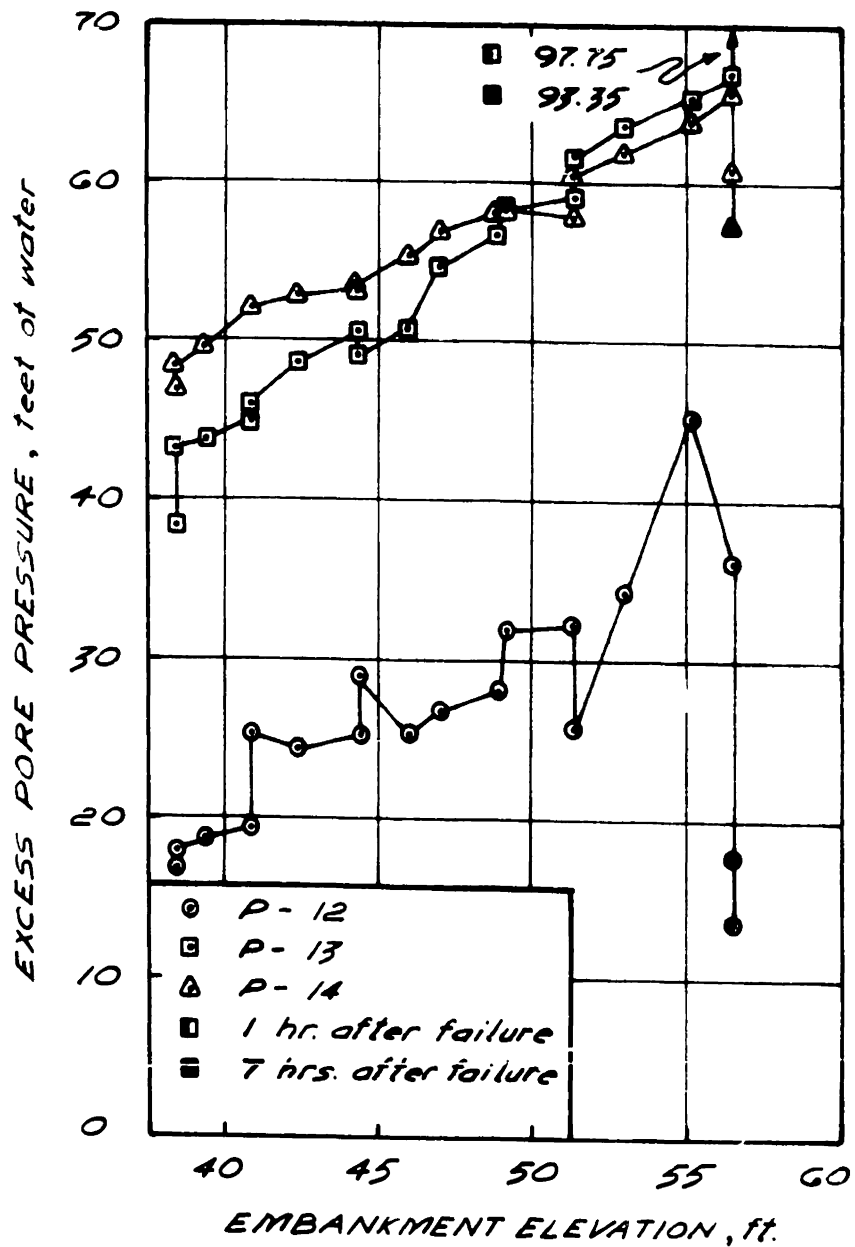
EXCESS PORE PRESSURE VS EMBANKMENT ELEVATION
STATION 267 TEST SECTION

FIGURE 3-5



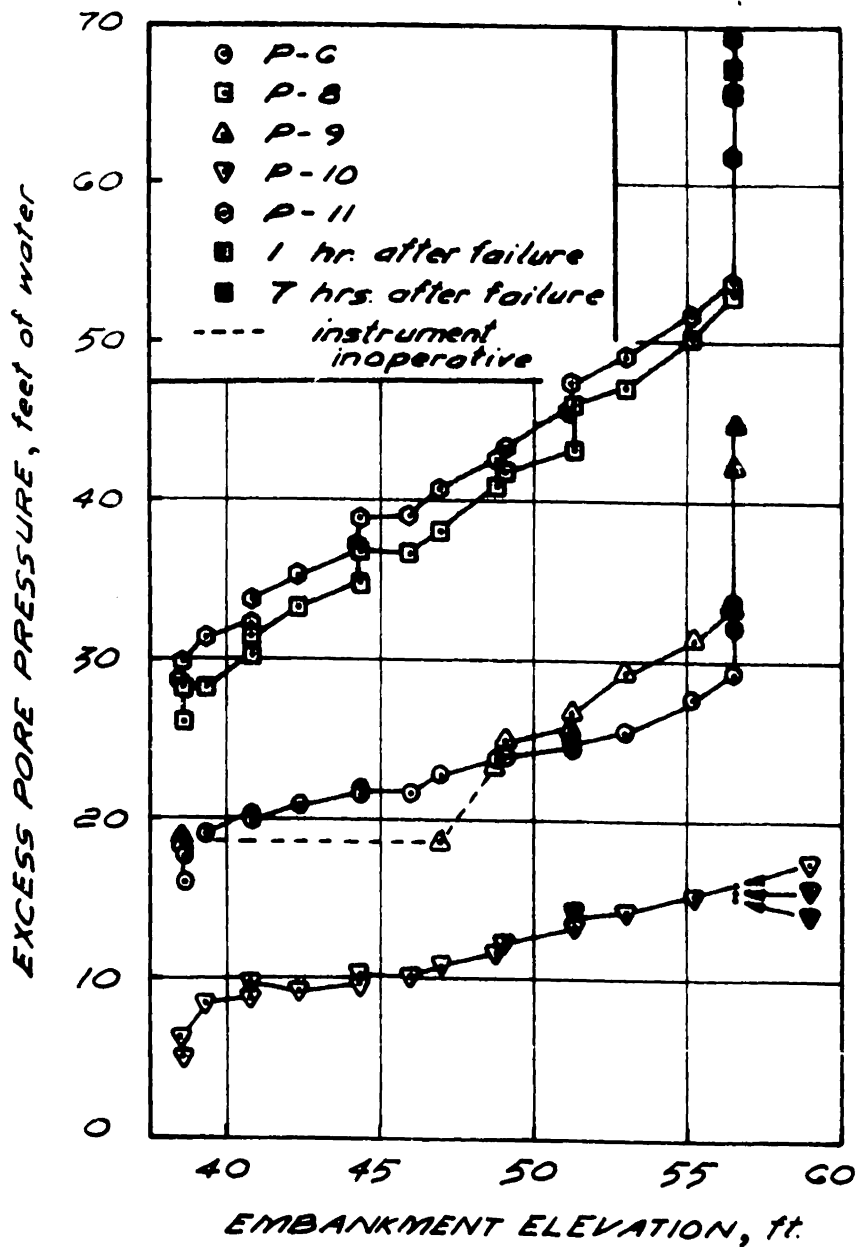
EXCESS PORE PRESSURE VS EMBANKMENT ELEVATION
STATION 263 TEST SECTION

FIGURE 3-6



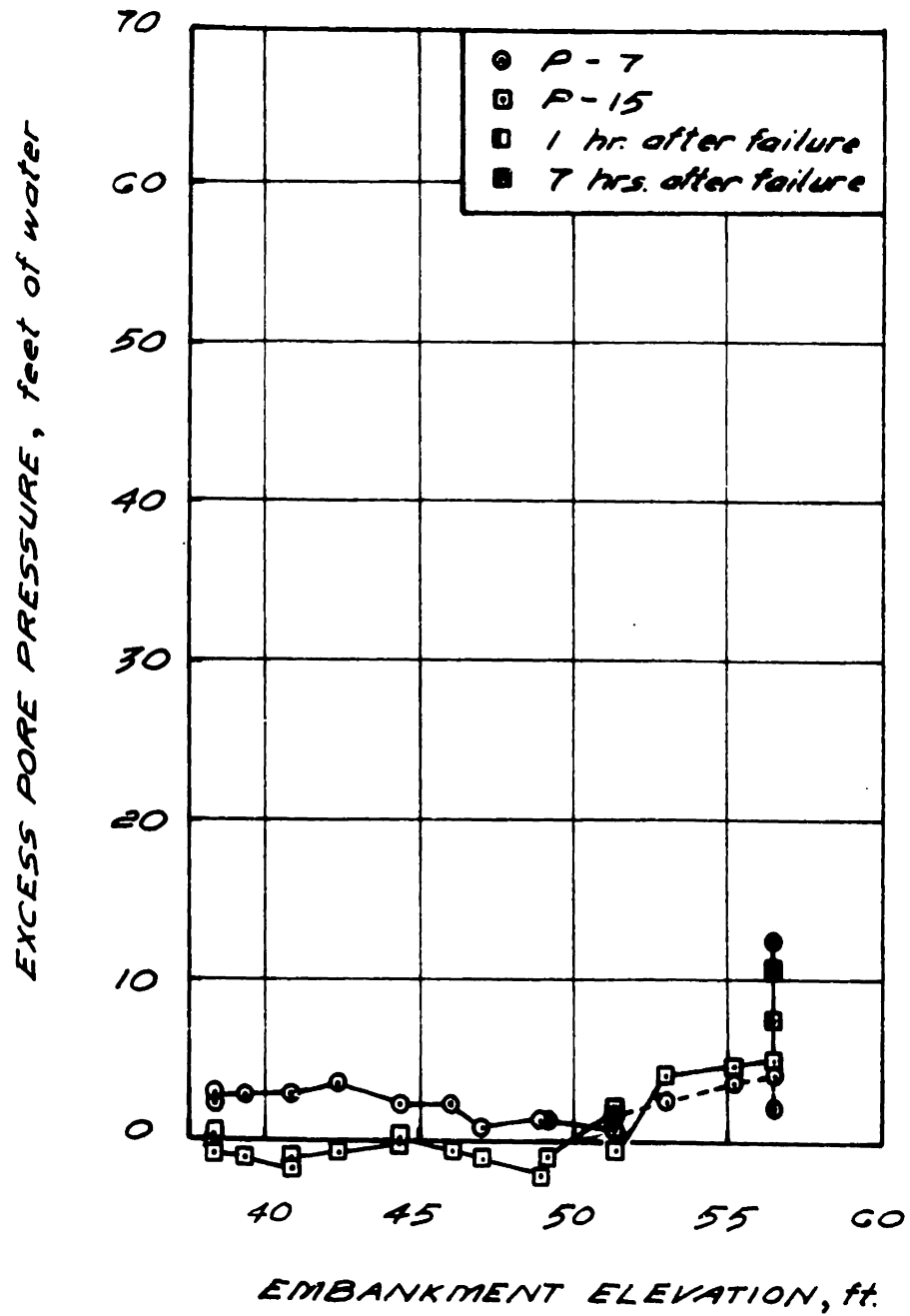
EXCESS PORE PRESSURE VS EMBANKMENT ELEVATION
STATION 263 TEST SECTION

FIGURE 3-7



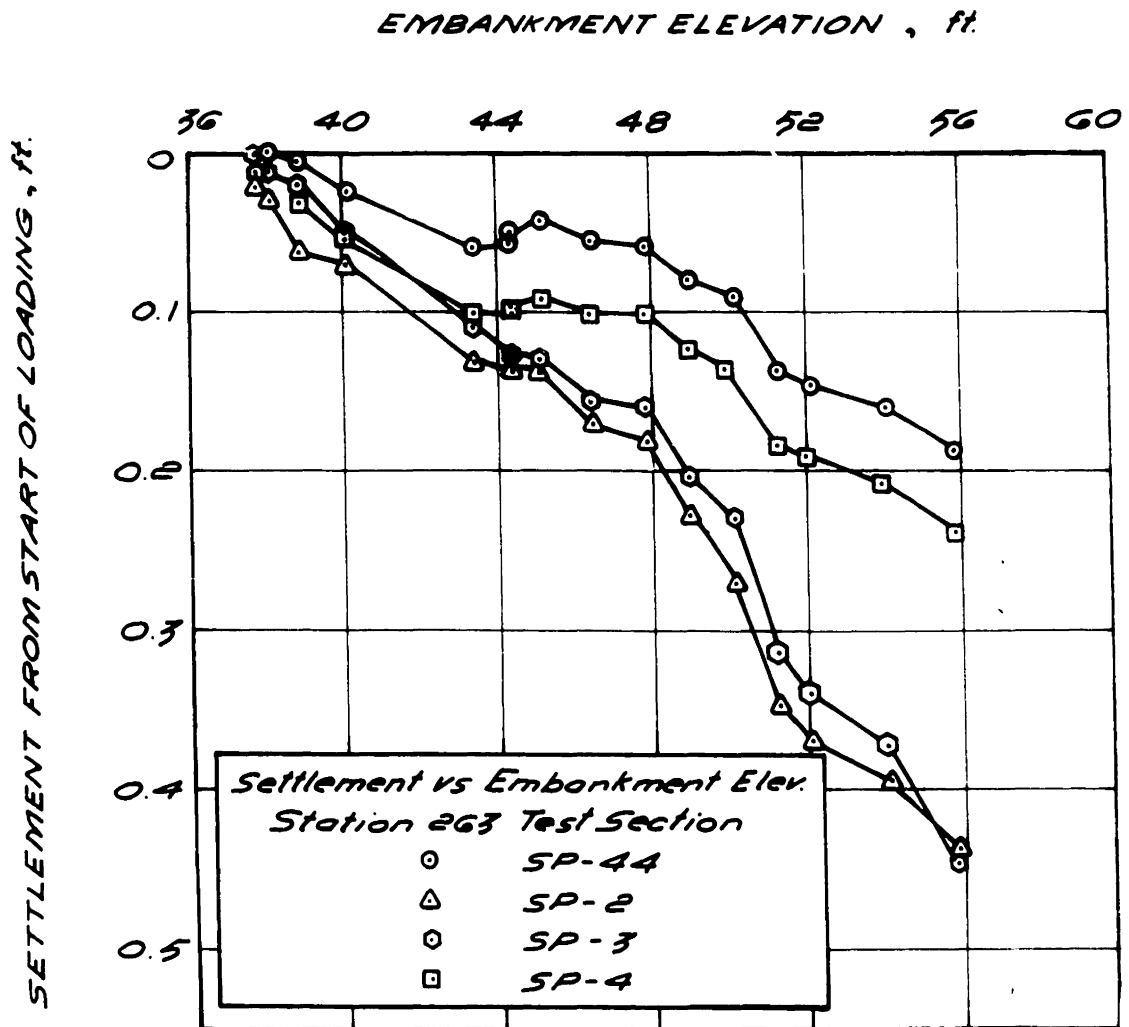
EXCESS PORE PRESSURE VS EMBANKMENT ELEVATION
STATION 263 TEST SECTION

FIGURE 3-8



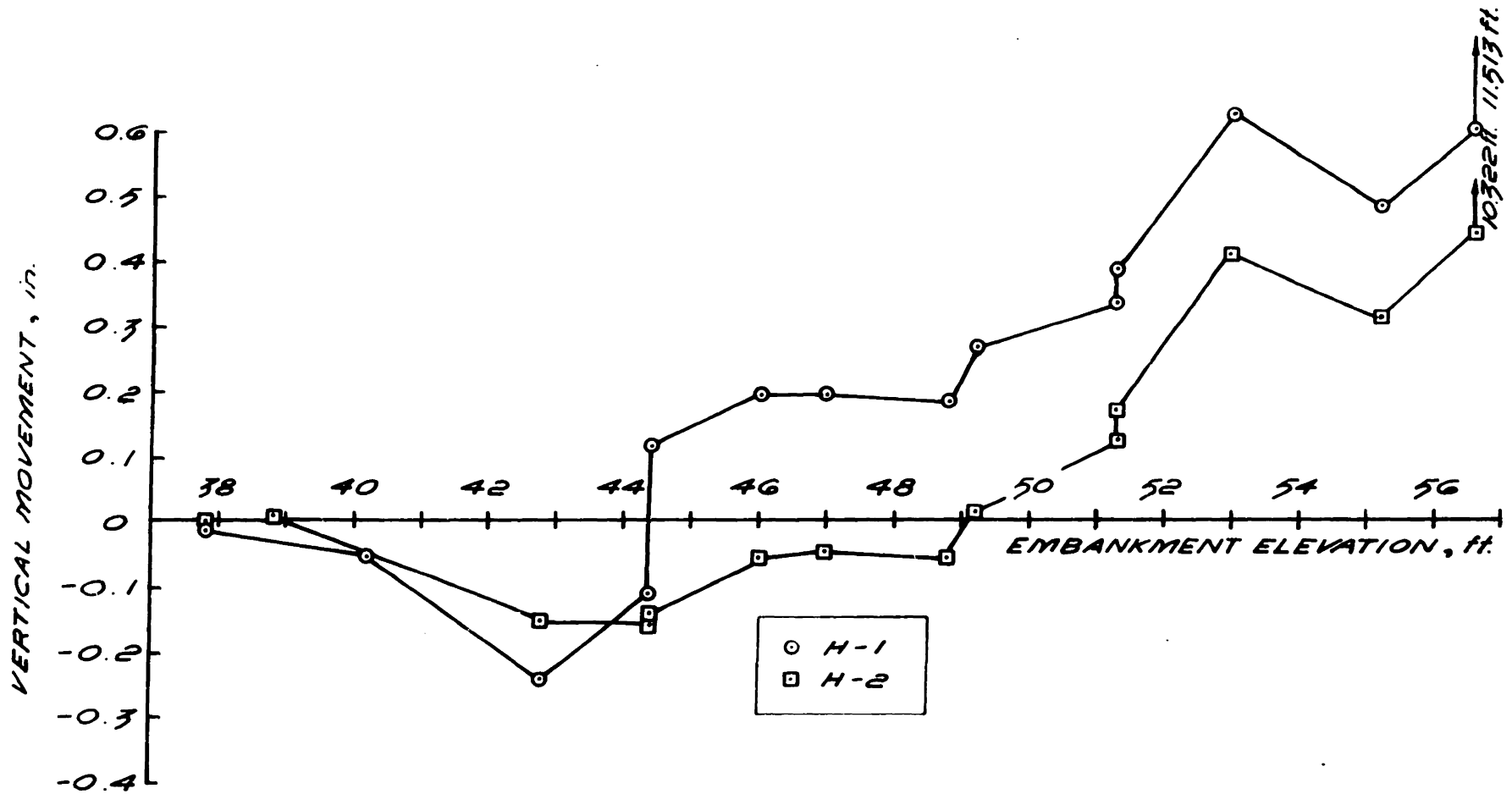
EXCESS PORE PRESSURE VS EMBANKMENT ELEVATION
STATION 263 TEST SECTION

FIGURE 3-9



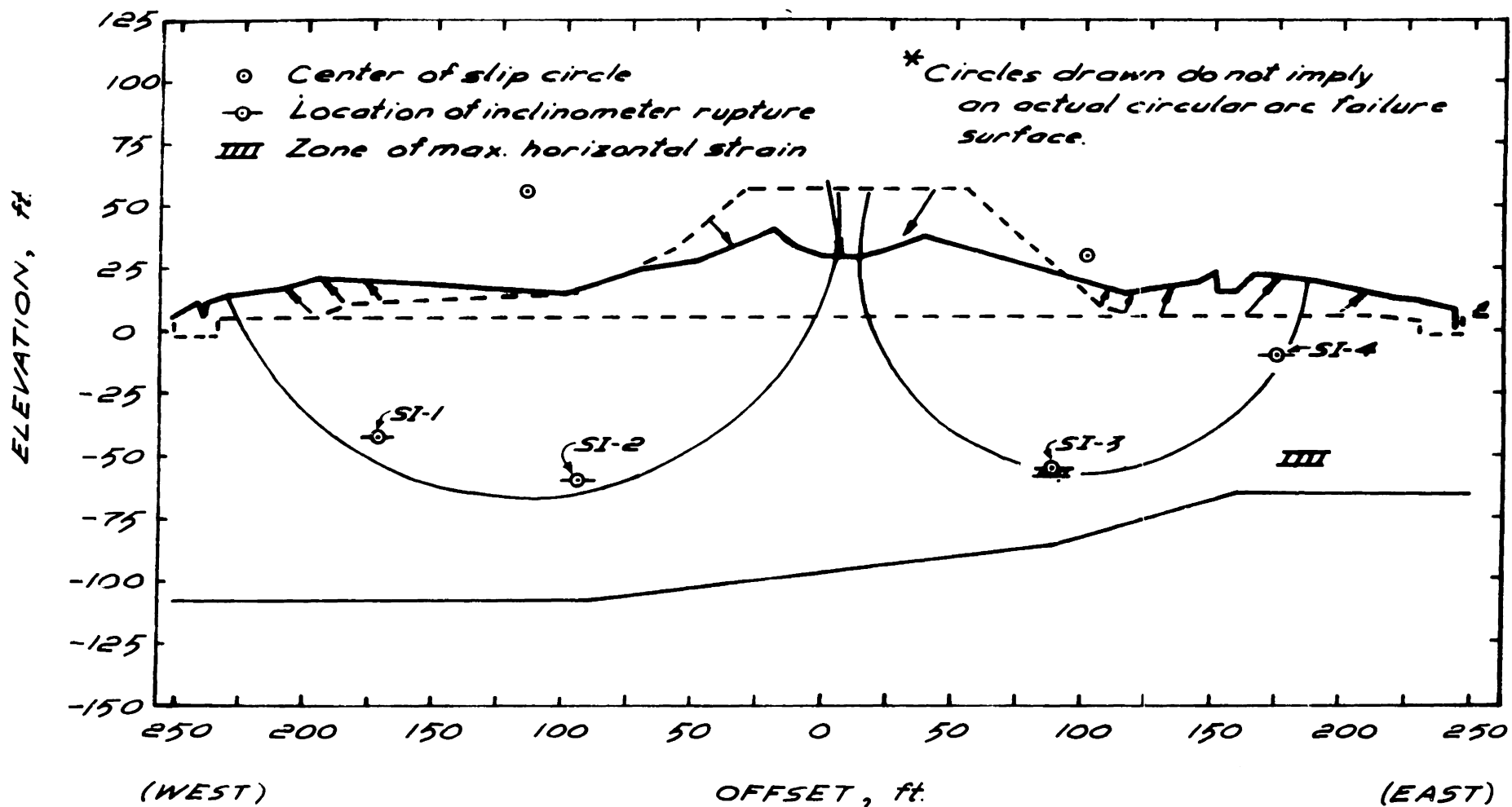
*SETTLEMENT VS EMBANKMENT ELEVATION
I-95, STATION 263 TEST SECTION*

FIGURE 3-10



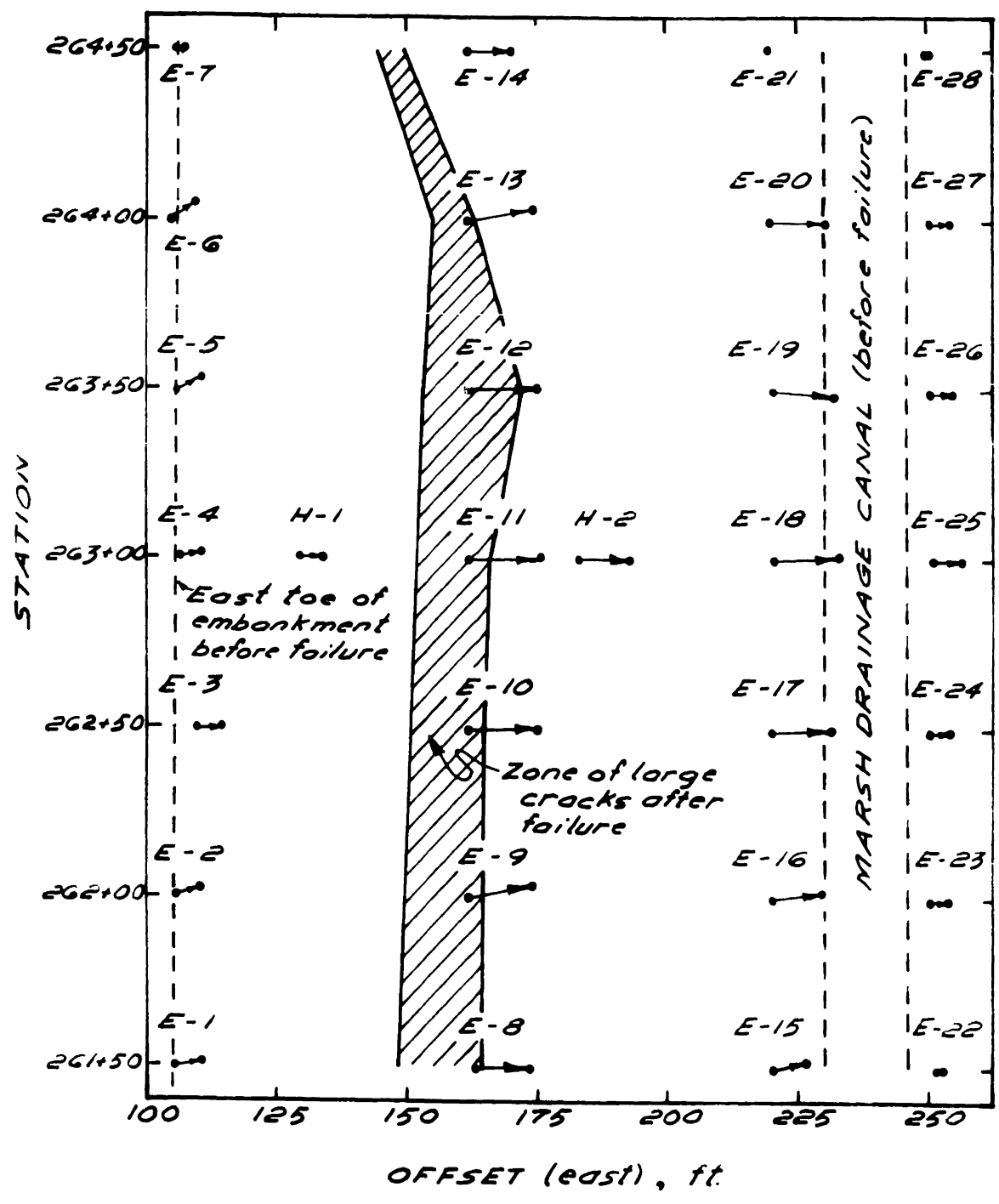
VERTICAL MOVEMENT VS EMBANKMENT ELEVATION (EAST SIDE)

FIGURE 3-11



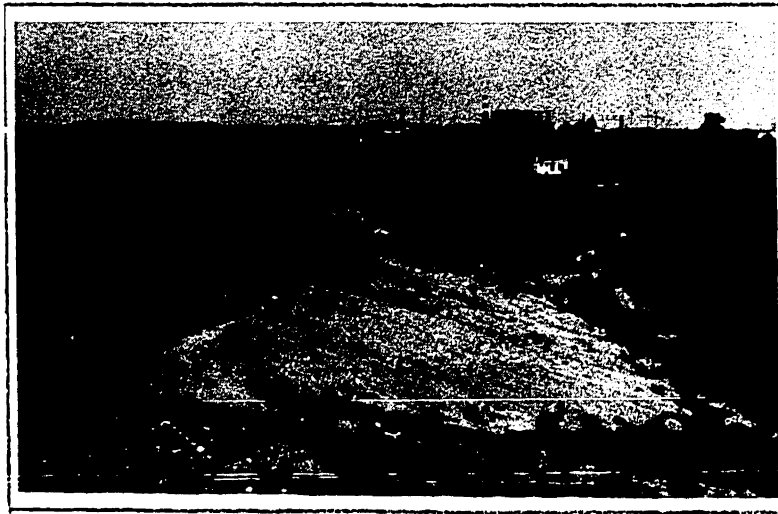
STATION 263 TEST SECTION BEFORE AND AFTER FAILURE

FIGURE 3-12



HORIZONTAL DISPLACEMENT OF SURFACE STAKES

FIGURE 3-13



Station 263 test section after failure (east side)

Figure 3-14



Large crack 140' east of embankment centerline at Sta 263

Figure 3-15

4. COMPARISON OF PREDICTIONS AND OBSERVED PERFORMANCE

The embankment crest elevations at failure predicted by various methods are summarized in table 4-1. The discrepancies in the predictions can be separated into two kinds: 1) those common to all the methods which affect equally all the results 2) those arising from the assumptions or procedures of a particular method.

4.1 Factors Contributing to Inaccuracies in All Predictions

4.1.1 Properties of the Sand Fill

The analyses presented in Table 4-2 were performed to investigate the effects of varying the fill weight and strength on the results of the most critical failure surface found during the SHANSEP prediction (Run #M-20). Except for the drastic assumption of $\bar{\phi} = 0^{\circ}$ (Run #M-23), a change in the friction angle of the sand had almost no effect on the computed factor of safety, (see Run #M-21).

The influence of varying the unit weight of the sand, however, was considerable (Run M-22). The unit weights used in the predictions came from results of field density tests at station 246 during construction of the original embankment as reported by Wolfskill & Soydemir (1971). The average γ_t was 119 lb/ft^3 , achieved by wetting down the sand and compacting with rubber tired rollers. The results from sand cone field density tests performed on September 1974 during the loading of station 263 test section are shown in table 4-3. The

average γ_t was 122 lb/ft³. The additional fill placed on the station 263 test section during loading was not systematically compacted as was the sand for the original 40 ft. high embankment. Therefore, it is reasonable to assume that the density of the original embankment was at least the same as that of the additional fill placed on the test section. The sand unit weights shown in table 4.2 for Run #M-24 are believed to represent better the actual field conditions and were used in all subsequent stability analyses.

4.1.2 Mode of Failure

The failure of the embankment was unusual both in its surprising length and in that it occurred to both sides of the embankment probably simultaneously. The stability analyses provided solutions for two dimensional problems and it would have been impossible to predict the longitudinal extent of the failure. The failure involved embankment sections of three different elevations and was probably propagated by a vertical shear mechanism. Its effect on the factor of safety as computed by two dimensional limiting equilibrium is not obvious. It is expected, however, that the computed factor of safety at failure would be less than one due to end effects. The magnitude of these end effects was estimated to be 6% from a series of progressively shallower slip surfaces.

The simultaneous failure to both sides was also impossible to predict by the methods employed. Chapter 2 showed that the factors of safety for both sides were essentially the same,

although slightly lower to the west than to the east. The similar factors of safety indicated an equal chance for failure to either side but all the slip surfaces considered assumed failure to one side only. With an incorrect failure surface close agreement between predicted and observed elevation at failure would be fortituous.

4.1.3 Time Effects

The loading of the test embankment was completed in about four weeks. Duncan, (1974), has found creep in samples from station 263 to be significant but loss in strength due to creep was not considered in the analyses performed. The undrained shear strength should had been decreased slightly to correct for time effects. The effect of neglecting creep, however, is probably small when compared to the effects of the incorrect weight of fill and incorrect failure surface.

4.2 U.C. and U.U. Case

The predictions based on Unconfined Compression and U.U. tests were both much too low, in agreement with results obtained by D'Appolonia, et al (1971). The actual elevation at failure was under estimated by 33%. Ladd (1971) attributes the low strengths in UC and UU tests to the loss in strength from sample disturbance. He estimated that UC and UU may underestimate undrained strengths by 20 to 50% for Boston Blue Clay. Clearly, the results from this field test indicate that the strengths measured do not provide a reliable estimate of the factor of safety in Boston Blue Clay, UC and UU test could be used only as strength

index tests or as a very conservative estimate of strength. -88-

4.3 Field Vane Analyses

The uncorrected Field Vane most closely predicted the embankment elevation at failure. With field vane strengths the failure elevation was underestimated by only 7.1%. The correction suggested by Bjerrum (figure 2-12) was in the wrong direction for the I-95 embankment and the correction based on the new data ($\mu=1.1$) was too high, but they both were within 10% of the right answer.

The field vane stability analyses show that the field vane is superior to the UC or UU tests as a strength index test for stability analyses.

4.4 SHANSEP Analysis

The SHANSEP prediction was the only one based on Morgenstern-Price analyses and was as good as the Field Vane but on the high side (+7.4% error). The main disadvantage in using M-P is the difficulty in locating the most critical failure surface. Unlike LEASE, where a large number of slip circles are analyzed in each run, M-P failure surfaces must be analyzed individually. Run M-24 in table 4.2 shows that, with the correct sand densities, the most critical failure surface found (M-20) yielded a factor of safety of 1.016 at the actual failure elevation. The error is only +1.6% which constitutes a very good prediction. Unfortunately, this would be a type "C" prediction, made after the results are known.

The use of the incorrect unit weight of sand together with

the possible inability to locate the most critical failure surface are believed to be the major contributors to the +7.4% error in the SHANSEP prediction. SHANSEP was the only method which could estimate the increase in strength of the partially consolidated foundation, without requiring additional field or laboratory strength tests. This capability makes SHANSEP particularly applicable to problems of embankments on partially consolidated foundations.

<i>METHOD</i>	<i>CLASS A PREDICTION OF EMBANKMENT ELEVATION AT FAILURE (feet)</i>	<i>ACTUAL EMBANKMENT ELEV. AT FAILURE (feet)</i>	<i>% ERROR</i>
<i>UNCONFINED COMPRESSION (BISHOP)</i>	<i>37.8</i>	<i>56.8</i>	<i>-33.1</i>
<i>UNCONSOLIDATED UNDRAINED (BISHOP)</i>	<i>37.8</i>	<i>"</i>	<i>-33.1</i>
<i>UNCORRECTED FIELD VANE (BISHOP)</i>	<i>52.5</i>	<i>"</i>	<i>-7.1</i>
<i>BJERRUM CORRECTED FIELD VANE (BISHOP)</i>	<i>50.5</i>	<i>"</i>	<i>-10.6</i>
<i>1.1*FIELD VANE (BISHOP)</i>	<i>61.1</i>	<i>"</i>	<i>+8.1</i>
<i>SHANSEP (M-P)</i>	<i>60.7</i>	<i>"</i>	<i>+7.4</i>

*COMPARISON OF PREDICTIONS
WITH OBSERVED BEHAVIOR*

TABLE 4-1

**SHANSEP STABILITY ANALYSES
EFFECT OF VARYING FILL PROPERTIES**

RUN NO.	PROPERTIES CHANGED	λ	F.S. (M-P)	Δ F.S., %												
M-20	<p><i>Starting Soil Properties</i></p> <table border="1"> <thead> <tr> <th>Soil #</th> <th>γ_t lb/ft³</th> <th>ϕ %</th> </tr> </thead> <tbody> <tr> <td>1</td> <td>119</td> <td>40</td> </tr> <tr> <td>3</td> <td>100</td> <td>30</td> </tr> <tr> <td>6</td> <td>110</td> <td>37</td> </tr> </tbody> </table>	Soil #	γ_t lb/ft ³	ϕ %	1	119	40	3	100	30	6	110	37	0.0451	1.008	—
Soil #	γ_t lb/ft ³	ϕ %														
1	119	40														
3	100	30														
6	110	37														
M-21	ϕ reduced 10% for Soils 1, 6, & 3 (on embankment slope)	0.0499	1.008	0												
M-22	γ_t increased 5% for Soils 6 & 3 (on embankment slope)	0.0446	0.992	-1.6%												
M-23	$\phi = 0$ for Soils 1 & 6	0.1790	0.969	-3.9%												
M-24	<p>Embankment Elevation reduced to +56.5 ft.</p> <p>γ_t changed to:</p> <p>122 pcf for Soil # 1</p> <p>122 pcf for Soil # 6</p> <p>115 pcf for Soil # 3 (on embankment slope)</p>	0.0424	1.016	N.A.												

TABLE 4-2

TEST NO.	DATE	SAMPLE ELEV.	DRY DENSITY lb/ft ³	WATER CONTENT, %	WET DENSITY lb/ft ³
1	5 SEPT 74	44'	118.0	5.79	124.5
2	"	"	115.5	4.92	121.5
3	"	"	102.5	3.63	108.5
4	6 SEPT 74	43.4'	128.0	7.05	137.0
5	"	43'	127.5	7.5	137.5
6	"	"	122.5	3.95	127.0
7	13 SEPT 74	48.7'	102.0	4.54	109.0
8	"	"	108.0	2.57	111.0

FIELD DENSITY TESTS

TABLE 4-3

Following the successful loading to failure, stability analyses were made using the best estimate of the actual field slip surface. Three possibilities were considered; 1) a circular arc failure surface through the locations at which the inclinometers sheared. 2) A non-circular failure surface through the same location. 3) A non-circular surface through the location of maximum horizontal strain before failure. No post failure analyses were performed with UC or UU strength data since, as shown earlier, the strengths are much too low.

5.1 Field Vane Analyses

Results of Simplified Bishop analyses with the slip circles shown in Figure 3-13 are shown in table 5.1. Surprisingly for both the east and west sides the computed factors of safety using the uncorrected field vane are higher than one. A $FS = 1$ was computed in Chapter 2 for a slip, surface compatible with failure to one direction at an embankment elevation 4 feet lower. The Bjerrum correction factor produced a reduction in the computer factor of safety of about 3% with the correction being in the right direction this time.

Two conclusions can be drawn from table 5.1 and Figure 3-13; first, the circles drawn in Figure 3-13 are at best an upper bound to the failure surfaces, if the failure surfaces were circular. In both sides, the most critical arc with the center as shown in Figure 3-13 passed below the location at which the inclinometers ruptured. Secondly, the failure mechanism appears

to have had a great influence in the embankment factor of safety. The Class A predictions indicated that the field vane yielded a factor of safety which was too low but the post failure analyses suggest that a field vane correction factor less than one should be used. This contradiction can only be explained by noting that the failure surface used for the predictions was not correct. The failure did not occur through the most critical surface for a one sided slide.

Based on the post failure field vane analyses, the appropriate correction factor (μ) for the east slide is 0.94 and for the west slide 0.92. These factors have been plotted in figure 5-1 for comparison but their meaning should be evaluated carefully. Bjerrum (1972), in suggesting his correction factor, assumed full mobilization of the shear strength in the sand fill if no cracks had been observed prior to failure. If cracks were present, the strength of the fill was ignored. No cracks were observed at the I-95 test embankment up to 13 hours before failure. Based on Bjerrum's criteria the analyses should include the shear strength of the sand, but Figure 2-11 indicates that most of the embankment sand is in the slice ignored by LEASE. The same is true for the circles shown in Figure 3-13. However, the arc through the fill is essentially vertical which makes the contribution of the sand to the resisting movement very small and probably negligible.

Perhaps more important than the fill strength used is the fact that all of the cases cited by Bjerrum started from

geostatic conditions. The additional fill for the station 263 test section was placed on an embankment with a partially consolidated foundation. The non- K_0 conditions existing at the site, combined with the fact that all the other cases reported involved failures to only one side of the embankment make the interpretation of the two new points in Figure 5-1 very difficult.

5.2 SHANSEP ANALYSES

The post-failure SHANSEP ANALYSES are presented in Table 5-2. Runs No. B-3 serve to compare the field vane and SHANSEP analyses of the assumed slip circle. The SHANSEP-LEASE results are essentially equal to the FV results, after applying Bjerrum's correction to the field vane strengths. Again, a failure surface deeper than the circle shown in Figure 3-13 is suggested.

The Morgenstern-Price analyses are illustrated in Figure 5-2. The failure surface through the zones of maximum computed horizontal strain (M-26) yields a factor of safety much too high, indicating that the failure surface did not follow the zones of maximum horizontal strain. A finite element analysis of the test embankment made by Hawkes (1975) using program FEECON predicted the pattern of horizontal deformations successfully. However, FEECON failed to predict the Plane Strain Passive section of the failure surface.

The minimum factor of safety obtained (run M-27) was about

10% too high. There is not yet enough field data to determine which failure surface most resembles the actual one. The most reasonable one given the present information is that shown in Figure 5-2 for run M-27.

5.3 Effective Stress Analysis

A prediction based on Effective Stress Analyses (ESA) was not included in Chapter 2 because of difficulties in obtaining reliable effective stress parameters and pore pressure predictions for Boston Blue Clay. A careful study of these parameters had never been done and it was not feasible to complete one before the start of the field test. For example, values of Henkle's "a" parameter back calculated by Ladd (1975) from field data obtained at station 246 during the construction of the original embankment varied by a factor of 4 to 6.

After the embankment failed, analyses were performed with the probable failure surfaces, soil properties which had been used previously at the site and field pore pressure measurements. The pore pressure measurements before and after failure are shown in table 5-3. The increase in pore pressures during failure was very large particularly under the embankment centerline. The last pore pressure readings before failure were taken 17 hours before failure, shortly after the last lift of fill was placed. These readings, plotted in Figure 5-3 were used in the stability analyses depicted in Figure 5-4. The pore pressure at any point within the clay is taken as the distance between that point and the corresponding piezometric line.

With a \bar{c} and a $\bar{\phi}$ specified, the analysis is similar to the undrained analysis described in Chapter 2

The same sand properties as in all other post-failure analyses were specified and two different sets of clay properties were used. Guertin (1967) suggested that values of $\bar{c} = 660 \text{ lb/ft}^2$ and $\bar{\phi} = 21.1^\circ$ for the over consolidated clay and $\bar{c} = 0$ with $\bar{\phi} = 26^\circ$ for N.C. were appropriate based on CIU tests. Kirby & Lambe (1972) used $\bar{c} = 0$ and $\bar{\phi} = 26^\circ$ as reasonable values for both the O.C. and N.C. strata.

The results of the ESA are presented in table 5-4. Although analyses with $\bar{c} = 660 \text{ lb/ff}^2$ and $\bar{\phi} = 21^\circ$ give a F.S. that is too high, those using $\phi = 26^\circ$ with no cohesion compare reasonably well with the Field Vane and SHANSEP post failure analyses. Factors of safety are greater than one for all the effective stress analyses but this is reasonable since the pore pressure used are only a lower bound to the actual pressure before failure. The ESA and TSA should yield the same factor of safety along the same failure surface. However, the difficulty involved in evaluating the parameters required \bar{c} make the ESA, Effective Stress Analysis a less powerful tool for the undrained stability analyses of embankments.

5.4 Effectiveness of Field Measurements as Indication of Impending Failure

One of the objectives of the instrumentation installed at the station 263 test section was to provide an advance warning of impending failure. As mentioned before, the failure was sudden and unexpected. In the paragraphs below, the field data

is examined for a possible warning of instability which might have been missed during the progress of the field test.

5.4.1 Pore Pressures

A common warning of impending failure obtained from piezometer data is a sudden, marked increase in pore pressure or a change in slope of the excess pore pressure v.s. embankment elevation relationship. Hoeg, et al (1969) and D'Appolonia et al (1971) attribute the change in slope to the local yielding that occurs when the maximum shear stress in the soil reaches the undrained shear strength. With the possible exception of P-7 and P-15 (Fig. 3-9) no change in slope of the excess pore pressure v.s. embankment elevation plots were observed. In P-7 a possible break point is detected at elevation +49 feet and similarly at elevation +52 feet for P-15. Since these piezometers are far away from the embankment (see figure 3-2) the indication of local yielding in their vicinity is significant. The soil at the toe of the potential failure surface will keep the mass from sliding, while the soil near the embankment has already failed (a clear indication that the factor of safety is not the same along the circle). When yielding occurs in the remaining intact soil, failure will take place. The location of the actual failure surface will be determined by the inclination of the failure planes at the toe of the sliding mass. Near the embankment, where shear stresses have exceeded the shear strength on all planes, the failure surface will follow a mechanism compatible with movements

along the failure planes formed at the toe.

-99-

Determination of the break point in the plots of P-7 and P-15 during construction was difficult due to the considerable scatter in the data and rapid dissipation of pore pressures. Therefore, whatever indication of failure they provided, if any, was not identified at the time. Construction proceeded for one more week and an additional 6.5 feet of fill were placed before failure occurred. For the station 263 test embankment pore pressure data did not provide a clear indication impending failure.

5.4.2 Settlements and Heave

The plot of settlement v.s. embankment elevation presented in figure 3-10 shows a change in the rate of movement of all the instruments at an embankment elevation of 49 feet. The change in slope of the settlement plots occurs at about the same elevation as the change in slope of the piezometer data from P-7 and P-15. Measurements obtained from the grid of surface stakes do not give any indication of instability. Initially, as shown in Fig. 3-11 for H-1 and H-2, a settlement was measured. The small magnitude of the reading however, falls within the margin of error of ± 0.02 " considered reasonable for the optical survey. The magnitude of the subsequent heave was small (less than 3 inches) and did not show any revealing trends.

Horizontal movements during loading might also be used to indicate whether failure was about to occur. Horizontal movement data were obtained during loading on 4 slope indicator

casings installed in the east side of the embankment. But ⁻¹⁰⁰⁻
data could not be processed quickly enough to use to control
construction Hawkes (1975) presents a full discussion of
these measurements and how they compare with predicted values.

5.4.3 Summary

The best indication of instability is given by the plots of the settlement plate data. However, the change in slope of the settlement v.s. embankment elevation plot is a conservative sign of impending failure. An additional 8 feet of fill were required to cause failure after the elevation at which the changes in slope occurred was reached. In an actual highway embankment project, where future deformations and loss in strength due to creep could be significant, this first sign of instability should indicate a stop of construction

**POST-FAILURE FIELD VANE ANALYSES
(LEASE METHOD)**

CLAY PROPERTIES	FAILURE SURFACE	F.S. (BISHOP)	F.S. (FELLENIUS)
UNCORRECTED FIELD VANE (EAST SIDE)	Circle shown in figure 3-12 Center coord: (+104, +30.4). Radius: 87.5'	1.224	0.941
	Similar to above but R = 95' (concentric circle w/minimum F.S.)	1.060	0.872
FIELD VANE WITH BJERRUM CORREC- TION (EAST SIDE)	Circle shown in figure 3-12 c @ (+101, +30.4). R = 87.5'	1.176	0.904
	Similar to above but R = 95' (Concentric circle w/minimum F.S.)	1.029	0.844
UNCORRECTED FIELD VANE (WEST SIDE)	Circle shown in figure 3-12 c @ (-116.3, +54.8) R = 121.8'	1.242	0.989
	Similar to above but R = 130'	1.087	0.886

TABLE 5-1

POST - FAILURE SHANSEP ANALYSES

RUN NO.	METHOD OF ANALYSIS	FAILURE SURFACE	COMPUTED F.S.	REMARKS
B-3(a)	LEASE (EAST SIDE)	Circle shown in figure 3-12 Center @ (+101., +30.4) Radius = 87.5'	F.S. (Bishop) = 1.159 F.S. (Fellenius) = 0.891	Best circular arc fit through locations where inclinometers sheared
B-3(d)		Similar to above, but R = 100'	F.S. (Bishop) = 1.034 F.S. (Fellenius) = 0.866	Similar to Run: B-3(a) but deeper circle
M-25	MORGENSTERN PRICE	SHOWN IN FIGURE 5-2	1.145	"Best fit" through locations where inclinometers sheared
M-26			1.410	"Best fit" through zones of maximum horizontal strain
M-27			1.105	Similar to M-20 previously considered the most critical failure surface

TABLE 5-2

TABLE 5-3

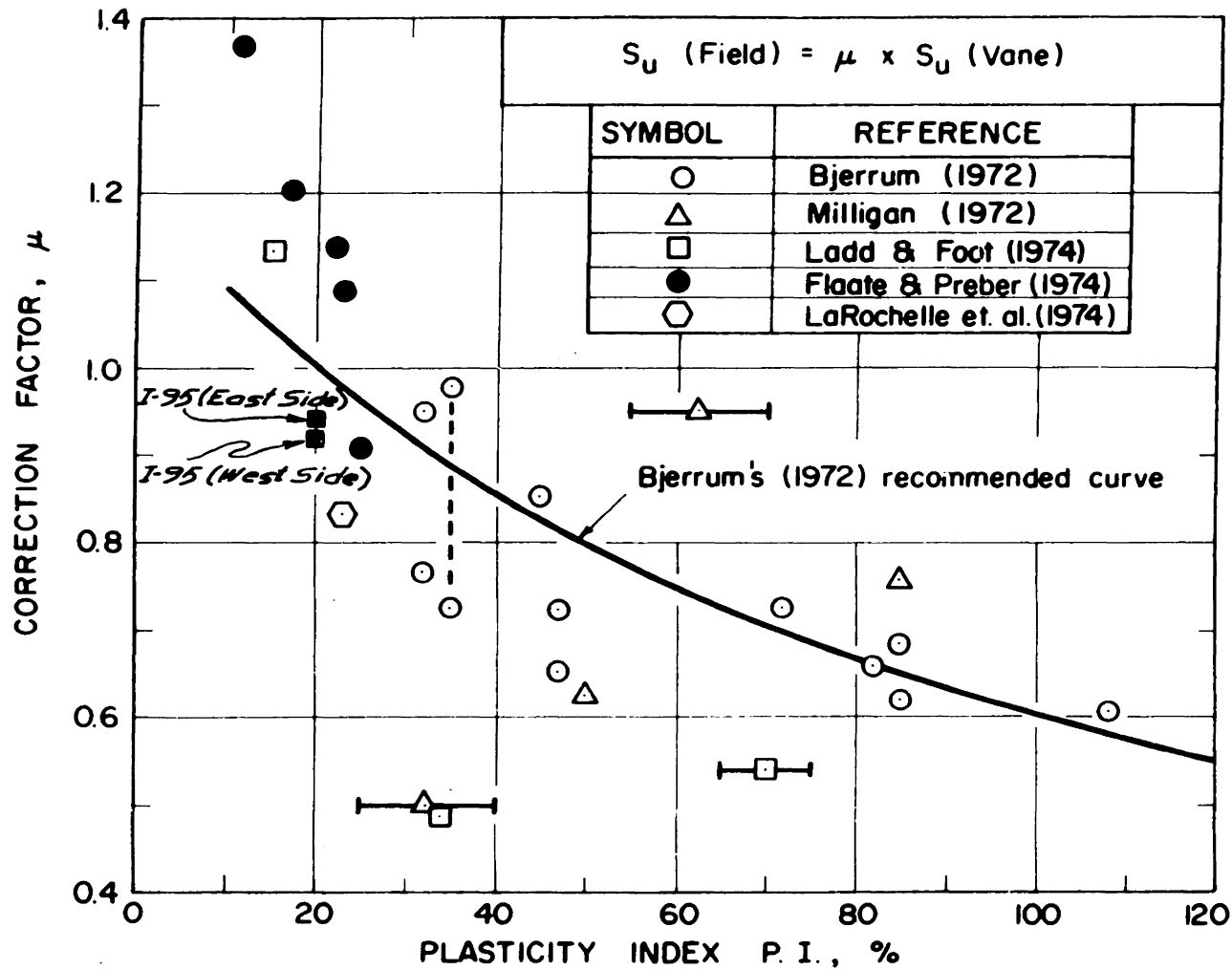
**PIEZOMETER WATER ELEVATION
BEFORE AND AFTER FAILURE**

PIEZ. NO.	SENSOR ELEV. (FT.)	WATER ELEVATION IN PIEZOMETER, FT.			
		before loading	17hrs. before failure	1hr. after failure	7hrs. after failure
P-1	-56.5	+19.6	+25.1	43.1	47.3
P-2	-53.5	+29.1	+41.3	62.0	57.8
P-3	-35.5	+29.7	+44.5	lost	lost
P-4	-57.5	+48.5	+73.1	≈119	≈119
P-5	-79.5	+49.9	+73.0	≈119	≈119
P-6	-40.5	+20.7	+31.5	39.4	36.8
P-7	-38.5	+7.8	+9.7	7.4	18.0
P-8	-58.8	+32.1	+59.1	73.3	71.8
P-9	-54.7	+24.1	+39.0	47.9	50.6
P-10	-22.7	+8.4	+19.4	19.0	18.5
P-11	-59.8	+34.1	+59.9	67.8	75.4
P-12	-35.8	+21.5	+40.8	18.3	22.2
P-13	-51.7	+43.1	+71.4	102.4	98.0
P-14	-73.1	+53.3	+72.0	67.2	64.0
P-15	-23.6	+3.8	+9.1	11.6	15.0

**POST-FAILURE EFFECTIVE STRESS ANALYSES
EAST SIDE, STATION 263 TEST SECTION**

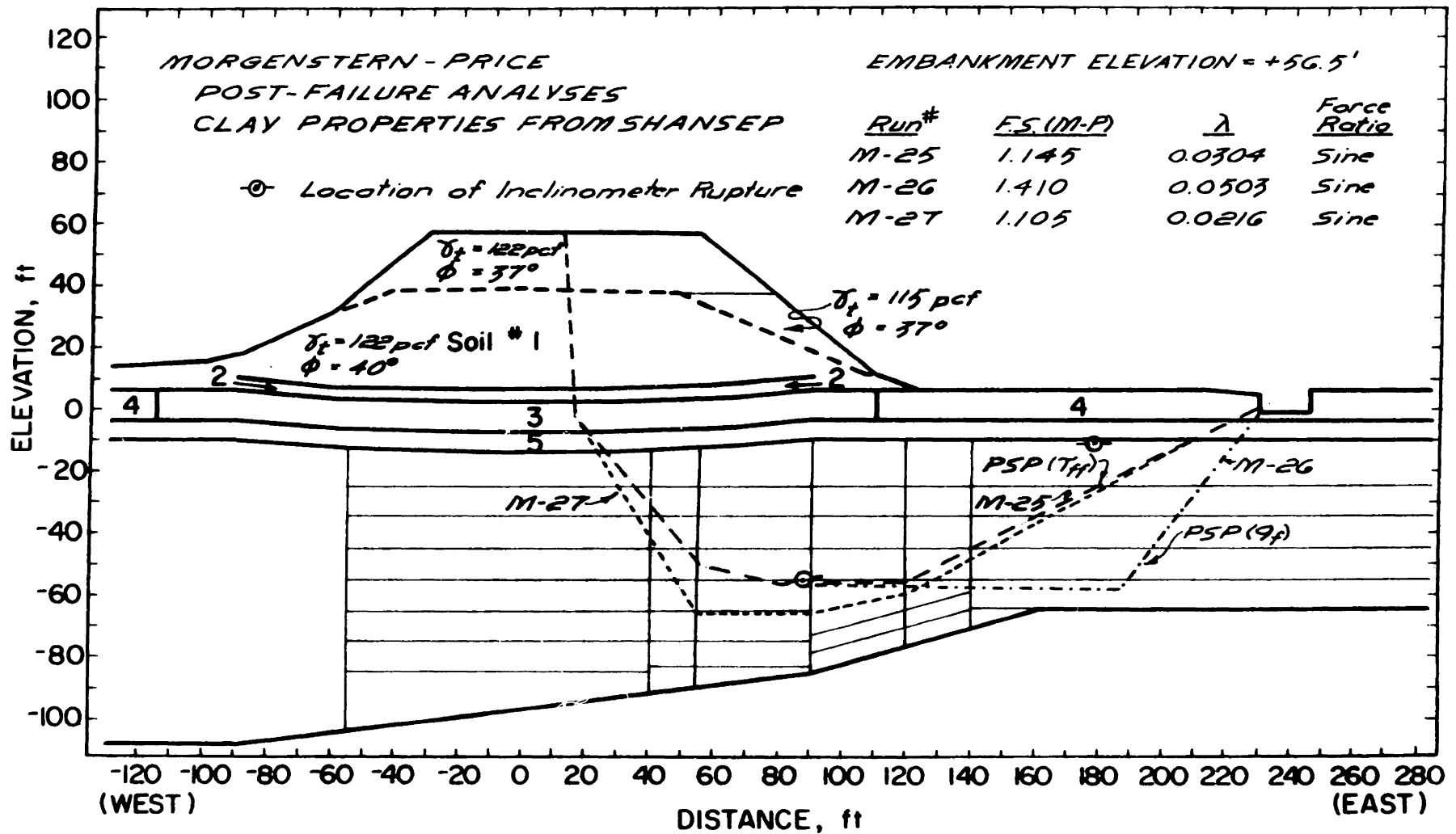
RUN NO.	METHOD OF ANALYSIS	CLAY PROPERTIES	FAILURE SURFACE	COMPUTED F.S.	REMARKS
—	LEASE (BISHOP)	OC $c=660^{lb/ft^2}$ $\phi=21.1^\circ$	Slip Circle shown in Fig. 3-12 (EAST SIDE)	1.589	F.S. decreases for deeper circles
		NC $c=0$ $\phi=25.1^\circ$		1.164	F.S. increases for deeper circles
M-28	MORGENSTERN - PRICE	OC $c=660^{lb/ft^2}$ $\phi=21.1^\circ$	Same as M-27 (Fig. 5-2)	1.545	$\lambda = 0.1687$
M-29		NC $c=0$ $\phi=25.1^\circ$	Same as M-25 (Fig. 5-2)	1.581	$\lambda = 0.1587$
M-30		OC $\left\{ \begin{array}{l} c=0 \\ \phi=26^\circ \end{array} \right.$ NC	Same as M-27 (Fig. 5-2)	1.262	$\lambda = 0.1916$
M-31			Same as M-25 (Fig. 5-2)	1.187	$\lambda = 0.1258$

TABLE 5-4

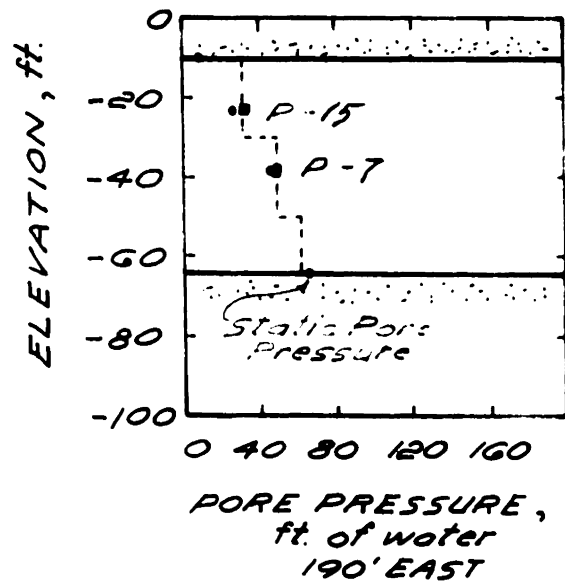
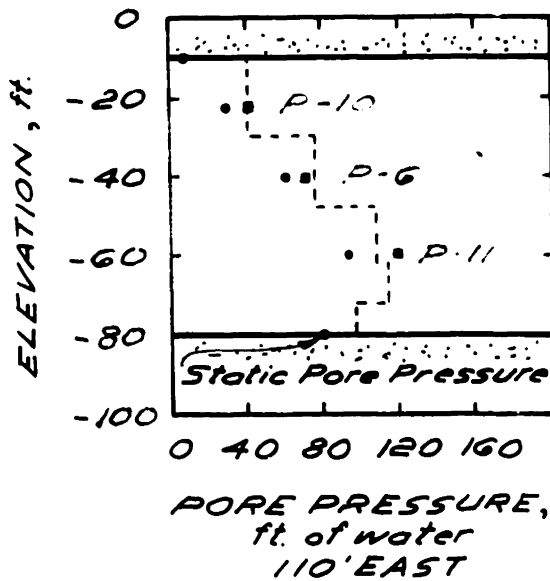
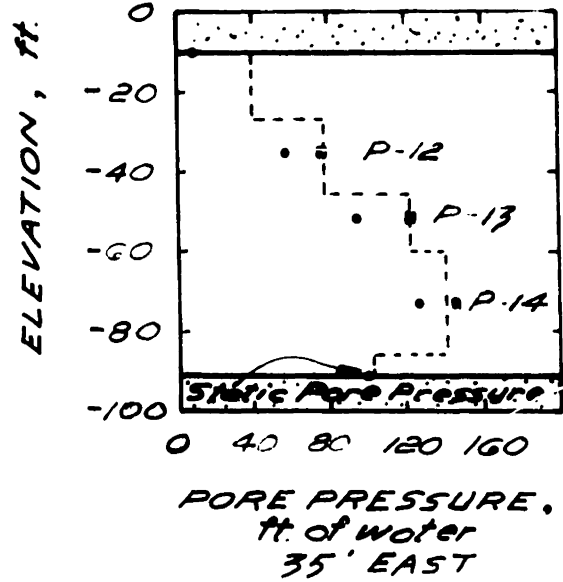
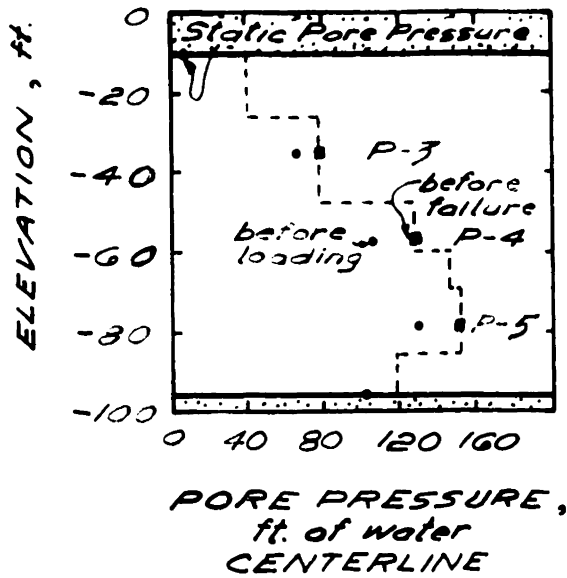


FIELD VANE CORRECTION FACTOR VS. PLASTICITY INDEX DERIVED FROM
EMBANKMENT FAILURES

FIGURE 5-1

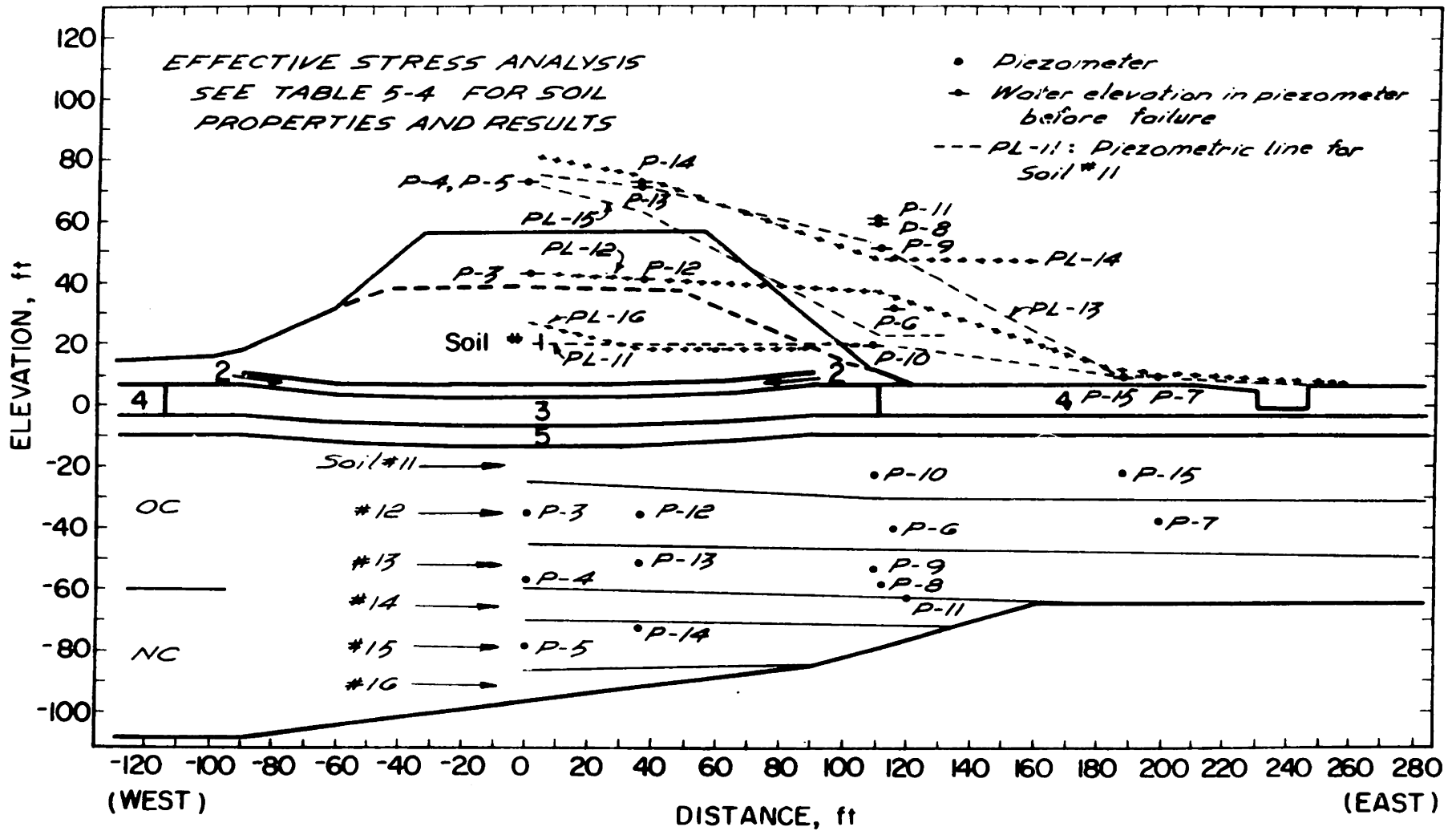


STABILITY ANALYSES I - 95 STATION 263
 FIGURE 5-2



PORE PRESSURES USED FOR
EFFECTIVE STRESS ANALYSIS
I-95 STATION 263

FIGURE 5-3



STABILITY ANALYSES I-95 STATION 263
 FIGURE 5-4

The I-95 failure study is far from being complete. Large amounts of valuable data have been obtained and there is more information to be collected in the field. Nevertheless, several significant conclusions can be derived from the study presented in this thesis:

1. The Unconfined Compression and Unconsolidated Untrained Triaxial tests yield undrained strengths that are much too low for use in stability analyses in Boston Blue Clay. The factors of safety computed from UC and UU strengths are extremely conservative unless modified by empirical correlations based on local experience.
2. The field vane shear test is superior to the UC or UU tests as a strength index test and should be used for preliminary stability computations whenever feasible. The usefulness of the field vane can be further improved with the development of more accurate semi-empirical correlations of the type suggested by Bjerrum (1972) and shown in figure 2-12. For the I-95 test embankment stability prediction based on uncorrected field vane strengths underestimated the embankment elevation at failure by only 7.1%. The average field vane correction factor, μ , back calculated from post failure LEASE analyses was 0.93.

3. SHANSEP yielded very reasonable stability predictions for the I-95 test embankment. The type A prediction over estimated the elevation at failure by 7.4% and the type C prediction, for which only the unit weight of the fill was changed to the in situ value, was only 1.6% over the actual elevation at failure.
4. The methods of analysis utilized (LEASE and M-P) were generally satisfactory. However, an improved version of LEASE with the capability of selecting the correct value of S_u depending on the position along the circular arc, would be a very worthwhile contribution to the use of computers for the solution of slope stability problems.
5. Due to the difficulty in working with pore pressures, the ESA appears to be inferior to the TSA for the undrained stability analysis of embankments on Boston Blue Clay. Back calculated pore pressure parameters varied a lot (Chapter 5) and piezometer data in table 5-3 shows that large changes in pore pressure occur during failure making it very difficult to select a value to input in the ESA.
6. The field instrumentation was not as successful in warning against impending failure as was expected. The only consistent but very conservative sign of instability was provided by the settlement plates. The pore pressure data proved to be an unreliable indication of impending failure for undrained loading on Boston Blue Clay.

In addition to the conclusions mentioned above several questions remain to be answered:

1. What is the actual failure surface? Based on the present information the writer believes that the failure surface is not circular as suggested in Section 5-2, and that the formation of the large crack shown in Figs. 1-1 and 3-14 was due to tension resulting from the shear forces generated along the bottom at the east toe of the sliding mass.
2. What is the effect of the failure mechanism on the computed factor of safety? Is a simultaneous failure to both sides equivalent to two independent failures to each side? A better understanding of the failure mechanism could provide some insight into the apparent discrepancy between the pre-failure and post-failure field vane analyses.

In order to completely evaluate the field test it would be necessary to define the failure surface more precisely. To locate additional points on the failure surface, several of the piezometer pipes could be retrieved below the embankment and between SI-3 and SI-4. In addition, field vane tests could be performed to locate a zone of low S_u since the clay has a sensitivity of about 3 to 4. However, the field vane data obtained in this manner will not be easy to evaluate in view of the very large movements that took place.

1. Bailey, W.A. and Christian, J.T. (1969) "ICES LEASE - I, A Problem - Oriented Language for Slope Stability Analysis" Research Report R69-22, Dept. of Civil Engineering, M.I.T.
2. Bishop, W.A. (1955), "The Use of the Slip Circle in the Stability Analysis of Slopes", Geotechnique, Vol. 5, No. 4, Dec. 1960, pp. 129-150.
3. Bjerrum, L. (1972), "Discussion Session 1", Embankments on Soft Ground, Proc. ASCE Specialty Conference on Performance of Earth and Earth-Supported Structures, Vol. 2, Purdue University, pp. 1-54.
4. Bromwell, L.G., Ryan, C.R., and Toth, W.E. (1971) "Recording Inclinomater for Measuring Soil Movement", Proc. 4th Panamerican Conference on Soil Mechanics and Foundation Engineering, Vol. 2, San Juan, Puerto Rico, pp. 333-343.
5. D'Appolonia. D.J., Lambe, T.W. and Poulos, H.G. (1971), "Evaluation of Pore Pressure Beneath an Embankment", ASCE, JSMFD, Vol. 97, No. SM6, pp. 881-897.
6. Duncan, J.M. (1974), Presentation of Prediction, Foundation Deformation Prediction Symposium, M.I.T., Nov., 1974.
7. Flaate, K. and Preber, T. (1974), "Stability of Road Embankments in Soft Clay", Can. Geot. Journal, Vol. 11, No.1, pp. 78-89.
8. Guertin, J.D. Jr., (1967), "Stability and Settlement Analyses of an Embankment on Clay", S.M. Thesis, Dept. of Civil Engineering, M.I.T.
9. Hawkes W.D. (1975), "Undrained Deformation Behavior of Partially Consolidated Boston Blue Clay" S.M. Thesis, Dept. of Civil Engineering, M.I.T.
10. Hoeg, K. Andersland, O.B. and Rolfsen, E.N. (1969) "Undrained Behavior of Quick Clay Under Load Test at Asrum", Geotechnique, Vol. 19, No. 1, March 1969.
11. Kenney, T.C. (1964), "Sea Level Movements and the Geologic Histories of the Post-Glacial Marine Soils at Boston, Nicolet, Ottawa and Oslo", Geotechnique, Vol, 14, pp. 203-230

12. Kirby, R.C. and Lambe, T.W. (1972), "Design of Embankments on Soft Soil", Research Report R72-36, Dept. of Civil Engineering, M.I.T.
13. Ladd, C.C. (1971), "Strength Parameters and Stress-Strain Behavior of Saturated Clays", Research Report R71-23, Dept. of Civil Engineering, M.I.T., Chapter 9.
14. Ladd, C.C. (1975), "Predicted Performance of an Embankment on Boston Blue Clay" Proc. Foundation Deformation Symposium, M.I.T. (to be published).
15. Lambe, T.W. (1951), Soil Testing for Engineers, John Wiley and Sons, New York, 165 pages.
16. Lambe, T.W., D'Appolonia, D.J., Karlsrud, K. and Kirby, R.C. (1971) "The Performance of the Foundation Under a High Embankment", Research Report R71-22, Dept. of Civil Engineering, M.I.T.
17. Lambe, T.W. (1973), "Thirteenth Rankine Lecture: Predictions in Soil Engineering", Geotechnique, Vol. 23, No. 2, June, 1973, pp. 149-202.
18. LaRochelle, P. Trak, B., Travenas, F., and Roy, M. (1974), "Failure of a Test Embankment on a Sensitive Champlain Clay Deposit", Can. Geot. Journal, Vol. 11, No. 1, pp. 142-164
19. Little, A.L. and Price, U.E. (1958), "The Use of an Electronic Computer for Slope Stability Analysis", Geotechnique, Vol. 8, No. 3, Sept. 1958, pp. 113-120.
20. Madera, G.A. (1969), "Slope Stability Analysis by Limiting Equilibrium", B.S. Thesis, Dept. of Civil Engineering, M.I.T. 1969.
21. Milligan, V. (1972), "Discussion Session 1, Embankments on Soft Ground", Proc. ASCE Specialty Conf. on Performance of Earth and Earth Supported Structures, Vol. 3., Purdue Univ. pp. 41-48.
22. Morgenstern, N.R. and Price, U.E. (1965), "The Analysis of the Stability of General Slip Surfaces", Geotechnique, Vol. 15, No. 1, March 1965, pp. 79-93.
23. Morgenstern, N.R. and Price, U.E. (1967), "A Numerical Method for Solving the Equations of Stability of General Slip Surfaces" The Computer Journal, Great Britain, Vol. 9, No. 4, Feb. 1967, pp. 388-393.

24. Simon, R.M., Ladd, C.C. and Christian, J.T. (1972), "Finite Element Program FEECON for Undrained Deformation Analyses of Granular Embankments on Soft Clay Foundations", Dept. of Civil Engineering Research Report R72-9, M.I.T., 1972.
25. Storch Engineers (1965), "Soils and Foundations Report for Interstate Route 95, Revere-Saugus, Massachusetts", Prepared for Highway Engineers, Inc., Boston, Mass.
26. Whitman, R.V. and Bailey, W.A. (1967) "Use of Computers for Slope Stability Analysis" ASCE JSMFD, Vol. 93, SM4, pp. 475-498.
27. Whittle, J.F. Jr. (1974), "Consolidation Behavior of an Embankment on Boston Blue Clay", SM Thesis, Dept. of Civil Engineering, M.I.T.
28. Wissa, A.E.Z. Christian, J.T., Davis, E.H. and Heiberg, S. (1971), "Consolidation at Constant Rate of Strain", ASCE, JSMFD, Vol. 97, SM10, pp. 1393-1413.
29. Wolfskill, L.A. and Soydemir, C. (1971), "Soil Instrumentation for the I-95 M.I.T.-MDPW Test Embankment", Dept. of Civil Engineering Research Report R71-28, M.I.T.

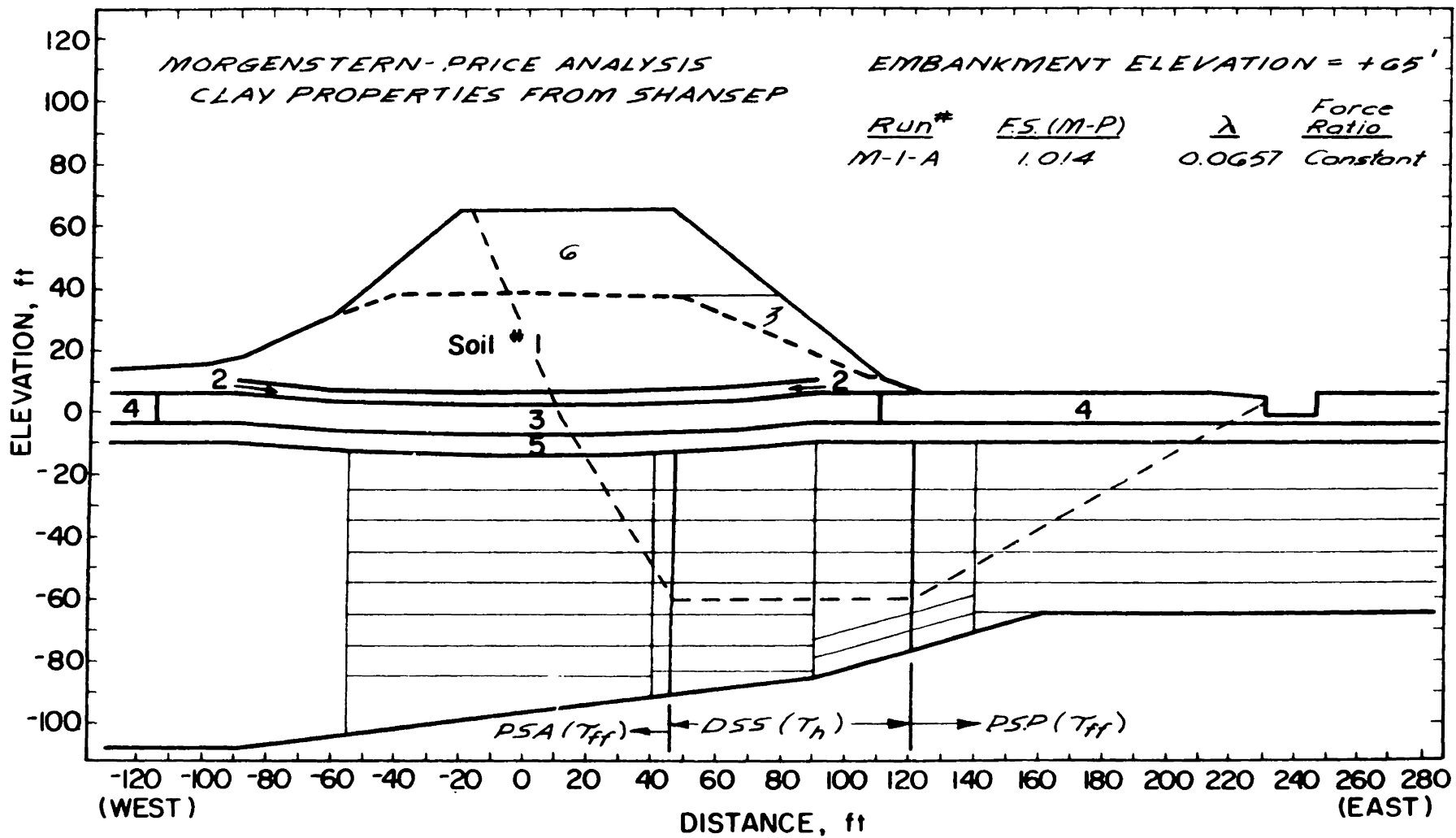
APPENDIX A

Morgenstern-Price SHANSEP
Stability Analyses

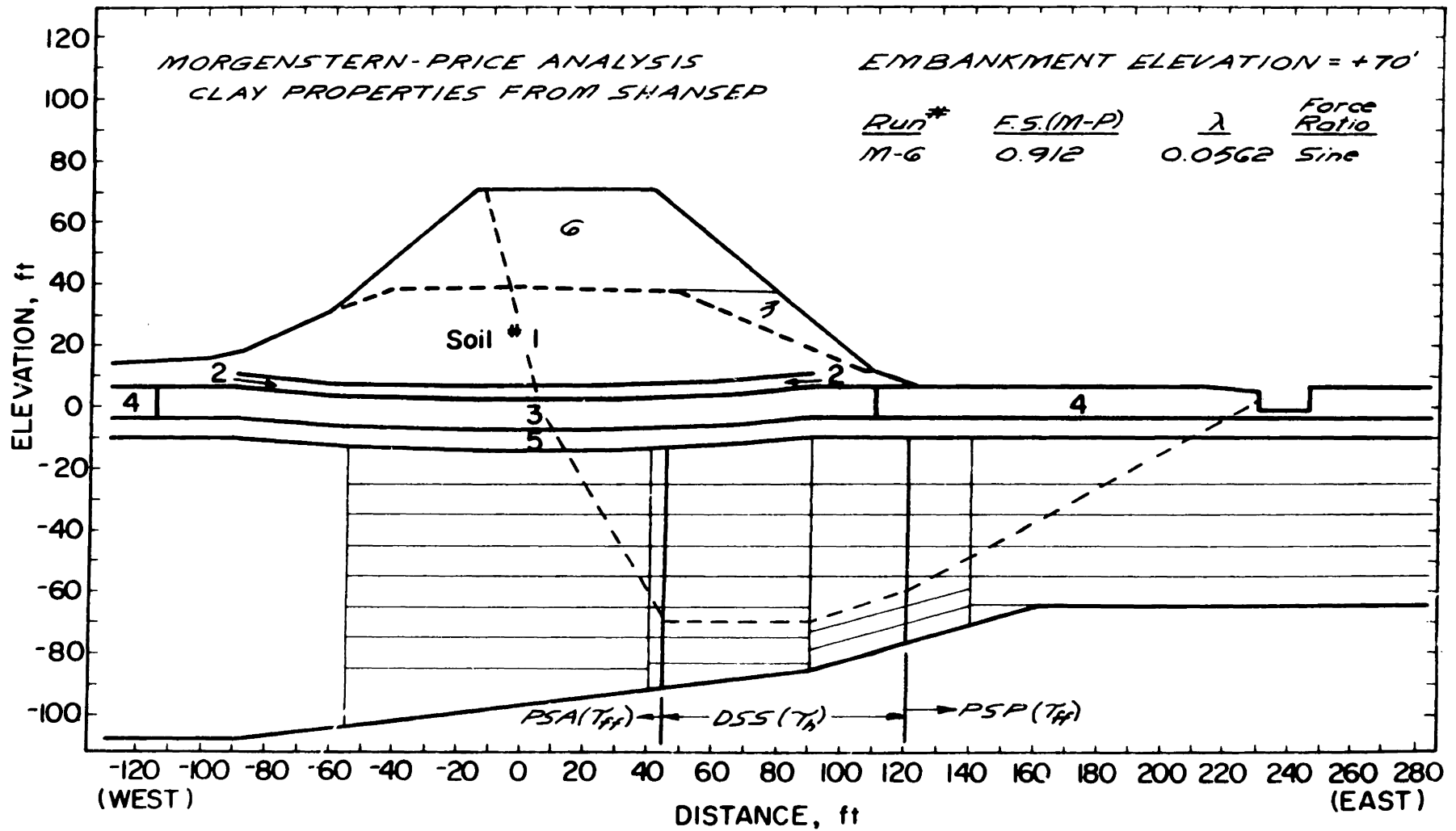
FILL ELEV.	RUN NO.	FACTOR OF SAFETY			FAILURE SURFACE POINTS COORDINATES						PSA	PSP	REMARKS
		CONST	SINE	BELL	1	2	3	4	5	6			
60'	14-A		1.104		-24,+62	+16,0	+50,-60	+120,-60	+232,+4		57°Tff	30°Tff	Effect of θ in fill is very small. Min @ θ \approx 75°
	14-B		1.099		-10,+61	"	"	"	"		67°Tff	"	
	14-C		1.096		0,+61	"	"	"	"		76°Tff	"	
	20		1.008		-27,+62	-10,0	+55,-70	+90,-60	+120,-60	+234,+4	9f	"	
62.5'	15		1.046		-1,+66	+15,0	+50,-60	+100,-60	+220,8		Tff	30°Tff	Effect of side force assumption very small.
	16		1.047		"	"	"	"	+232,3		Tff	"	
	17	0.998	1.005	1.000	"	"	+55,-70	+90,-70	+120,-60	+232,+4	Tff	"	
	18		0.997		-22,+66	-10,0	"	"	"	"	9f	"	
	19-A		0.981		"	"	"	"	+266,+8	9f	9f		
65'	1	1.16	1.17	1.19	-22,+74	+11,0	+46,-60	+120,-60	+250,+14		Tff	53°Tff	Error in Pl. 5 PSP @ 30° more critical. Deeper wedge more critical. PSA under crest (1-A) more critical.
	1-A	1.014	1.02		"	"	"	"	+250,+15		"	30°Tff	
	5		0.973		-19,+66	+6,0	+46,-70	+90,-70	+120,-60	+234,+8	"	"	
	7		1.039		"	-5,0	+40,-60	+135,-60	+240,0		"	"	
	8		1.056		"	"	+30,-60	"	"		"	"	
	9		0.924		"	+4,0	+30,-45	+86,-65	+120,-65	+232,0	"	"	
	11		1.013		"	-1,0	+40,-70	+90,-70	+226,+8		"	"	
	12		0.969		-20,+66	+10,-1	+50,-70	"	+120,-60	+236,+7	"	"	
	13		1.059		"	"	"	"	+190,+10	"	45°9f	PSP @ 30° more critical.	
70'	2	1.116	1.13		-16,+80	+11,0	+46,-60	+120,-60	+250,+14		Tff	53°Tff	Error in Pl. 5
	2-A	0.962	0.97		"	"	"	"	+250,+18		"	30°Tff	
	6		0.912		-12,+71	+6,0	+46,-70	+90,-70	+120,-60	+234,+8	"	"	

SUMMARY OF MORGENSTERN-PRICE (SHANSEP)
STABILITY ANALYSES

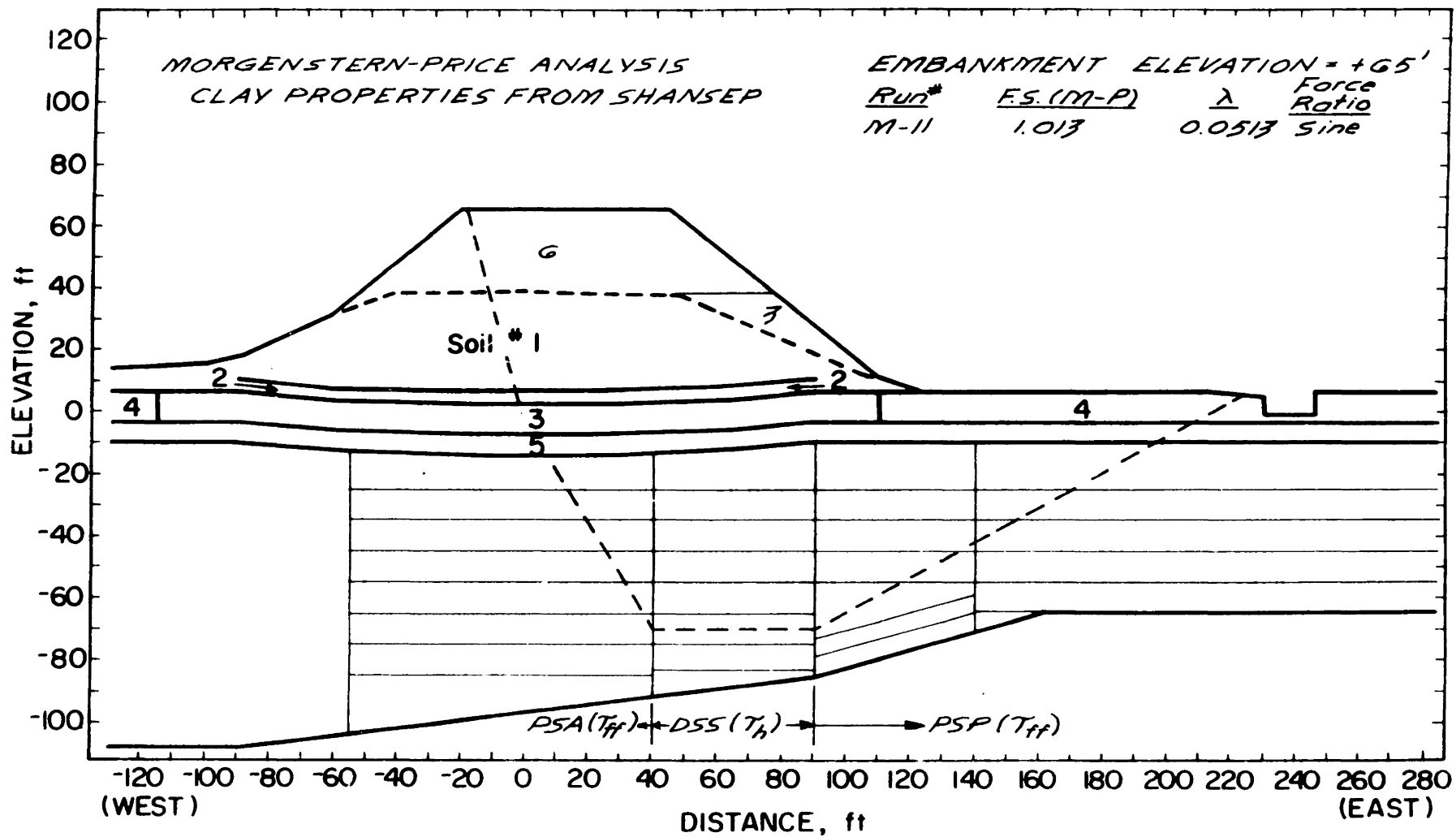
TABLE A-1



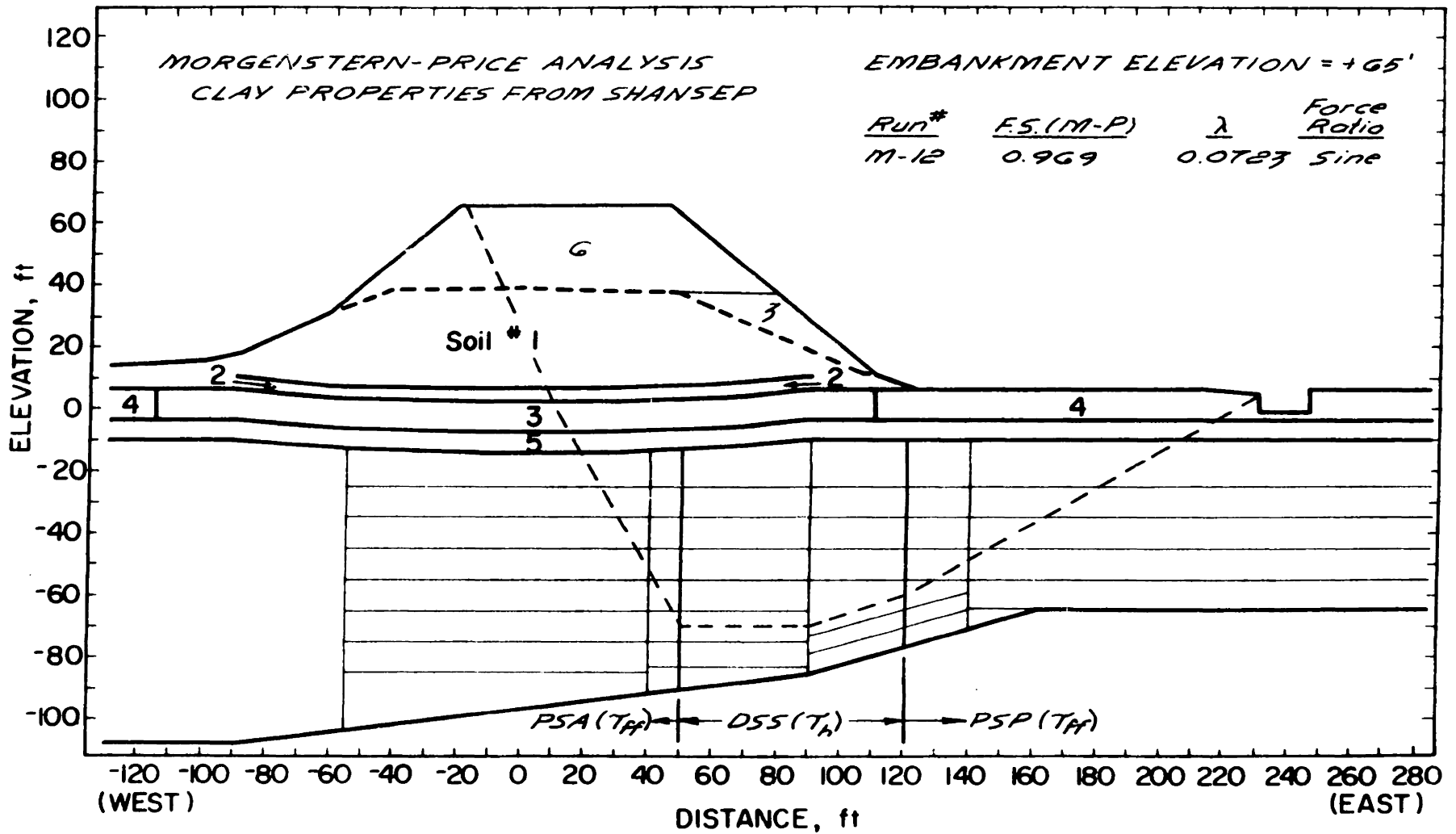
STABILITY ANALYSES I-95 STATION 263
FIGURE A-1



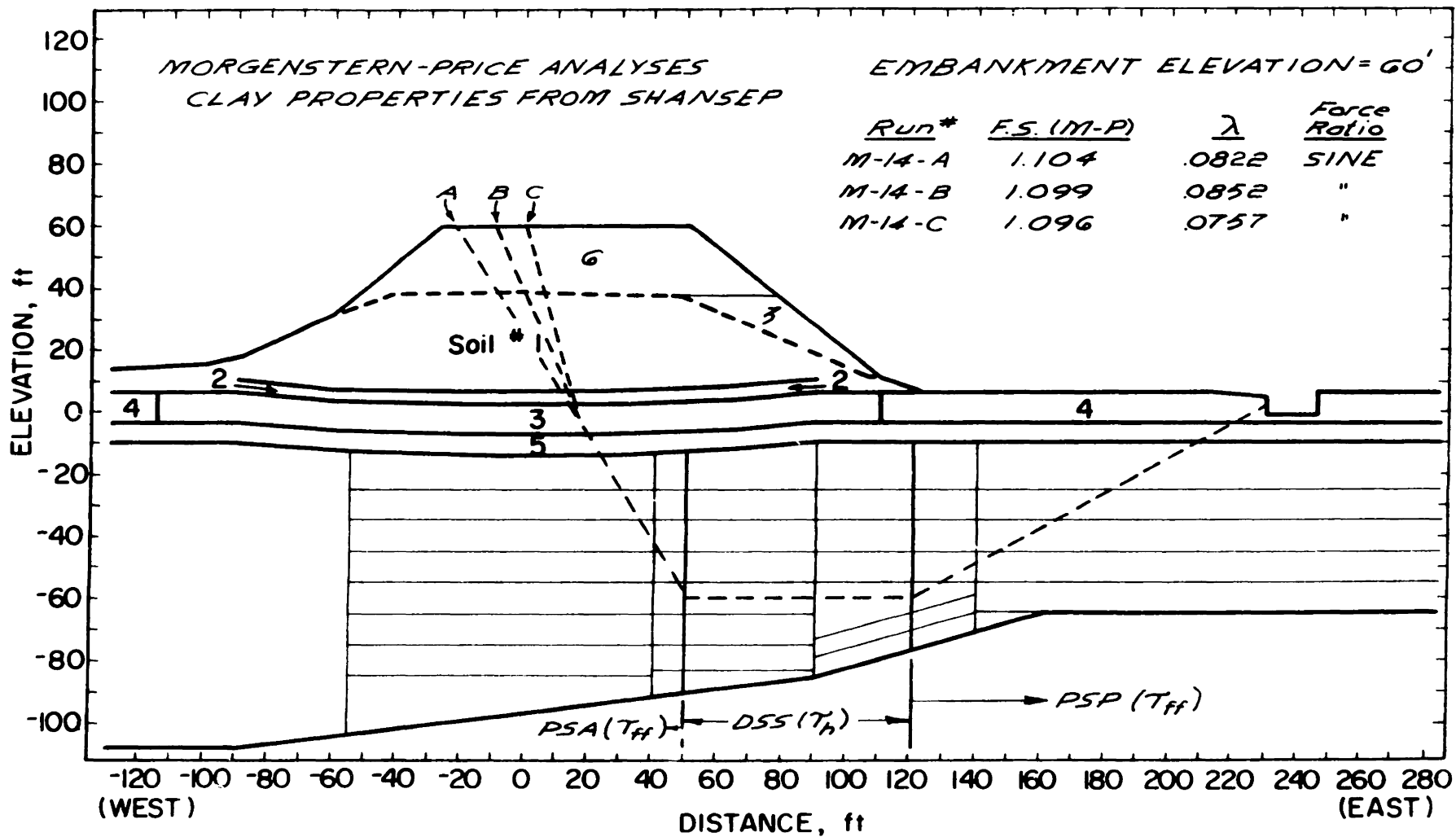
STABILITY ANALYSES I-95 STATION 263
FIGURE A-2



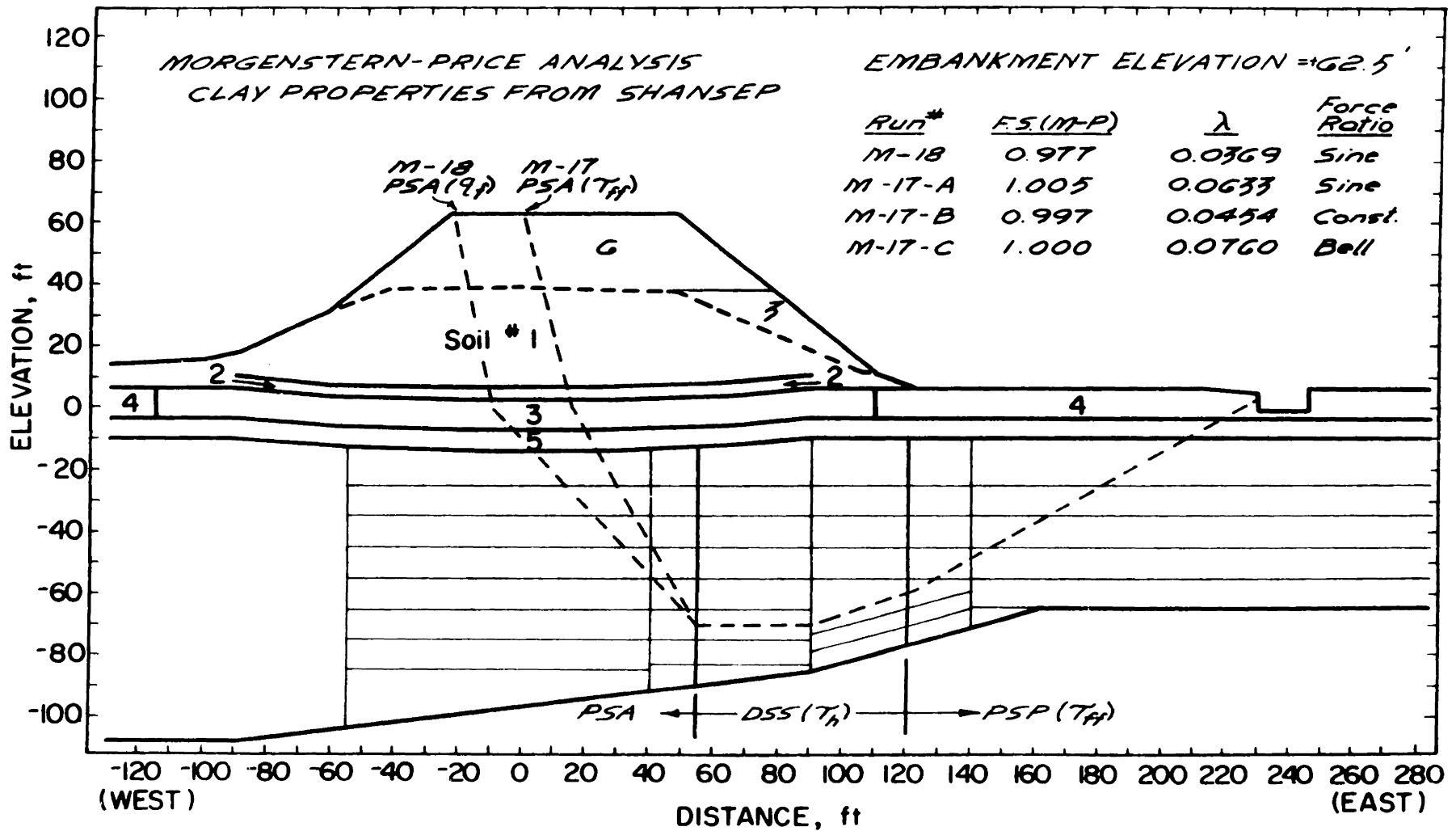
STABILITY ANALYSES I-95 STATION 263
FIGURE A-3



STABILITY ANALYSES I-95 STATION 263
FIGURE A-4

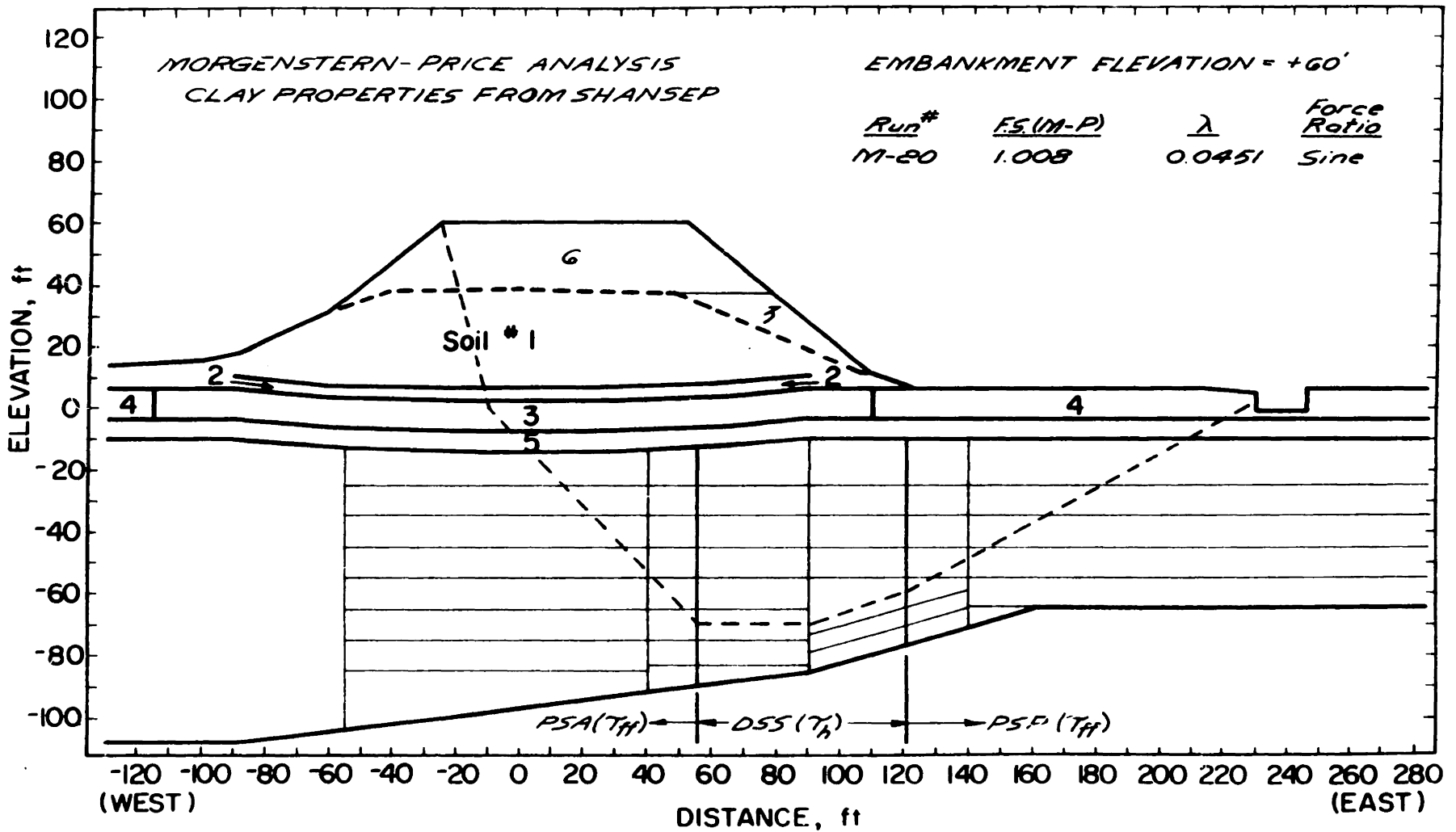


STABILITY ANALYSES I-95 STATION 263
FIGURE A-5



STABILITY ANALYSES I-95 STATION 263

FIGURE A-6



STABILITY ANALYSES I-95 STATION 263
FIGURE A-7